TOXICITY MECHANISM OF ANTHROPOGENIC WATER CONTAMINANTS: DRINKING WATER DISINFECTION BY-PRODUCTS (HALOACETIC ACIDS) AND PARTICLE ASSOCIATED CONTAMINANTS FROM SEALCOATS (POLYAROMATIC HYDROCARBONS) IN LAKE SEDIMENTS

BY

AZRA DAD

DISSERTATION

Submitted in partial fulfillment of the requirements
for the degree of Doctor of Philosophy in Crop Sciences
in the Graduate College of the
University of Illinois at Urbana-Champaign, 2016

Urbana, Illinois

Doctoral Committee:

Professor Michael J. Plewa, Chair
Professor Charles J. Werth
Professor A. Lane Rayburn
Professor Jodi Flaws

ABSTRACT

Drinking water disinfection was one of the major public health accomplishments of 20th century. Water disinfection helps in reducing waterborne diseases like typhoid fever, cholera, and hepatitis A. However, chemical water disinfection also produces unwanted toxic chemicals, known as water disinfection by-products (DBPs). Most of the DBPs are cytotoxic, neurotoxic, genotoxic, mutagenic, carcinogenic and teratogenic but the toxicity mechanism is not completely understood. Therefore, the objectives of this dissertation were to i) understand the toxicity mechanisms and identify the molecular targets of all the regulated and non-regulated haloacetic acids (HAAs) water DBPs, ii) to differentiate among the toxicity mechanisms of mono-, di-, and triHAAs, iii) to evaluate the toxicity potential of chlorinated and chloraminated wastewater effluents, and iv) to evaluate the mutagenicity potential of the particle associated contaminants such as polyaromatic hydrocarbons (PAHs) associated with coal tar and soot, extracted from lake core sediments.

Studies based on the toxicity mechanism of HAAs water DBPs demonstrated that monoHAAs were the strongest inhibitors of glyceraldehyde-3-phosphate dehydrogenase (GAPDH) where, di-, and triHAAs were weaker inhibitors. MonoHAAs greatly reduced the ATP contents of the cells. Unlike monoHAAs, triHAAs increased the cellular ATP levels as compared to the negative controls. Exogenous pyruvate supplementation rescued cells from monoHAA-induced DNA damage and ATP depletion. These results confirmed that monoHAA-induced genotoxicity was due to GAPDH inhibition. HAAs not only affected the GAPDH kinetics and disturbed the cellular energy homeostasis but also increased pyruvate dehydrogenase complex (PDC) activity. Increased PDC activity by monoHAAs was due to changes in metabolite ratios e.g., ATP/ADP, and NADH/NAD ratio but the increase induced by di-, and triHAAs was due to the inhibition of pyruvate dehydrogenase kinase (PDK). Results demonstrated that HAA-induced toxicity is due to disruption in cellular energy homeostasis. This research demonstrated that there was a difference among the HAA-induced toxicity mechanisms and their molecular targets. MonoHAAs had an indirect effect on mitochondrial metabolism by inhibiting GAPDH, affecting the generation of pyruvate, inducing oxidative stress and reducing the final output of mitochondria in the form of ATP. Among monoHAAs, the rank order of toxicity was iodoacetic acid > bromoacetic acid >> chloroacetic acid (IAA > BAA >> CAA). This toxicity pattern was directly correlated with the inhibition of GAPDH kinetics, ATP depletion, and PDC activation.

Whereas, di- and triHAAs induced toxicity by directly affecting mitochondrial metabolism by PDK inhibition, which led to PDC activation.

The toxicity potential of chlorinated and chloraminated wastewater effluents extracted with XAD-8 and XAD-4 resins was evaluated. For chlorinated water, the organic extracts eluted from XAD-8 were more cytotoxic than that of the chloraminated wastewater extracts. However, the XAD-4 extracts of the chlorinated wastewaters and chloraminated wastewaters did not show any significance difference. Unlike the cytotoxicity analyses, the chloraminated wastewater XAD-8 extracts showed a higher genotoxic effect in mammalian cells than the XAD-4 extracts. Thus the major cytotoxicity and genotoxicity components in wastewater effluents were associated with hydrophobic acid fractions as compared to the transphilic acid fractions.

The mutagenicity evaluation of the coal tar and soot associated polyaromatic hydrocarbons (PAHs) from lake sediments demonstrated that the coal tar and soot extracts were not direct acting mutagens but needed S9 microsomal activation. It was also found that coal tar extracts induced a higher rate of base pair substitution mutations as compared to the induction of frameshift mutations. Soot extracts induced a relatively higher rate of frameshift mutations as compared to the coal tar extract frameshift mutation rate.

"Have ye observed the water that ye drink? Is it ye who shed it from the raincloud, or are do we? If we willed we verily could make it salt. Why, then, give ye not thanks? (Quran 56: 68-70).

ACKNOWLEDGMENTS

"...Say, "Sufficient for me is Allah; upon him rely the reliers." (Quran 39:38).

First and foremost, I give thanks to Lord Almighty, for his blessings throughout my Ph.D. to accomplish my goals and complete my research successfully.

My Ph.D. journey would have been improbable without the support, encouragement, and inspiration of the people around me. I would like to express my deepest gratitude to my advisor professor Michael Plewa. He has been a great mentor and taught me how to develop my hypotheses, think like a scientist, and tackle the hardships along the way, during my Ph.D. scientific journey. I would like to thank Dr. Wagner for training me in the lab, for providing all the research supplies in time, and for proofreading my manuscripts. I also would like to thank my committee members, Dr. Jodi Flaws, Dr. Lane Rayburn, and Dr. Charles Werth for their insightful questions and comments to polish my skills and make me a better scientist.

I would like to thank all the Crop sciences, and Interdisciplinary Environmental Toxicology Program faculty and staff for organizing and administering the departments efficiently and providing me an opportunity to pursue my Ph.D in these programs and for introducing me to great scientists in the field. I would especially like to thank Dianne Carson and Synthia Lane for their cooperation as I went through the process.

I would like to thank all the graduate students in Dr. Plewa's laboratory for their cooperation and thought provoking discussion that helped me to easily adapt to the new environment and develop my research project along the way. Thanks to Dr. Justin Pals, Dr. Yukako Komaki, Dr. Clara Jeong, and Jennifer Osiol for all of their help.

I also would like to thank all the funding organizations i.e. Comsats Institute of Information Technology, Islamabad Pakistan, U.S. Geological Survey, and Interdisciplinary Environmental Toxicology Program for their financial support.

Finally, it would be remiss of me if I do not extend my gratitude to my dear family. I would like to thank my Mum and Dad and also my siblings for all of their support and encouragement.

Azra Dad

TABLE OF CONTENTS

CHAPTER 1

INTRODUCTION AND LITERATURE REVIEW

1.1. INTRODUCTION

Contaminated water is a major health risk throughout the world; contamination, whether natural or anthropogenic affects the quality of life and the public health (World Health Organization 2011; Ngwenya et al. 2013). Drinking water disinfection was the greatest public health achievement of the 20th century (Cutler and Miller 2005). When water from melted snow and rain flows into source water such as lakes and rivers, it collects a variety of toxic chemicals from variety of surfaces with some from the sealcoating of roads, streets and parking lots e.g. polyaromatic hydrocarbons (PAHs) and pathogens e.g. bacteria and viruses that come from wastewaters. These different sources of pollutions may generate drinking water contamination and habitat degradation for aquatic life. In order to provide safe drinking water to hundreds of millions of Americans, source water is processed and disinfected to reduce pollutants and waterborne diseases. Water disinfectants are powerful oxidizing agents and they react with the natural organic matter and other water contaminants and inadvertently produce toxic water disinfection by-products (DBPs) (Richardson et al. 2007a; Richardson and Postigo 2012). Safe drinking water is a pivotal factor of the quality of human life and lakes and rivers provide habitats for aquatic life and are used as source water for drinking water. It is an important goal to study the toxicity of water contaminants (Plewa and Wagner 2015). In this dissertation, I discuss the toxicity mechanism of haloacetic acid water DBPs, DBPs generated in water after chlorination of wastewaters, and toxic agents associated with contaminants originating from sealcoats in lake sediments and wastewaters. Thus the overall theme of this dissertation is water and the generation of anthropogenic mediated toxic contaminants in water.

1.2. WATER DISINFECTION BY-PRODUCTS AND ADVERSE HEALTH OUTCOMES

The introduction of water disinfection was associated with the recognition that drinking water was a significant source of infectious disease transmission. Drinking water disinfection safeguarded against waterborne diseases, e.g., typhoid fever, cholera, amoebiasis, shigellosis, salmonellosis, and hepatitis A (Akin et al. 1982). In water treatment processes, controlling waterborne diseases by eliminating microbiological contaminants is achieved by two basic approaches, removing pathogens from the water or inactivating the pathogens. Inactivating

pathogens as a water treatment strategy is referred to as disinfection. In 1881, Koch, demonstrated that chlorine can inactivate pathogenic bacteria (Koch 1881). In the United States, chlorine was first used for water disinfection in New Jersey, in 1908 (American Chemistry Council 2015). In water works practice, the purpose of disinfection is not just the inactivation of microorganisms in the source water (primary disinfection) but also to avoid regrowth of these pathogens by maintaining a disinfectant residual in the treated-water distribution system (secondary disinfection) (Crittenden et al. 2012). Disinfectants are powerful oxidants and they not only kill harmful microorganisms but also generate toxic water disinfection by-products (DBPs) (Krasner 2009). DBPs are formed when chemical disinfectants (chlorine, chlorine dioxide, chloramine, and ozone) react with organic precursors such as, natural organic matter (NOM), and inorganic precursors such as halide ions. Disinfectants oxidize organic and inorganic precursors and convert them into DBPs (Krasner 2009). More than 600 DBPs have been identified (Richardson et al. 2007b). The spectrum of DBPs in water is influenced by a variety of factors, which include the type of disinfectant used, the concentration of disinfectant, reaction time, NOM concentrations and other organic chemical as dissolved organic carbon (DOC), pH, and temperature. In chlorinated water, the most abundant classes of DBPs are the trihalomethane (THMs) and the haloacetic acids (HAAs) (Krasner et al. 2006; Krasner 2009).

The first DBPs identified were THMs reported in chlorinated drinking water, in 1974 (Bellar et al. 1974; Rook 1974). Rook showed for the first time that THMs were produced due to the reaction of chlorine with NOM in raw surface water (Rook 1974). After the discovery of chloroform in chlorinated drinking water, National Cancer Institute (NCI) published the results of a rodent cancer bioassay on chloroform, in 1976 (U. S. Environmental Protection Agency 2001; Hrudey 2009), health concerns associated with chloroform and THMs lead to the adoption of drinking water guidelines and the development standards to control DBPs and reduce the level of consumer's exposure to these hazardous chemicals. In 1979, under the Safe Drinking Water Act, the U.S. Environmental Protection Agency (U.S. EPA) issued the Total Trihalomethane Rule with a regulatory standard for THM4 (sum of chloroform, bromodichloromethane, chlorodibromomethane, and bromoform) at 100 μg/L (U. S. Environmental Protection Agency 1979). The U.S. EPA published the final Stage 1 Disinfectants/Disinfection By-Product (D/DBP) Rule in 1998 with the lowered THM4 maximum contaminant level (MCL) to be 80 μg/L and regulated HAA5 (chloroacetic acid (CAA), dichloroacetic acid (DCA), trichloroacetic

acid (TCA), bromoacetic acid (BAA), and dibromoacetic acid (DBA)) to a total maximum contaminant level of 60 μg/L (U. S. Environmental Protection Agency 1998). Afterwards, in 2006, the final stage 2 DBP rule was established. The stage 2 DBP rule continued with the previous MCLs from stage 1 rule but added changes to monitoring design and determination of compliance of the rule (U. S. Environmental Protection Agency 2006).

Concerns regarding the adverse health outcomes of DBPs initiated epidemiological studies to evaluate the health effects of these hazardous complex mixtures present in disinfected water. Epidemiological studies demonstrated a relationship between lifetime chronic exposure to DBPs and colorectal cancer (King et al. 2000; Bove et al. 2002; Rivera-Núñez and Wright 2013; Rahman et al. 2014), bladder cancer (King et al. 2000; U. S. Environmental Protection Agency 2001; Villanueva et al. 2007), skin cancer (Karagas et al. 2008) and to a lesser extent adverse pregnancy outcomes (Chisholm et al. 2008; Jeong et al. 2012; Rivera-Núñez and Wright 2013). However, these DBPs showed a different carcinogenicity potential in animal studies and discrepancies in it's carcinogenicity potential among males and females were also found (David and Elsebeth 1999). The discrepancies in carcinogenic potency of different DBPs might be because of the target organ specificity and species differences in sensitivity (Bull et al. 2011), but a gap in the knowledge connecting DBPs exposure and adverse health outcomes continues.

Drinking water disinfection has undoubtedly improved the quality of life by inactivating pathogenic microorganisms present in source-waters and by controlling waterborne diseases in the developed countries. However, the unwanted generation of hazardous DBPs in drinking water chronically exposes a population to toxic agents and increases potential health risks associated with the drinking water disinfection. Different modes of toxicity for these DBPs were proposed including genotoxicity and oxidative stress but the mechanisms linking these toxicities to increased risk of cancer and other adverse health outcomes are not well understood. Further research on the molecular mechanism of toxicity of specific DBPs complexes and individual DBPs is essential to understand their cumulative effects and adverse health outcomes. Understanding DBP modes of action may also help in the identification of populations susceptible to the toxic effects of DBPs due to genetic polymorphisms for different genes e.g. those responsible for DNA repair, metabolic functions, and responses to oxidative stress.

Formation, Occurrence and Toxicity of Mono-, Di-, and Trihaloacetic acids

Formation and Occurrence of HAAs

There are 10 HAAs commonly identified in drinking water; iodoacetic acid (IAA), chloroacetic acid (CAA), dichloroacetic acid (DCA), trichloroacetic acid (TCA), bromoacetic acid (BAA), dibromoacetic acid (DBA), bromochloroacetic acid (BCA), bromodichloroacetic acid (BDCA), chlorodibromoacetic acid (CDBA) and tribromoacetic acid (TBA) (Health Canada 2008). HAAs belong to the family of halogenated aliphatic carboxylic acids and carry two carbon carboxylic acids in which one or more halogen atoms take the place of the hydrogen atoms attached to the α-carbon relative to the carboxylic acid (Figure 1.1). HAAs are present in water at neutral pH as salts or acetates (European Comission 2003) but in this document I refer to them as acids. HAAs are generated in treated water when chlorine or other disinfectants react with NOM e.g., fulvic acids and humic acids and inorganic DBP precursors e.g., halide ions (Br^- and I^-) naturally present in the raw water (WHO 2000; Stuart 2009). Various water treatment methods including chlorination, ozonotaion, and chloramination, lead to the formation of chlorinated, brominated and iodinated acetic acids. In the case of chlorination, hypochlorous acid (HOCl) and the hypochlorite ion (OCl) are formed, which then react with a bromide ion present in the water and oxidize it to hypobromous acid and hypobromite ion, respectively. Hypochlorous acid and hypobromous acid then react with NOM to form different DBPs, including HAAs. The chlorinated HAAs generally dominate; however, in high-bromide waters, the formation of brominated HAAs may be more frequent. Chloramination also results in HAA production if chloramine is produced by chlorination followed by ammonia addition (WHO 2000; Health Canada 2008). HAA formation may be more prevalent when drinking water is chlorinated under a slightly acidic pH. Whereas THM formation increases with increasing pH, HAA formation decreases, hydrolysis likely being a significant factor (Krasner et al. 1989; Pourmoghaddas and Stevens 1995).

HAAs are the second most abundant classes of DBPs in chlorinated drinking water (Krasner et al. 2006). In 1989, a study on 35 U.S. utilities analyzed 19 different halogenated DBPs. The halogenated compounds, collectively, accounted for between 30 and 60% of the total organic halogen (TOX) found in those samples (Krasner et al. 1989). Hua et al conducted a study on the effect of 5 different oxidation treatments on the formation of DBPs using seven diverse

natural waters in the U.S. They found that the free chlorine formed more HAAs and TOX than chloramines or chlorine dioxide. The TOX produced by chlorination was 45.1% with the HAAs accounted for 15.4%, pre-ozonation/post-chlorination produced 43.4% and HAAs accounted for 14.4%, chloramination produced 19.2% and HAAs accounted for 15.4%, preozonation/chloramination produced 16% and HAAs accounted for 11.2%, and chlorine dioxide produced 19.7% with HAAs accounted for 17.3% (Hua and Reckhow 2007). Among halogenated DBPs, the di-, and tri-halogenated acetic acids with multiple chlorine, or mixed chlorine and bromine species were the most prevalent, however, the source waters with high Br- and I-, brominated DBPs may be the most dominant species (Krasner et al. 2006). A nationwide survey of DBPs occurrence at 12 water treatment plants was conducted in the U. S. It was found that in the plant effluents, the TOX on a median basis was 178 μg/L as Cl^- with HAAs accounted for 12% on a median basis. The sum of the 9 HAAs in the surveyed plants ranged from 5 μg/L to 130 μg/L with a median of 34 μg/L (Krasner et al. 2006). A survey of DBPs occurrence at 3 different water supplies was performed in the U.K. to evaluate the levels of HAAs in the water and the relationship between HAAs and THMs, pH, temperature, and free and total chlorine. The source water for most of the samples was surface water. Some of the samples showed levels of total HAAs above 200 μg/L. MCAA was not measured and DCA levels were very high, above 100 μg/L, which is above world health organization (WHO) level of 50 μg/L, while the TCA levels were lower than DCA. The overall mean value for the total HAAs was 35-95 μg/L with a maximum concentration of 244 μg/L. Total THMs were not a good indicator of HAAs levels and the ratios of total THMs and HAAs was significantly correlated with the temperature, pH, and free and total chlorine (Malliarou et al. 2005). A study was conducted to investigate the concentration of different DBPs including 9 HAAs in the water from 11 different Spanish provinces. HAAs concentration ranged from 0.9 to 86.9 μg/L with a median of 26.4. While DCA and TCA had the highest concentrations of 7.3 and 6.5 μg/L (median value), respectively, among other 9 HAAs, CAA and TBA occurred at lowest concentrations with 60% and 50% samples below the quantification limit, respectively. The sum of dihalo- and trihaloacetic acids showed similar concentrations of 12.7 and 13.3 μg/L (median value), respectively (Villanueva et al. 2012).

In most studies, 9 HAAs were studied but not IAA. IAA was first discovered in the nationwide occurrence study in the U. S., (Plewa et al. 2004a; Krasner et al. 2006). One recent survey of DBP occurrence investigated 13 drinking water plants, in Shanghai China. The source waters were from the Yangtze or Huangpu rivers; the disinfectant was chloramine. In these water systems 9 HAAs ranged from 3.31 μg/L to 48.55 μg/L; IAA was also detected in all the water supplies and the concentration ranged from 0.04 μg/L to 1.66 μg/L. The maximum IAA concentration of 1.66 μg/L was due to the higher concentration of I^- (18 μg/L) in the source water (Wei et al. 2013a).

In vivo and epidemiological and experimental studies demonstrated that DBPs are toxic. Epidemiological studies showed that increased risk of bladder and colorectal cancer was associated with DBPs (Villanueva et al. 2007). U. S. EPA estimated that 2-17% of bladder cancer cases in the U.S. may be induced by DBPs (U.S. Environmental Protection Agency 1998). Furthermore, DBPs in chlorinated drinking water were associated with spontaneous abortion in a prospective study of 5144 pregnant women (Waller et al. 1998). In *in-vivo* studies, HAAs (DCA, TCA, and DBA) induced hepatocellular adenomas and hepatocellular carcinomas in B6C3F1 mice and F344 rats (Health Canada 2008) and DCA, DBA, and bromochloroacetic acid (BCA) altered intestinal microflora and metabolism in rats, which could also have an effect on bioactivation of promutagens or procarcinogen(George et al. 2000) . IAA induced malignant transformation in NIH/3T3 mouse embryonic fibroblast cells and when implanted in Balb/c nude mice, developed into highly aggressive fibrosarcomas (Wei 2013). Gestational exposure of mixture of HAA5 resulted in pregnancy loss and eye malformation in rats (Narotsky et al. 2011). Under *ex-vivo* conditions, monoHAAs were teratogenic and induced dysmorphogenesis in CD-1 mouse embryos and affected neural tube development, eye development and produced anomalies in heart development (Hunter et al. 1996). HAAs were cytotoxic and genotoxic in Chinese hamster ovary (CHO) cells (Plewa et al. 2010), mutagenic in *Salmonella typhimurium* and CHO cells (Hunter et al. 1996; Kargalioglu et al. 2002; Zhang et al. 2010).

In vitro studies showed that monoHAAs were more toxic than the diHAAs and diHAAs were more toxic than the triHAAs (Hunter et al. 1996; Kargalioglu et al. 2002; Plewa et al. 2002; Plewa et al. 2010). A variety of studies demonstrated that of the monoHAAs, IAA was the most toxic and CAA was the least toxic. These data indicated that the toxicity of these monoHAAs

was dependent on the type of halogen substituent (Hunter Iii and Tugman 1995; Plewa et al. 2004b; Pals et al. 2011; Dad et al. 2013)

The focus of my project is on the toxicity mechanism of 10 HAAs (Figure 1.1). I present the toxicity mechanism(s) of the mono, di-, and trihaloacetic acids with variability in their chemical structures based on the number and type of their halogen substituent. The toxicity of the HAAs reported in the literature is reviewed below.

Toxicity of HAAs

HAAs are cytotoxic and genotoxic in mammalian cells (Plewa et al. 2002; Plewa et al. 2010) mutagenic in *Salmonella* strain TA100 (Kargalioglu et al. 2002), induce reproductive and developmental toxicity (Narotsky et al. 2015; Teixido et al. 2015) , and carcinogenic (Pan et al. 2014).

HAAs Induced Mutagenicity

HAAs are mutagenic in variety of cell-based studies (Kargalioglu et al. 2002; Wang et al. 2011). Nelson et al studied the effect of cecal microbiota on the mutagenicity of HAAs and also the changes in the intestinal microflora and changes in the enzyme activities produced by the intestinal microflora. 1 mg/mL of CAA, BAA, DCA, DBA, TCA, TBA, and BCA in PYG medium was inoculated with rat cecal homogenate and was incubated at 37°C. HAAs mutagenicity in *Salmonella* TA100 was determined using microsuspension bioassay. After 15 h of incubation, the activities of beta-glucuronidase, beta-galactosidase, beta-glucosidase, azoreductase, nitroreductase, dechlorinase, and dehydrochlorinase was also determined. Results showed that all the HAAs except BCA were toxic to microflora. DBA, TBA, and BCA were mutagenic in the microsuspension assay, but the presence of the intestinal microflora did not significantly alter the mutagenicity. BCA increased the activities of several enzymes involved in the biotransformation of xenobiotics (Nelson et al. 2001). HAAs were mutagenic in CHO-K1 cells, when evaluated using hypoxanthine-guanine phosphoribosyltransferase (HGPRT) mutation assay (Zhang et al. 2010). The mutagenicity of HAAs was evaluated in *Salmonella typhimurium* strains TA98, TA100, and RSJ100 +/- S9. Among the three different strains used in the study for mutagenicity evaluation, TA100 - S9 was the most sensitive to the HAAs induced mutagenicity. The rank order for the mutagenic potency for HAAs excluding other DBPs involved in the study

was BAA > DBA > DCA > CAA with TBA and TCA not mutagenic. The mutagenic and cytotoxic potential of the different HAAs showed that brominated HAAs were more toxic than the chlorinated ones. Moreover, the mutagenicity potential of these HAAs had an inverse relationship with the number of halogen atoms present on the HAAs molecules (Kargalioglu et al. 2002).

Genotoxicity and DNA Damage

Studies demonstrated that HAAs induce DNA damage (Plewa et al. 2002; Plewa et al. 2010). Escobar et al studied the genotoxic and clastogenic effect of HAAs in primary human lymohocytes. All monoHAAs were genotoxic in the human lymphocytes with IAA being the most toxic followed by BAA and then CAA. The human lymphocytes showed less HAA-induced DNA damage repair as compared to the other mammalian cells. HAAs induced chromosomal aberrations in these human cells (Escobar-Hoyos et al. 2013). Using SOS/umu test with *S. typhimurium*, TA1535/pSK1002 without S9 activation, the genotoxic effect of the brominated HAAs and brominated THMs was investigated in a comparison study of the genotoxic effect of the treated and untreated water. It was found that the brominated HAAs induced genotoxic effect. However, the brominated THMs were more toxic than the brominated HAAs (Wang et al. 2011). The cytotoxic and genotoxic potential of the 12 individual HAAs was investigated using CHO cell line AS52. It was found that most of the HAAs included in the study were cytotoxic with the rank order of IAA > BAA > TBAA > CDBAA > DIAA > DBAA > BDCAA > BCAA > CAA > BIAA > TCAA > DCAA. The rank order for genotoxicity was IAA > BAA > CAA > DBAA > DIAA > TBAA > BCAA > BIAA > CDBAA. DCAA, TCAA, and BDCAA were not genotoxic. The trend for the cytotoxicity and genotoxcity for all the HAAs was again iodinated HAAs > brominated HAAs > chlorinated HAAs (Plewa et al. 2010). The evaluation of the cytotoxicity and genotxocity of haloacetic acids using microplate-based cytotoxicity assay and CHO hypoxanthine-guanine phosphoribosyltransferase (HGPRT) gene mutation assay in CHO-K1 cells showed some toxicity. The chronic cytotoxicity of the HAAs showed some variation among the HAAs included in the study. They were rank ordered in the following descending order IAA >BAA > DBA > CAA > DCA > TCA. All HAAs were mutagenic to CHO-K1 cells in the HGPRT mutation study. The DBPs included in the mutation assay were rank ordered as follows: IAA > DBA > BAA > CAA > DCA > TCA. The cytotoxicity and HGPRT mutation

induced by these HAAs were significantly correlated showing that these two endpoints are suitable for comparing their toxic potentials quantitatively (Zhang et al. 2010). The genotoxocity and the clastogenic and/or aneugenic effects of the monoHAAs treated TK6 cells were evaluated using cytokinesis-block micronucleas assay. Results showed that none of the three monoHAAs included in the study was able to significantly increase the frequency of micronucleus in the binucleated TK6 cells. The rank order for the cytotoxicity potential was IAA > BAA >> CAA (Liviac et al. 2010).

Carcinogenicity

HAAs are carcinogenic. Ronald et al, investigated the carcinogenic potency of DBA. Male and female F344/N rats and B6C3F1 mice were exposed to 0, 50, 500 and 1000 mg/L of DBA for different time periods, ranging from 2 weeks to 2 years. In the 2 year study, neoplasms were induced in rats and mice at different sites, including mononuclear cell leukemia and abdominal cavity mesothliomas in rats, and lung and liver cancer in mice. The liver cancer incidence was increased in male mice even at the lowest concentration of 50 mg/L (≈4 mg/kg dose) (Melnick et al. 2007). Another study by the National Toxicology Program (NTP), evaluated DCA for its carcinogenic effect. Results showed that 500 mg/kg of DCA exposure for 39 weeks induced squamous cell papillomas at the site of application in male and female Tg.AC hemizygous mice (National Toxicology 2007), which is a transgenic mouse line created by a pronuclear injection of v-Ha-ras oncogene fused to a fetal zeta globulin protein at 5' and to a SV-40 polyadenylation/ splice site sequence at the 3' end in the FVB/N mouse strain (Tennant et al. 2001). A few bronchiolar/alveolar carcinomas were also appeared in both males and females when they were exposed to 1000 mg/L of DCA for 41 weeks. There was an increased occurrence of pulmonary adenomas or carcinomas compared to the control group in both dermally and orally exposed groups for a period of 39-41 weeks (National Toxicology Program 2007). Heren et al studied the carcinogenic effect of trichloroethylene (TCE) and its major metabolite TCA and minor metabolite DCA. Since TCE and its metabolites induce peroxisome proliferation so they were evaluated as tumor promoters in mouse liver. Male B6C3F1 mice were exposed intraperitoneally to 0, 2.5, or 10 μg/g body weight ethylnitrosourea (ENU) on Day 15 of age. At 28 days of age, the mice were exposed to TCE (3 or 40 mg/liter), TCA (2 or 5 g/liter), or DCA (2 or 5 g/liter drinking water containing either) in drinking water. After 61 weeks of exposure, the

animals were killed; they found that DCA and TCA were carcinogenic at a concentration of 5 g/liter without prior initiation with ENU, resulting in hepatocellular carcinomas in 81 and 32% of the animals, respectively. None of the untreated animals had hepatocellular carcinomas; this study indicated that DCA and TCA are complete hepatocarcinogens in B6C3F1 mice (Herren-Freund et al. 1987). Recently, IAA was reported to induce malignant transformation in NIH/3T3 mouse embryonic fibroblast cells and malignant cells progressed to a highly aggressive fibrosarcoma when implanted in Balb/c nude mice (Wei et al. 2013b). These studies demonstrated many of the HAAs are carcinogenic excluding CAA (DeAngelo et al. 1997). It is interesting that the U.S. EPA regulated DBP has not been studied for carcinogenicity (e.g., BAA) (Richardson et al. 2007b).

HAAs Toxicity Mechanism

HAAs are alkylating agents and follow S_N2 reactivity. In S_N2 reaction (Figure 1.2) the bond between the carbon and the halogen is polarized. The halogen is slightly more electronegative than the carbon so the halogen is partially negatively charged while the carbon has a partial positive charge. When a nucleophile presents itself, it attacks the partial positive carbon. The nucleophilic attack on the carbon and electron withdrawing from the carbon by the halogen group happens simultaneously. Therefore, the nucleophilic attack on the carbon happens from the opposite side of the halogen-leaving group. This process is known as substitution nucleophilic bimolecular (S_N2) reaction because the rate of this reaction is dependent on the concentration of the two reactants (R-X and Nu). Hence, the rate law for this reaction is R= K[R-X] [Nu]. This process is also dependent on the carbon-halogen bond length and the bond dissociation energy. For the three monoHAAs, the α-carbon-halide (αC-X) bond length follows the pattern of C-I > C-Br > C-Cl, which implies that the greater the bond length, the lower the dissociation energy required to react with the target molecule (Plewa et al. 2004b) (Table 1.1) (Loudon 1995). Cytotoxic and genotoxic potencies of monoHAAs expressed the pattern of IAA > BAA >> CAA. The toxic potential of monoHAAs was highly correlated with the pattern of S_N2 reactivity, αC-X bond length and bond dissociation energy (Plewa et al. 2004b). The mutagenicity of the monoHAAs in *S. typhimurium* and CHO cells did not require any exogenous metabolic activation. These agents were classified as direct acting mutagens (Plewa et al. 2004b). HAAs are alkylating agents and the specific biological molecules alkylated by all the mono-, di-,

and triHAAs and the disturbance induced in cellular homeostasis are discussed in this dissertation.

IAA inhibits glyceraldehyde-3-phosphate dehydrogenase (GAPDH) (Hernández-Fonseca et al. 2008; Schmidt and Dringen 2009; Pals et al. 2011). GAPDH is a member of the dehydrogenase enzyme family and is a pivotal enzyme in glucose metabolism (Sirover 1999). It exists as a homologue tetramer, monomer and dimer (Carlile et al. 2000). The tetrameric form is comprised of four chemically identical subunits, O, P, Q, and R (Figure 1.3) and is present in the cytoplasm. The monomeric form is localized to the nucleus and contains two binding domains; an N terminal, NAD^+-binding domain and a C-terminal catalytic, or glyceraldehyde-3-phosphate (G3P)-binding domain (Jenkins and Tanner 2006). IAA is a thiol reagent; it is frequently used as an alkylating agent to modify the sulfhydryl group of a thiol molecule in the active sites of different enzymes containing a cysteine residue in their active sites (Albrecht et al. 1993; Gali and Board 1997). IAA inhibits GAPDH irreversibly by making a thioether bond with the cysteine residue in the active site of GAPDH or in the G3P binding domain and make the G3P binding domain unavailable for binding the physiological substrate glyceraldehyde-3-phosphate (G3P) to carry on the following reaction. Therefore, IAA renders GAPDH inactive (Schmidt and Dringen 2009).

$$\text{Glyceraldehyde-3-phosphate} + NAD^+ + Pi \overset{\text{GAPDH}}{\leftrightarrows} \text{1,3-bisphposphoglycerate} + NADH$$

GAPDH is a pivotal metabolic enzyme; any disturbance in glycolysis due to the inactivation of GAPDH enzyme disturbs the cellular energy homeostasis (Kahlert and Reiser 2000; Hernández-Fonseca et al. 2008; Dad et al. 2013), leads to cytosolic Ca^{2+} toxicity (Kahlert and Reiser 2000; Hernández-Fonseca et al. 2008), oxidative stress (Hernández-Fonseca et al. 2008), hypoglycemia and ischemia (Hernández-Fonseca et al. 2008) in CHO cells (Dad et al. 2013), rat hippocampus astrocytes (Kahlert and Reiser 2000)and cultured hippocampus neurons (Hernández-Fonseca et al. 2008). Since brain cells are very sensitive to hypoglycemia and very vulnerable to oxidative stress, IAA is commonly used to study the role of metabolism in different neurodegenerative diseases; especially, the role of glycolysis by IAA-induced inhibition of GAPDH and ultimately glycolysis (Kahlert and Reiser 2000; Rodríguez et al. 2010).

Cellular Ca^{2+} homeostasis is crucial for different cellular functioning. In all cells including brain cells, the regulation of cytosolic Ca^{2+} concentration is a major part of the different signaling pathways linked to the control of metabolism, apoptosis and survival of neurons. At rest, the cytosolic Ca^{2+} is lower than the extracellular Ca^{2+}. In order to regulate the Ca^{2+} concentration in the cytosol, different systems are available e.g., plasma membrane Ca^{2+} ATPase powered by ATP and Na^{+}/Ca^{2+} - exchangers fuelled by the Na^{+} gradient, push the Ca^{2+} outside the cytosol into the extracellular space, while sarcoendoplasmic reticulum Ca^{2+} ATPase (SERCA) pumps Ca^{2+} into endoplasmic reticulum (ER), which can be transported into the mitochondria. The distribution of Ca^{2+} into its proper cellular compartments requires energy, which is produced by metabolism (Szalai et al. 1999; Kahlert and Reiser 2000). Studies showed that different glycolytic products e.g., phosphoenol pyruvate and ATP produced by glycolysis were directly associated with the Ca^{2+} compartmentalization especially with the Ca^{2+} uptake by the SERCA pump into ER (Xu et al. 1995). The inhibition of glycolysis and oxidative phosphorylation reduced the ATP content by 85%. It was believed that the Ca^{2+} excitotoxicity is due to the influx of Ca^{2+} through N-methyl-D-aspartate receptor (NMDA), which further leads to oxidative stress. Hernanadaz et al compared the two mechanisms and found that during the severe impairment of glycolysis due to the inhibition of GAPDH by IAA (100 μM), the cellular ATP level was drastically reduced, which increased the cytosolic Ca^{2+} and induced ROS. Moreover, they found that the BAPTA-AM, a Ca^{2+} chelator rescued the cells against the IAA (100 μM) induced ROS. However, an antagonist of the NMDA receptor MK-801 did not significantly reduce the IAA induced ROS. This proved that the Ca^{2+} excitoxicity induced oxidative stress in the IAA treated cultured hippocampal neurons, was due to the ATP depletion (Hernández-Fonseca et al. 2008). IAA also affected the GSH content of the cells (Schmidt and Dringen 2009). Studies showed that not only IAA but other HAAs also inhibit GAPDH and reduce ATP contents of the cells. The ROS induced by the HAAs lead to DNA damage and apoptosis. It was found that CAA down-regulated Bcl-2 and Mcl-1 (anti-apoptotic protein), while up-regulated Bax (pro-apoptotic protein) level, which was also associated with the cytochrome c release and pro-caspace cascade activation. The apoptotic effects induced by CAA was reversed by the N-acetyl-cysteine (NAC), which is an antioxidant; proving that HAAs inhibit glycolysis by inactivating GAPDH, reduced ATP levels, increased cytosolic Ca^{2+} concentration, induced ROS, leading to DNA damage, and inducing apoptosis (Chen et al. 2013).

Allosteric Changes in Pyruvate Dehydrogenase Kinase (PDK) Regulate Pyruvate Dehydrogenase Complex (PDC) Activity

In 1974, Whitehouse et al discovered that DCA activates pyruvate dehydrogenase complex by inhibiting pyruvate dehydrogenase kinase (Whitehouse et al. 1974); this finding was confirmed by other studies (Kline et al. 1997; Sutendra and Michelakis 2013; Ferriero et al. 2015). The pyruvate dehydrogenase complex (PDC) is a member of the α-ketoacid dehydrogenase complex family. PDC is responsible for the oxidative decarboxylation of pyruvate and its conversion into acetyl-CoA in the presence of different cofactors including thiamine pyrophosphate (TPP), CoA, and NAD^+. Mammalian PDC has multiple copies of 6 different components; they are pyruvate dehydrogenase (E1), dihydrolipoamide acetyltransferase (E2), dihydrolipoamide dehydrogenase (E3), E1 specific kinases, phospho-E1 phosphotase and X protein (De Marcucci and Lindsay 1985; Jilka et al. 1986). E1, E2, and E3 are the major catalytic components, which are responsible for the stepwise decarboxylation and dehydrogenation of the pyruvate into acetyl- CoA (Patel and Roche 1990).

The E1 component is a tetramer ($\alpha_2\beta_2$). The tetrameric E1 contains two sites for TPP binding, which is required for the first step of pyruvate decarboxylation. In the first step, E1 catalyzes the TPP dependent decarboxylation of pyruvate to hydroxyethyl TPP and also leaves an acetyl group, which is covalently linked to lipoamide group of E2. $E_1\alpha$ component of the tetrameric E1 is inactivated/phosphorylated by pyruvate dehydrogenase kinase (PDK) enzyme and activated/dephosphorylated by a specific phosphatase enzyme. The dephosphorylation of these sites by phospho-E1-phosphotase leads to the activation of the enzyme (Frey et al. 1989; Patel and Roche 1990). (Figure. 1.4)

E2 is responsible for transferring the acetyl group from acetyl-lipoyl to CoA and generation of acetyl-CoA. Sixty percent of the NH_2-terminal of the E2 component is a multidomain structure and comprises three 80-amino acid domains, each of these domains carries a lipoyl prosthetic group attached to a specific lysine residue, followed by a 50-amino acid subunit binding domain that precedes the remaining 40% of the structure that forms the oligomeric inner domain (Stephens et al. 1983). Between each of these domains are interdomain sequences, which are rich in alanine, proline, and charged amino acids (Texter et al. 1988; Perham and Packman 1989). The number of E2 domains is different in different organisms.

Human E2 has 2 lipoyl domains presented as L1 and L2. The E2B or subunit-binding domain is responsible for binding E1 and E3. The inner domain (E-I) catalyzes the transacetylation reaction and self-association to form the dodecahedral structure, which contain 60 subunits. The E2 component also plays a crucial role in the activation and inactivation of the pyruvate dehydrogenase by providing a binding site to the PDK and phospho-E1-phosphotase enzymes (Patel and Roche 1990; Patel and Korotchkina 2003) (Figure.1.5)

E3 transfers electrons from dihydrolipoamide to NAD^+. It is a homodimer and each polypeptide noncovalently binds to a molecule of FAD. (Patel and Roche 1990)

Pyruvate dehydrogenase kinase (PDK) plays an important role in regulating the PDC. PDK has four isoforms and exhibit tissue specific expression; PDK1 is detected in heart, pancreatic islets, and skeletal muscles; PDK2 is expressed in all tissues; PDK3 is present in testes, kidney, and pancreatic islets. Phosphorylation of E1p by PDK occurs at three different serine residues (S264: site 1, S271: site 2, and S203: site 3). Among the three conserved phosphorylation sites, site 1 is the most rapidly phosphorylated site where site 3 is the slowest phosphorylated site (Sale and Randle 1981; Korotchkina and Patel 1995). Structural studies of the PDKs showed that all the four isoforms of PDKs phosphorylate sites 1 and 2, but only PDK1 modifies Site 3 (Korotchkina and Patel 2001).

Different mitochondrial protein kinases comprising PDKs and some related BCKs do not carry the motif, which are normally present in eukaryotic Ser/Thr/Tyr protein kinases. The rat PDK2 structure revealed that these proteins have two distinct domains; the C-terminal domain is an α/β structure with a five strand β sheet. These enzymes also have four conserved motifs (N-G1-,G2-, and G3-boxes), which build a unique ATP-binding fold. The ATP-binding fold has a structure known as the "ATP lid". The conformational changes in ATP-lid are linked with the ATP hydrolysis and protein-protein interaction. (Wigley et al. 1991; Ban et al. 1999) The N-terminal domain of these kinases consists of a four-helix bundle that resembles the histidine phosphoryl-transfer domains of the two component systems (Davie et al. 1995). The binding of the PDKs to the L2 domain of the E2p subunit of the PDC activates PDK activity, but this activation of different PDK isoforms occurs in a different fashion (Kato et al. 2005). Crystal structures of the PDK3-L2 complex with or without (apo) bound nucleotides (ATP or ADP) indicated that the C-terminal domain of PDK3 binds ATP or ADP through conserved motifs. The

ATP binding site is present on the sidewall of the C-terminal domain facing the cleft between the N and C terminal domains (Dutta and Inouye 2000) (Figure 1.6). The ϒ-phosphate of the bound ATP in the cleft is accessible to the E1p subunit for its serine residue phosphorylation and eventually inactivation. The PDK3-L2 structure showed that there is no direct interaction between the bound L2 and the active-site cleft so L2 exerts its effect on PDK3 through an allosteric mechanism (Kato et al. 2005).

The crystal structure of PDK3 with and without L2 binding showed that in the closed conformation, the C-terminal tails in the PDK3 dimer are disordered and keeps the ATP lid in the active-site cleft in a partially ordered form, which traps ADP with high affinity and renders PDK3 inactive. In the L2-binding-induced open conformation, both C- terminal tails are ordered and exist in a crossover configuration. The crossover configuration induces the opening of the active-site cleft with a disordered ATP lid. The disordered ATP lid has a low affinity for the ADP binding, which leads to the release of ADP and results in the removal of PDK3 inhibition caused by bound ADP, resulting in the L2-stimulated PDK3 activity (Kato et al. 2005). (Figure 1.7).

These structural studies demonstrated that PDKs are regulated by the classic allosteric mechanism of R(relaxed) to T(tight) equilibrium between the L2-bound and free PDK3, with the L2 bound form facilitating the R or open conformation (Kato et al. 2005).

DCA Induces Allosteric Conformational Changes in PDK and Modulates PDC Activity

Recent mutational studies and the PDK2 structure with dichloroacetic acid (DCA) revealed that DCA binds to the N-terminal domain of PDK2. The E2P/E3BP scaffold-free activity showed that DCA reduces PDK1 and PDK3 activity in a similar fashion to 4% and 17%, respectively (Kato et al. 2007). L2 binding promotes the opening of the active-site cleft and destabilizes the ATP lid facilitating ADP dissociation in the PDK3-L2 complex, which renders PDK active (Kato et al. 2005). Kinetic studies showed that exposure to DCA prevents the ADP dissociation from the active-site cleft resulting in PDK inhibition. ADP binding to PDK reduces the affinity of this enzyme for L2 binding by 3-fold; the presence of DCA and ADP synergistically decreases the affinity of the PDK for L2 by 130-fold as compared to ADP alone and eventually affects the L2-induced activation of the PDK. The inhibition of the PDK by DCA

induced allosteric change keeps the PDC in its active state and accelerates the tricarboxylic acid (TCA) cycle (Kato et al. 2007).

DCA is Used to Activate PDC in Different Disease States

Bonnet et al showed that DCA induces apoptosis in the tumor cells by reversing the Warburg effect (Bonnet et al. 2007). They found that DCA activates PDC by inhibiting PDK and shifts the glycolytic-based metabolism to mitochondria in the tumor cells. The results demonstrated that DCA decreased the mitochondrial membrane potential ($\Delta\Psi m$) by activating TCA cycle, generating more protons by mitochondria, and by decreasing cytosolic Ca^{++} concentration. The decrease in $\Delta\Psi m$ also induced mitochondrial transition pore (MTP) opening. The opening of MTP activated the release of cytochrome-C, which is required for the caspase activation and apoptosis induction. DCA induced activation of mitochondrial metabolism and it activates complex-I induced ROS generation. The complex-I induced ROS generation upregulated the K^+ channel Kv1.5 expression and decreased K^+ concentration, which also helped in the activation of apoptosis in the tumor cells (Bonnet et al. 2007). DCA was also used to lower the plasma lactate, alanine, cholesterol, and glucose levels in adult, noninsulin-dependent diabetic patients (Stacpoole et al. 1978). Studies showed that DCA also reduced lactic acidosis in patients with pyruvate dehydrogenase deficiency (Stacpoole et al. 2006). DCA showed oncolysis in attenuated oncolytic measles virus Edmonston strain (MV-Edm) caused glioblastoma cells by inhibiting aerobic glycolysis. It was found that DCA enhanced the MV-Edm replication (increasing bioenergetic consumption) and inhibited glycolysis (decreasing bioenrgetic production), which, in combination, accelerated bioenergetic exhaustion leading to necrotic cell death (Li et al. 2015).

Rationale for Research

Water disinfection greatly reduces exposure to water-borne pathogens but exposure to the inadvertently produced toxic DBPs is unavoidable (Akin et al. 1982; Krasner 2009). Different epidemiological and experimental studies concluded that disinfecting water increases the risk of bladder cancer (Villanueva et al. 2007), colorectal cancer (King et al. 2000; Bove et al. 2002) and adverse pregnancy outcomes (Chisholm et al. 2008; Jeong et al. 2012; Rivera-Núñez and Wright 2013). Some of the HAAs e.g., IAA the mode of action for toxicity induction is based on oxidative DNA damage and GAPDH inhibition. However, the difference among the toxicity

mechanisms of the different classes of HAAs present in the disinfected water and their link to the adverse health outcomes is unknown. In order to fill this gap additional research is required.

The monoHAAs inhibit GAPDH and induce toxicity; it is important to find out if there is a link between the GAPDH inhibition HAA-induced genotoxicity. The difference among the mono-, di-, and triHAA toxicity mechanisms are also unknown. In this dissertation a link between the HAA-induced GAPDH inhibition and genotoxicity is discussed. Furthermore, the difference between the toxicity mechanisms of the mono-, di-, and triHAAs are explored.

My working hypothesis is that the monoHAAs inhibit GAPDH depleting glycolytic ATP and reducing the generation of pyruvate used as a mitochondrial substrate during tricarboxylic acid (TCA) cycle for the further production of ATP. The unavailability of pyruvate for the TCA cycle disturbs the normal generation of reducing power (NADH and $FADH_2$). Reducing power produced by the TCA cycle is required for oxidative phosphorylation for the complete reduction of O_2 to water. During O_2 reduction through oxidative phosphorylation, electromotive force is generated, which is utilized by ATP synthase to produce ATP. Glycolytic and mitochondrial ATP is required to maintain cellular Ca^{2+} homeostasis. Since the monoHAAs inhibit GAPDH and reduce the generation of pyruvate they disturb the normal production of reducing power through the TCA cycle. Due to the unavailability of reducing power O_2 is not completely reduced to H_2O and incomplete O_2 reduction generates superoxide radicles (O_2^-) or hydroxyl radicles ($^{\bullet}\dot{O}H$), also known as reactive oxygen species (ROS). The unavailability of reducing power not only produces ROS but also disrupts the mitochondrial membrane potential and electromotive force generated during oxidative phosphorylation and ultimately affects ATP synthesis and disturbs cellular Ca^{2+} homeostasis. Increased ROS and ATP depletion due to monoHAA-induced GAPDH inhibition leads to genomic DNA damage (Figure 1.8. A). If this hypothesis is correct, then supplementing monoHAA-treated cells with exogenous pyruvate should restore cellular ATP levels and prevent or reduce genomic DNA damage. (Figure 1.8. B)

Unlike the monoHAAs the di-, and triHAAs are not the good inhibitors of the GAPDH. Considering the toxicity mechanism of di-, and triHAAs, I postulate that increased activation of PDH activity by diHAAs and triHAAs due to PDK inhibition accelerates pyruvate transport in mitochondria, which is coupled with Ca^{2+} influx and enhance the oxidative decarboxylation of pyruvate into acetyl CoA, which in turn will produce more reducing power in the form of

NADH. The NADH will be further utilized by oxidative phosphorylation to produce more ATP. The accelerated TCA cycle due to PDH activation and enhanced NADH formation will consumes more O_2 as a final electron acceptor, which might lead to hypoxia and eventually ROS production. In order to keep providing the pyruvate supply required by di-, and triHAAs induced activated PDH, the cells will consume more glucose and will accelerate the release of pyruvate, lactate and alanine from cells (Evans and Stacpoole 1982), which in turn will disturb the glucose homeostasis and may lead to toxicity. The chronic exposure to diHAAs and triHAAs through drinking water may be involved with hypolactatemia, disturbed glucose homeostasis and hepatotoxicity in humans especially sensitive populations (featuses). (Figure 1.9)

To test the mentioned hypothesis illustrated in (figure 1.8, 1.9) I propose the following objectives.

Objectives

1. To study the effect of HAAs on GAPDH inhibition kinetics. (Chapter 3)
2. To investigate the effect of HAAs on cellular energy homeostasis by measuring the ATP content in HAA-treated cells. (Chapter 3)
3. To study the relationship of HAA-induced GAPDH inhibition and genomic DNA damage in HAA-treated cells by supplementing cells with exogenous pyruvate. (Chapter 2)
4. To study the relationship of HAA-induced GAPDH inhibition with the ATP content of the cells by supplementing cells with the exogenous pyruvate. (Chapter 2)
5. To investigate the difference among mono-, di- and triHAA toxicity mechanisms by measuring PDH activity in HAA-treated cells. (Chapter 3)
6. To study the oxidative stress in HAA-treated cells. (Chapter 2)

1.3. TOXICITY OF DBPS GENERATED AFTER CHLORINATION OF WASTE WATER EFFLUENTS

Domestic wastewaters have several health safety concerns. Pathogenic microorganisms present in wastewater include enteric bacteria, viruses, and protozoan cysts. In order to provide protection against these pathogens, wastewater is treated with different chemical disinfectants. The target disinfectant is usually chlorine and is the most commonly used chemical disinfectant in both Kingdom of Saudi Arabia (KSA) and USA. In this study, the target waters are

wastewater effluents containing ammonia and nitrogenous organic matter. Ammonia and organic nitrogen presence in excess with respect to the chlorine dose result in a very fast conversion of the free chlorine into monochloramine and organic chloramines. Chloramines then react with both inorganic and organic constituents in water forming a large number of disinfection byproducts (DBPs). Relevant reactions to this study involving inorganic species are the oxidation of iodide ion (I^-) by monochloramine (NH_2Cl) to form hypoiodous acid (HOI) (Bichsel and von Gunten 1999). In this study, the cytotoxicity and genotoxicity potentials of the chlorinated and chloraminated wastewater effluents extracts, extracted through XAD-8 and XAD-4 were analyzed.

Objectives

The objectives of this part of my research include the following;

1. To determine the cytotoxicity and genotoxicity potential of the chlorinated wastewater effluents extracted through XAD-8 and XAD-4 resin. (Chapter 4)

2. To analyze the cytotoxicity and genotoxicity potential of the chloraminated wastewater effluents extracted through XAD-8 and XAD-4 resin. (Chapter 4)

1.4. TOXICITY OF POLYCYCLIC AROMATIC HYDROCARBONS ASSOCIATED WITH COAL TAR PARTICLES IN URBAN LAKES

Particle-associated contaminants (PACs) are hazardous to flora and fauna in the aquatic systems and also to humans because most of the PACs are highly stable, bioaccumulative and toxic. Studies demonstrated that most of the PACs are persistent in nature and continue to occur in the environment years after their use was abandoned (Mahler and Van Metre 2003). Results from water quality surveys (Van Metre and Mahler 2005; Chalmers et al. 2007) showed that metal, polychlorinated biphenyls and DDT concentrations decreased in water since the 1970's after their regulation. However, total concentrations of polycyclic aromatic hydrocarbons (PAHs) have increased (Van Metre and Mahler 2005) with increasing urbanization.

PAHs are atmospheric pollutants found in soil, air and water, which have two or more single or fused aromatic rings sharing a carbon atoms pair between the rings in their molecules, e.g. benzo(α)pyrene. PAHs containing six fused aromatic rings are known as small PAHs while those with more than 6 are known as large aromatic hydrocarbons (Buha 2011). The major

sources of PAHs include the incomplete combustion of organic material such as cigarette smoke, vehicle exhausts, wildfires, agricultural burning and residential wood burning; other sources are asphalt roads, coal, coal tar, municipal and industrial waste incineration and hazardous waste sites (Mumtaz and Julia 1995). Sources of particle associated PAHs in urban lake sediments are automobile and industry emission-based combustion sources, coal-tar and asphalt based sealcoats on parking lots, driveway pavements, roofs and vulcanized rubber products such as automobile tires (Hoffman et al. 1984; Mahler et al. 2005). Particles worn from coal-tar pavements are transported into urban lakes and streams via runoff and can be a primary source of PAHs in these urban water bodies (Mahler et al. 2005; Yang et al. 2010).

Total PAH concentrations in coal-tar sealcoat particles are higher than other particles including particles from unsealed concrete, asphalt parking lots, road dust and residential soils. Moreover, coal tar seal coat contributes 84% of the total PAH in urban lakes (Yang et al. 2010). A study using contaminant mass-balance receptor modeling showed that coal tar sealcoat is the main source of PAHs over the past 20 years in 40 lakes located throughout the United States (Van Metre and Mahler 2010). PAHs are lipophilic in nature and are generally found adsorbed on particles surface in water and bioaccumulate in edible marine organisms. Background levels of PAHs in drinking water ranged from 4 to 24 ng per liter. The U.S. EPA selected 17 PAHs and profiled them in a single group based on their highest concentrations at national Priority List (NPL) sites, their level of harmful effects, exposure and the available information for these PAHs (Mumtaz and Julia 1995). These PAHs were genotoxic and carcinogenic (Farmer 2003) and induced lung cancer in workers exposed to coal tar pitch volatiles measured as benzene-soluble matter (Armstrong 1994). Several fractions of creosote P1 were found as mutagenic in *Salmonella typhimurium* strain TA98. The mutagenicity of creosote fractions was due to the presence of 0.18 and 1.1% of benzo(α)pyrene and benz(α)anthracene, respectively (Bos et al. 1984). The fate of PAHs from coal tar sealcoat in aquatic systems is not well understood. It is not clear if PAHs redistribute in water and lose their toxic potential or if they are lost to the water column with ageing. A mechanistic and quantitative approach is needed to understand the distribution of PAHs in water and the changes in the toxic potential of PAHs associated with its distribution in aquatic systems.

Hypothesis

In order to determine the best management practices to alleviate the impact of coal tar seal coating and associated PAHs in sediments, it is important to study the fate and toxicity of PAHs in water. I shall determine the mutagenicity of the PAHs associated with coal tar and other carbonaceous material particles in urban lake sediments. We hypothesize that the toxicity of pore water in sediments decreases with time as PAHs and other organic pollutants redistribute from less strongly sorbing carbonatious materials like coal tar to more strongly sorbing black carbon, and as less recalcitrant pollutants are biologically degraded over time. Urban lakes are sources of recreation and/or drinking water for large populations, and understanding contribution of coal tar toxicity is an important step in protecting the environment and public health.

Objectives

The objectives of this project are listed below.

1. To compare the toxicity of PAHs associated with the less strongly sorbing carbonatious material like coal tar and more strongly sorbing carbonatious material like soot. (Chapter 5)
2. To analyze these PACs linked PAHs for mutagenicity using the plate incorporation assay with *S. typhimurium* cells strains TA100 and TA98 and determine the induction of base-pair substitution mutation versus frameshift mutations. (Chapter 5)

1.5. FIGURES AND TABLES

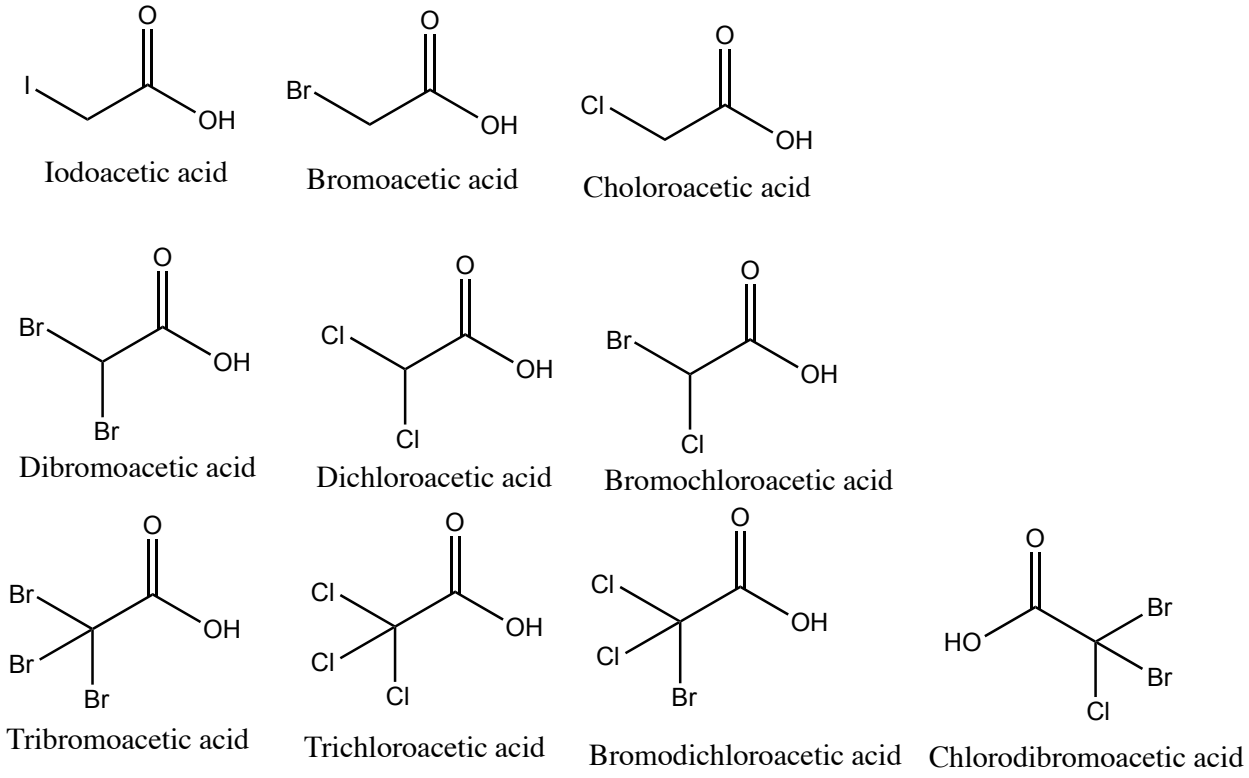

Figure 1.1. Different regulated and nonregulated mono-, di-, and triHAAs

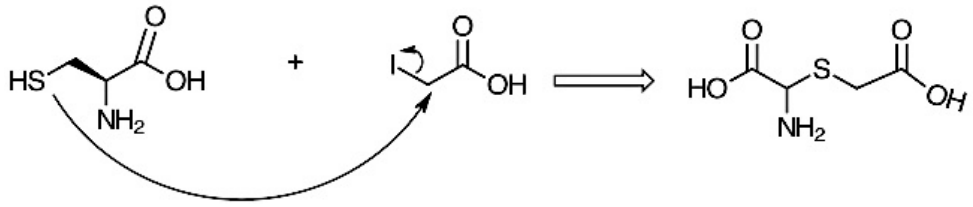

Figure 1.2. S_N2 reaction between cysteine and iodoacetic acid. SH group of cysteine acts as a nucleophile and attacks "C " of the halogen-leaving group.

Table 1.1. Monohaloacetic acid characteristics, sources and purities.							
HAA [a]	CASN	MW (g/mol)	C−X [b]	Bond Length (Å) [c]	Dissociation Energy (kcal/mol) [d]	Source	Purity
IAA	64-69-7	185.95	C−I	2.14	57.4	Sigma-Aldrich	>99%
BAA	79-08-3	138.95	C−Br	1.93	65.9	Fluka	>99%
CAA	79-11-8	94.50	C−Cl	1.77	78.5	Fluka	>99%

[a] Abbreviations: HAA, haloacetic acids. IAA, iodoacetic acid; BAA, bromoacetic acid; CAA, chloroacetic acid. [b] α-Carbon-halogen bond. [c] C−X bond length summarized from (Loudon 1995). [d] C−X bond dissociation energy summarized from (Loudon 1995).

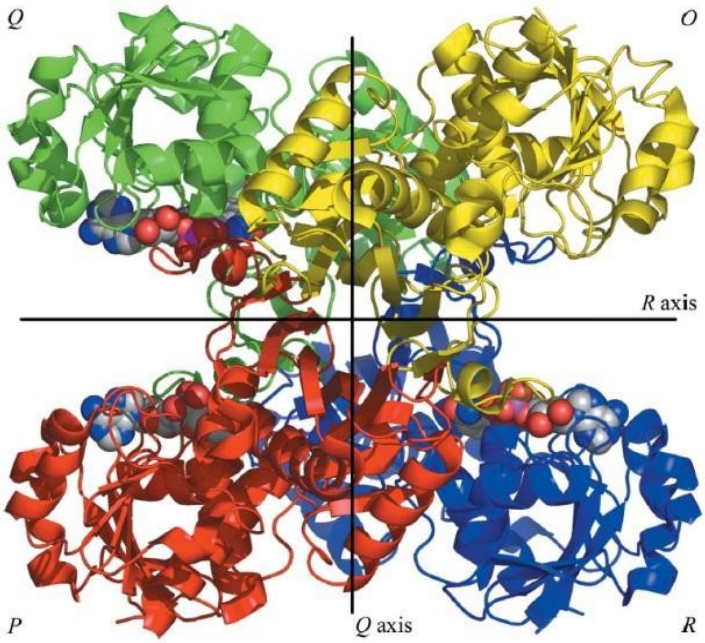

Figure 1.3. Ribbon view of the human placental GAPDH, subunits O, P, Q, and R. GAPDH active-sites clefts are indicated by arrows on each of the asymmetric subunits, P, Q, and R (Jenkins and Tanner 2006)

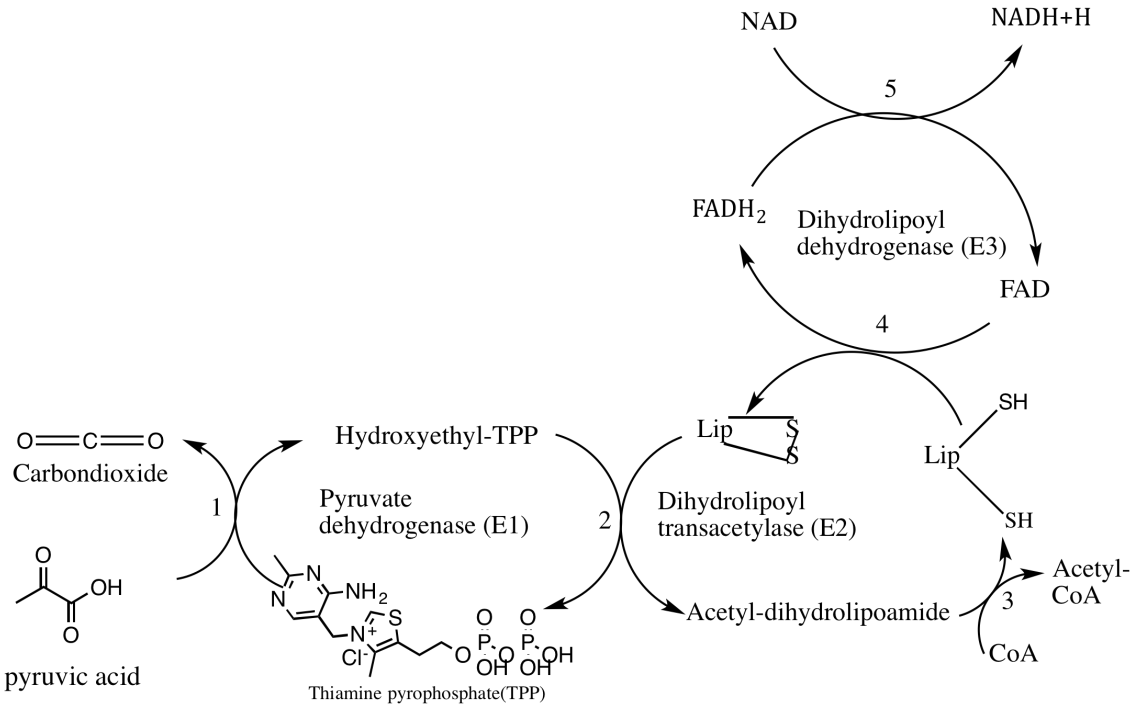

Figure 1.4. Different components of the pyruvate dehydrogenase complex activity

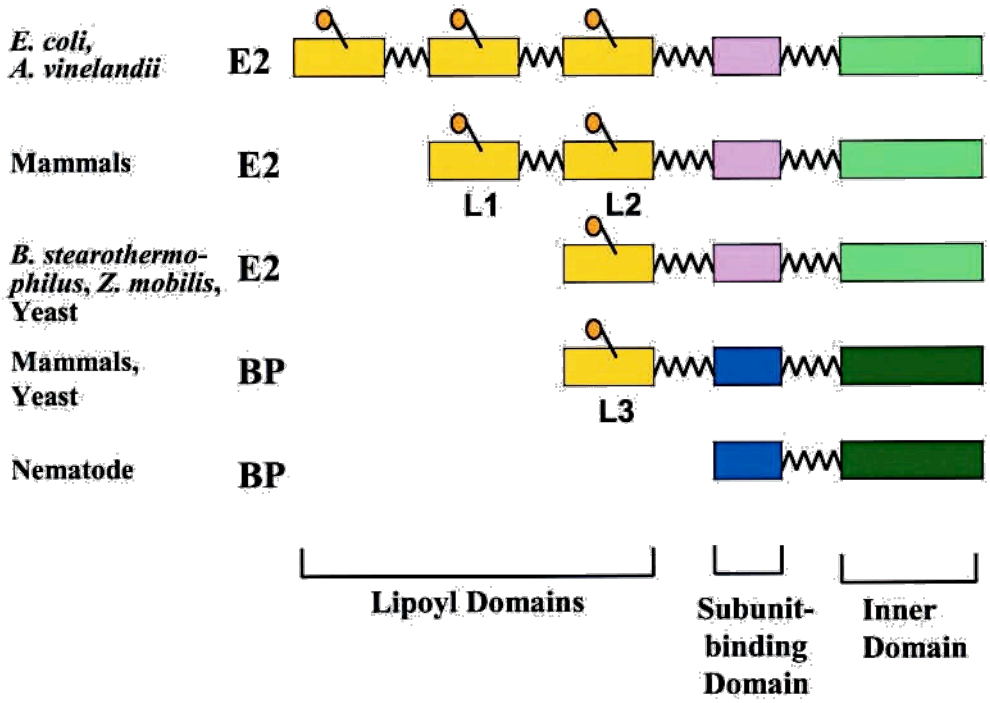

Figure 1.5. The structural domains of E2 and binding protein of pyruvate dehydrogenase complex (Patel and Korotchkina 2003)

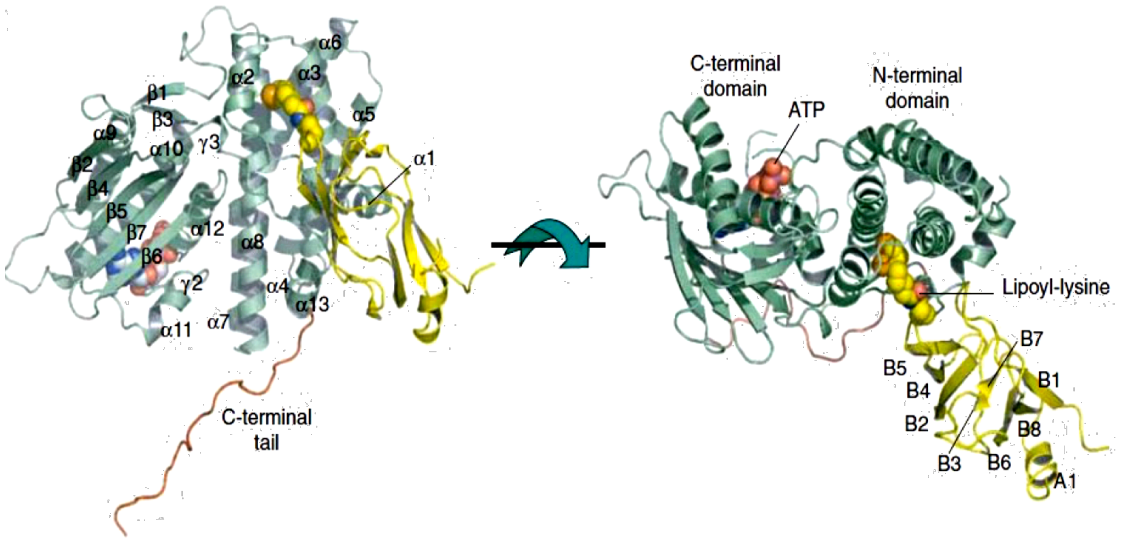

Figure 1.6. The position of ATP binding site between the N and C-terminal domain of PDK3 (Kato et al. 2005)

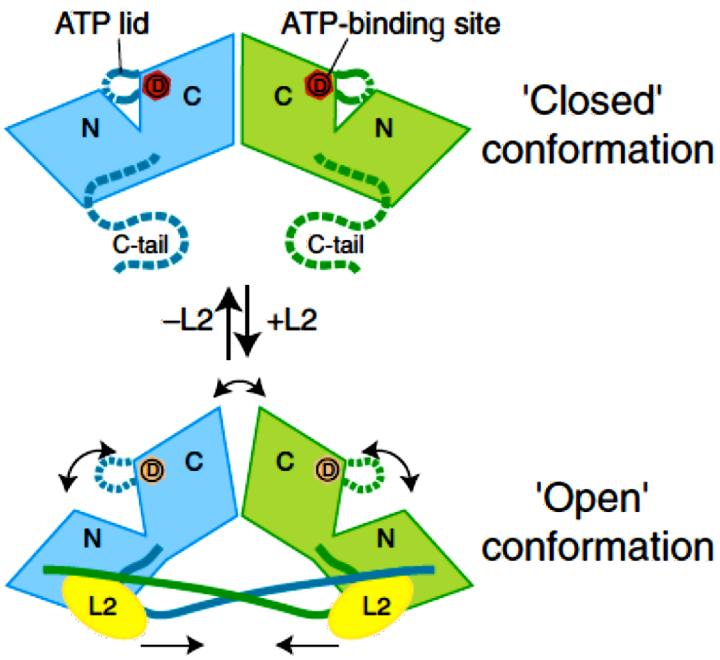

Figure 1.7. Closed and open confirmation of ATP lid of PDK3 in response to L2 and ADP binding (Kato et al. 2005)

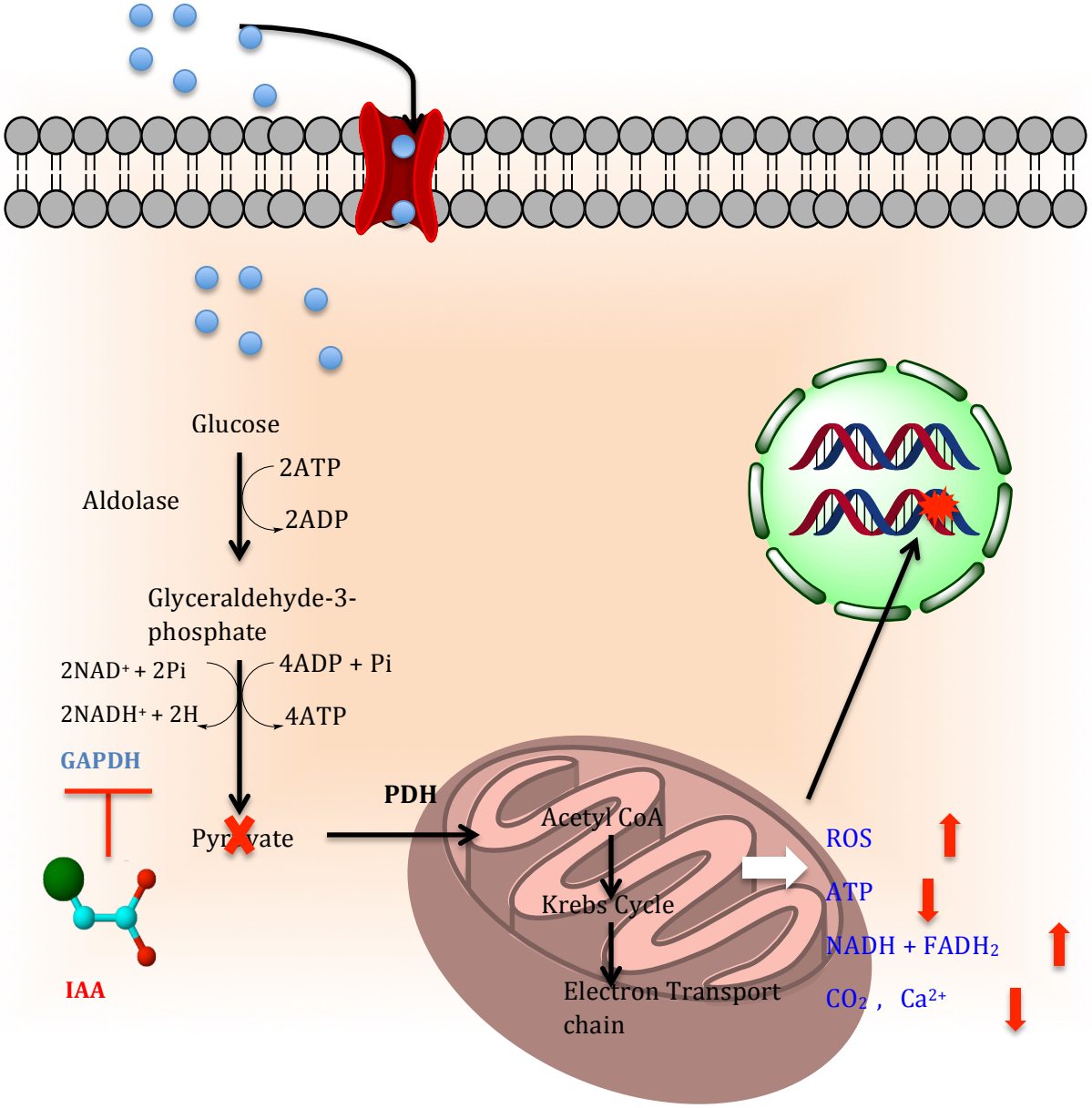

Figure 1.8. (A) Effect of IAA on the ATP contents and genome integrity of the cell in response to GAPDH inhibition.

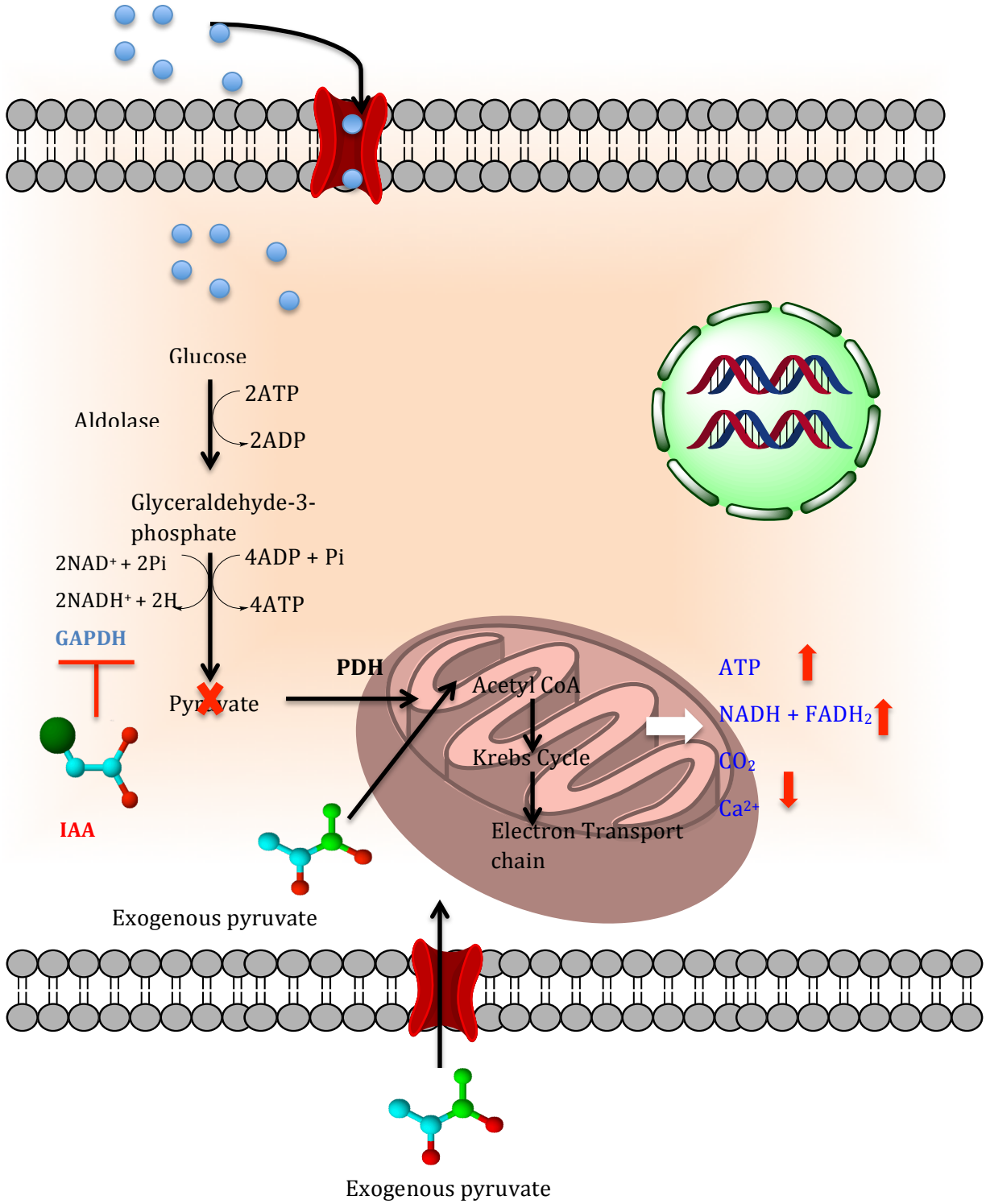

Figure 1.8 (B)**.** The effect of exogenous pyruvate on the oxidative DNA damage and reduction in the ATP contents of the cells induced by IAA mediated GAPDH inhibition.

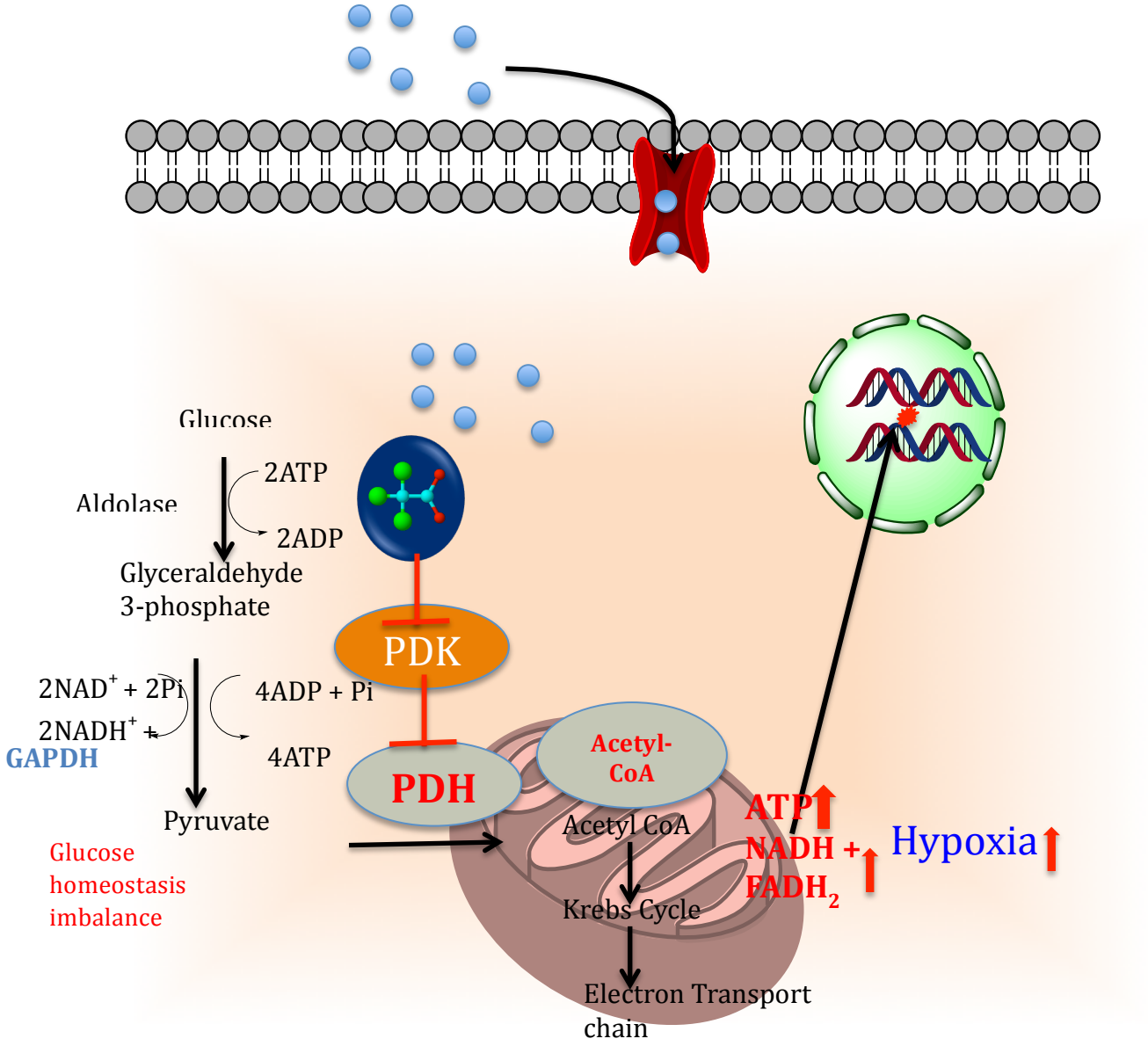

Figure 1.9. Effect of a triHAA on pyruvate dehydrogenase kinase (PDK) controlled pyruvate dehydrogenase complex (PDC) activity and its ultimate effect on mitochondrial metabolism.

1.6. REFERENCES

Akin EW, Hoff JC, Lippy EC. 1982. Waterborne outbreak control: which disinfectant? Environmental Health Perspectives Vol. 46:7-12.

Albrecht J, Talbot M, Kimelberg HK, Aschner M. 1993. The role of sulfhydryl groups and calcium in the mercuric chloride-induced inhibition of glutamate uptake in rat primary astrocyte cultures. Brain Research 607(1–2):249-254.

American Chemistry Council. 2015. Chlorine Chemistry: Essential to Safer Water for 100 Years, and Running. http://chlorine.americanchemistry.com/Safer-Water.

Armstrong B. 1994. Lung cancer mortality and polynuclear aromatic hydrocarbons: A case-cohort study of aluminum production workers in Arvida, Quebec, Canada. Am J Epidemiol 139(3):250-262.

Ban C, Junop M, Yang W. 1999. Transformation of MutL by ATP binding and hydrolysis: a switch in DNA mismatch repair. Cell 97(1):85-97.

Bellar TA, Lichtenberg JJ, Kroner RC. 1974. Occurence of organohalides in chlorinated drinking waters Journal American Water Works Association 66(12):703-706.

Bichsel Y, von Gunten U. 1999. Oxidation of iodide and hypoiodous acid in the disinfection of natural waters. Environmental Science & Technology 33(22):4040.

Bonnet S, Archer SL, Allalunis-Turner J, Haromy A, Beaulieu C, Thompson R, Lee CT, Lopaschuk GD, Puttagunta L, Bonnet S, Harry G, Hashimoto K, Porter CJ, Andrade MA, Thebaud B, Michelakis ED. 2007. A mitochondria-K+ channel axis is suppressed in cancer and its normalization promotes apoptosis and inhibits cancer growth. Cancer Cell 11(1):37-51.

Bos RP, Theuws JLG, Leijdekkers CM, Henderson PT. 1984. The presence of the mutagenic polycyclic aromatic hydrocarbons benzo(a)pyrene and benz(a)anthracine in creosote-P1 Mutat Res 130(3):153-158.

Bove F, Shim Y, Zeitz P. 2002. Drinking Water Contaminants and Adverse Pregnancy Outcomes: A Review. Environ Health Perspect 110 Suppl 1:61.

Buha A. 2011. Polycyclic Aromatic Hydrocarbons.

Bull RJ, Reckhow DA, Li X, Humpage AR, Joll C, Hrudey SE. 2011. Potential carcinogenic hazards of non-regulated disinfection by-products: Haloquinones, halo-cyclopentene and cyclohexene derivatives, N-halamines, halonitriles, and heterocyclic amines. Toxicology 286(1–3):1-19.

Carlile GW, Chalmers-Redman RM, Tatton NA, Pong A, Borden KE, Tatton WG. 2000. Reduced apoptosis after nerve growth factor and serum withdrawal: conversion of tetrameric glyceraldehyde-3-phosphate dehydrogenase to a dimer. Mol Pharmacol 57(1):2-12.

Chalmers AT, Van Metre PC, Callender E. 2007. The chemical response of particle-associated contaminants in aquatic sediments to urbanization in New England, U.S.A. J Contam Hydrol 91(1-2):4-25.

Chen CH, Chen SJ, Su CC, Yen CC, Tseng TJ, Jinn TR, Tang FC, Chen KL, Su YC, Lee k I, Hung DZ, Huang CF. 2013. Chloroacetic acid induced neuronal cells death through oxidative stress-mediated p38-MAPK activation pathway regulated mitochondria-dependent apoptotic signals. Toxicology 303:72-82.

Chisholm K, Cook A, Bower C, Weinstein P. 2008. Risk of birth defects in Australian communities with high levels of brominated disinfection by-products. Environ Health Perspect 116(9):1267-1273.
Crittenden JC, Trussell RR, Hand DW, Howe KJ, Tchobanoglous G. 2012. Disinfection. MWH's Water Treatment: Principles and Design, Third Edition: John Wiley & Sons, Inc. p 903-1032.
Cutler D, Miller G. 2005. The role of public health improvements in health advances: The twentieth-century United States. Demography 42(1):1-22.
Dad A, Jeong CH, Pals JA, Wagner ED, Plewa MJ. 2013. Pyruvate Remediation of Cell Stress and Genotoxicity Induced by Haloacetic Acid Drinking Water Disinfection By-Products. Environmental and Molecular Mutagenesis 54(8):629-637.
David DM, Elsebeth L. 1999. Chloroform http://monographs.iarc.fr/ENG/Publications/techrep42/TR42-16.pdf.
Davie JR, Wynn RM, Meng M, Huang YS, Aalund G, Chuang DT, Lau KS. 1995. Expression and characterization of branched-chain alpha-ketoacid dehydrogenase kinase from the rat. Is it a histidine-protein kinase? J Biol Chem 270(34):19861-19867.
De Marcucci O, Lindsay JG. 1985. Component X. An immunologically distinct polypeptide associated with mammalian pyruvate dehydrogenase multi-enzyme complex. European Journal of Biochemistry 149(3):641-648.
DeAngelo AB, Daniel FB, Most BM, Olson GR. 1997. Failure of monochloroacetic acid and trichloroacetic acid administered in the drinking water to produce liver cancer in male F344/N rats. J Toxicol Environ Health 52(5):425-445.
Dutta R, Inouye M. 2000. GHKL, an emergent ATPase/kinase superfamily. Trends Biochem Sci 25(1):24-28.
Escobar-Hoyos LF, Hoyos-Giraldo LS, Londono-Velasco E, Reyes-Carvajal I, Saavedra-Trujillo D, Carvajal-Varona S, Sanchez-Gomez A, Wagner ED, Plewa MJ. 2013. Genotoxic and clastogenic effects of monohaloacetic acid drinking water disinfection by-products in primary human lymphocytes. Water Res 47(10):3282-3290.
European Comission 2003. European Comission Report: Scientific Committee on Toxicity, Ecotoxicity and the Environment (CSTEE); Opinion on the Results of the Risk Assessment of Monochloroacetic acid (MCCA) Environmental Part (Cas NO. 79-11-8)
Evans OB, Stacpoole PW. 1982. Prolonged hypolactatemia and increased total pyruvate dehydrogenase activity by dichloroacetate. Biochem Pharmacol 31(7):1295-1300.
Farmer PB. 2003. Molecular epidemiology studies of carcinogenic environmental pollutants - Effects of polycyclic aromatic hydrocarbons (PAHs) in environmental pollution on exogenous and oxidative DNA damage. Mutat Res 544(2-3):397-402.
Ferriero R, Iannuzzi C, Manco G, Brunetti-Pierri N. 2015. Differential inhibition of PDKs by phenylbutyrate and enhancement of pyruvate dehydrogenase complex activity by combination with dichloroacetate. J Inherit Metab Dis.
Frey PA, Flournoy DS, Gruys K, Yang YS. 1989. Intermediates in reductive transacetylation catalyzed by pyruvate dehydrogenase complex. Annals of the New York Academy of Sciences 573:21-35.
Gali RR, Board PG. 1997. Identification of an essential cysteine residue in human glutathione synthase. Biochem J 321 (Pt 1):207-210.
George SE, Nelson GM, Swank AE, Brooks LR, Bailey K, George M, DeAngelo A. 2000. The disinfection by-products dichloro-, dibromo-, and bromochloroacetic acid impact

intestinal microflora and metabolism in Fischer 344 rats upon exposure in drinking water. Toxicol Sci 56(2):282-289.
Health Canada. 2008. Guidelines for Canadian Drinking Water Quality: Guideline Technical Document — Haloacetic Acids.
Hernández-Fonseca K, Cárdenas-Rodríguez N, Pedraza-Chaverri J, Massieu L. 2008. Calcium-dependent production of reactive oxygen species is involved in neuronal damage induced during glycolysis inhibition in cultured hippocampal neurons. J Neurosci Res 86(8):1768-1780.
Herren-Freund SL, Pereira MA, Khoury MD, Olson G. 1987. The carcinogenicity of trichloroethylene and its metabolites, trichloroacetic acid and dichloroacetic acid, in mouse liver. Toxicol Appl Pharmacol 90(2):183-189.
Hoffman EJ, Mills GL, Latimer JS, Quinn JG. 1984. Urban runoff as a source of polycyclic aromatic-hydrocarbons to coastal waters Environ Sci Technol 18(8):580-587.
Hrudey SE. 2009. Chlorination disinfection by-products, public health risk tradeoffs and me. Water Research 43(8):2057-2092.
Hua G, Reckhow DA. 2007. Comparison of disinfection byproduct formation from chlorine and alternative disinfectants. Water Research 41(8):1667-1678.
Hunter ES, 3rd, Rogers EH, Schmid JE, Richard A. 1996. Comparative effects of haloacetic acids in whole embryo culture. Teratology 54(2):57-64.
Hunter Iii ES, Tugman JA. 1995. Inhibitors of glycolytic metabolism affect neurulation-staged mouse conceptuses in vitro. Teratology 52(6):317-323.
Jenkins JL, Tanner JJ. 2006. High-resolution structure of human D-glyceraldehyde-3-phosphate dehydrogenase. Acta Crystallogr D Biol Crystallogr 62(3):290-301.
Jeong CH, Wagner ED, Siebert VR, Anduri S, Richardson SD, Daiber EJ, McKague AB, Kogevinas M, Villanueva CM, Goslan EH, Wentai L, Isabelle LM, Pankow JF, Grazuleviciene R, Cordier S, Edwards SC, Righi E, Nieuwenhuijsen MJ, Plewa MJ. 2012. Occurrence and toxicity of disinfection byproducts in european drinking waters in relation with the HIWATE epidemiology study. Environ Sci Technol 46(21):12120-12128.
Jilka JM, Rahmatullah M, Kazemi M, Roche TE. 1986. Properties of a newly characterized protein of the bovine kidney pyruvate dehydrogenase complex. J Biol Chem 261(4):1858-1867.
Kahlert S, Reiser G. 2000. Requirement of glycolytic and mitochondrial energy supply for loading of Ca2+ stores and InsP(3)-mediated Ca2+ signaling in rat hippocampus astrocytes. J Neurosci Res 61(4):409-420.
Karagas MR, Villanueva CM, Nieuwenhuijsen M, Weisel CP, Cantor KP, Kogevinas M. 2008. Disinfection byproducts in drinking water and skin cancer? A hypothesis. Cancer Cause Control 19(5):547-548.
Kargalioglu Y, McMillan BJ, Minear RA, Plewa MJ. 2002. Analysis of the cytotoxicity and mutagenicity of drinking water disinfection by-products in Salmonella typhimurium. Teratogenesis Carcinogenesis and Mutagenesis 22(2):113-128.
Kato M, Chuang JL, Tso SC, Wynn RM, Chuang DT. 2005. Crystal structure of pyruvate dehydrogenase kinase 3 bound to lipoyl domain 2 of human pyruvate dehydrogenase complex. Embo j 24(10):1763-1774.

Kato M, Li J, Chuang JL, Chuang DT. 2007. Distinct structural mechanisms for inhibition of pyruvate dehydrogenase kinase isoforms by AZD7545, dichloroacetate, and radicicol. Structure 15(8):992-1004.
King WD, Marrett LD, Woolcott CG. 2000. Case-control study of colon and rectal cancers and chlorination by-products in treated water. Cancer Epidemiol Biomarkers Prev 9(8):813-818.
Kline JA, Maiorano PC, Schroeder JD, Grattan RM, Vary TC, Watts JA. 1997. Activation of pyruvate dehydrogenase improves heart function and metabolism after hemorrhagic shock. J Mol Cell Cardiol 29(9):2465-2474.
Koch R. 1881. Über Desinfektion. Mitt kaiserl Gesundheitsamte 1:234–282.
Korotchkina LG, Patel MS. 1995. Mutagenesis studies of the phosphorylation sites of recombinant human pyruvate dehydrogenase. Site-specific regulation. J Biol Chem 270(24):14297-14304.
Korotchkina LG, Patel MS. 2001. Site specificity of four pyruvate dehydrogenase kinase isoenzymes toward the three phosphorylation sites of human pyruvate dehydrogenase. J Biol Chem 276(40):37223-37229.
Krasner SW. 2009. The formation and control of emerging disinfection by-products of health concern. Philos Trans A Math Phys Eng Sci 367(1904):4077-4095.
Krasner SW, McGuire MJ, Jacangelo JG, Patania NL, Reagan KM, Marco Aieta E. 1989. Occurrence of disinfection by-products in US drinking water. Journal / American Water Works Association 81(8):41-53.
Krasner SW, Weinberg HS, Richardson SD, Pastor SJ, Chinn R, Sclimenti MJ, Onstad GD, Thruston Jr AD. 2006. Occurrence of a new generation of disinfection byproducts. Environ Sci Technol 40(23):7175-7185.
Li C, Meng G, Su L, Chen A, Xia M, Xu C, Yu D, Jiang A, Wei J. 2015. Dichloroacetate blocks aerobic glycolytic adaptation to attenuated measles virus and promotes viral replication leading to enhanced oncolysis in glioblastoma. Oncotarget 6(3):1544-1555.
Liviac D, Creus A, Marcos R. 2010. Genotoxicity testing of three monohaloacetic acids in TK6 cells using the cytokinesis-block micronucleus assay. Mutagenesis 25(5):505-509.
Loudon GM. 1995. Organic Chemistry 3rd ed. Redwood, CA: Benjamin/Cummings Publ. Co.
Mahler BJ, Van Metre PC. 2003. A simplified approach for monitoring hydrophobic organic contaminants associated with suspended sediment: Methodology and applications. Arch Environ Contam Toxicol 44(3):288-297.
Mahler BJ, van Metre PC, Bashara TJ, Wilson JT, Johns DA. 2005. Parking Lot Sealcoat: An Unrecognized Source of Urban Polycyclic Aromatic Hydrocarbons. Environ Sci Technol 39(15):5560-5566.
Malliarou E, Collins C, Graham N, Nieuwenhuijsen MJ. 2005. Haloacetic acids in drinking water in the United Kingdom. Water Research 39(12):2722-2730.
Melnick RL, Nyska A, Foster PM, Roycroft JH, Kissling GE. 2007. Toxicity and carcinogenicity of the water disinfection byproduct, dibromoacetic acid, in rats and mice. Toxicology 230(2/3):126-136.
Mumtaz M, Julia G. 1995. Toxicologial profile for polycyclic aromatic hydrocarbons Toxic substances portal-polycyclic aromatic hydrocarbons (PAHs).
Narotsky MG, Best DS, McDonald A, Godin EA, Hunter ES, 3rd, Simmons JE. 2011. Pregnancy loss and eye malformations in offspring of F344 rats following gestational exposure to mixtures of regulated trihalomethanes and haloacetic acids. Reprod Toxicol 31(1):59-65.

Narotsky MG, Klinefelter GR, Goldman JM, DeAngelo AB, Best DS, McDonald A, Strader LF, Murr AS, Suarez JD, George MH, Hunter ES, 3rd, Simmons JE. 2015. Reproductive Toxicity of a Mixture of Regulated Drinking-Water Disinfection By-Products in a Multigenerational Rat Bioassay. Environ Health Perspect.

National Toxicology P. 2007. NTP report on the toxicology studies of dichloroacetic acid (CAS No. 79-43-6) in genetically modified (FVB Tg.AC hemizygous) mice (dermal and drinking water studies) and carcinogenicity studies of dichloroacetic acid in genetically modified [B6.129-Trp53(tm1Brd) (N5) haploinsufficient] mice (drinking water studies). Natl Toxicol Program Genet Modif Model Rep(11):1-168.

National Toxicology Program. 2007. NTP report on the toxicology studies of dichloroacetic acid (CAS No. 79-43-6) in genetically modified (FVB Tg.AC hemizygous) mice (dermal and drinking water studies) and carcinogenicity studies of dichloroacetic acid in genetically modified [B6.129-Trp53(tm1Brd) (N5) haploinsufficient] mice (drinking water studies). Natl Toxicol Program Genet Modif Model Rep(11):1-168.

Nelson GM, Swank AE, Brooks LR, Bailey KC, George SE. 2001. Metabolism, microflora effects, and genotoxicity in haloacetic acid-treated cultures of rat cecal microbiota. Toxicol Sci 60(2):232-241.

Ngwenya N, Ncube EJ, Parsons J. 2013. Recent advances in drinking water disinfection: successes and challenges. Rev Environ Contam Toxicol 222:111-170.

Pals JA, Ang JK, Wagner ED, Plewa MJ. 2011. Biological mechanism for the toxicity of haloacetic acid drinking water disinfection byproducts. Environ SciTechnol 45(13):5791-5797.

Pan S, An W, Li H, Su M, Zhang J, Yang M. 2014. Cancer risk assessment on trihalomethanes and haloacetic acids in drinking water of China using disability-adjusted life years. J Hazard Mater 280:288-294.

Patel MS, Korotchkina LG. 2003. The biochemistry of the pyruvate dehydrogenase complex*. Biochemistry and Molecular Biology Education 31(1):5-15.

Patel MS, Roche TE. 1990. Molecular biology and biochemistry of pyruvate dehydrogenase complexes. FASEB J 4(14):3224-3233.

Perham RN, Packman LC. 1989. 2-Oxo acid dehydrogenase multienzyme complexes: domains, dynamics, and design. Ann N Y Acad Sci 573:1-20.

Plewa MJ, Cemeli E, Anderson D, Wagner ED. 2004a. The genotoxicity of the drinking water disinfection by-product iodoacetic acid is reduced by modulators of oxidative stress. Environmental and Molecular Mutagenesis 44(3):220-220.

Plewa MJ, Kargalioglu Y, Vankerk D, Minear RA, Wagner ED. 2002. Mammalian cell cytotoxicity and genotoxicity analysis of drinking water disinfection by-products. Environmental and Molecular Mutagenesis 40(2):134-142.

Plewa MJ, Simmons JE, Richardson SD, Wagner ED. 2010. Mammalian Cell Cytotoxicity and Genotoxicity of the Haloacetic Acids, A Major Class of Drinking Water Disinfection By-Products. Environmental and Molecular Mutagenesis 51(8-9):871-878.

Plewa MJ, Wagner ED. 2015. Charting a New Path to Resolve the Adverse Health Effects of DBPs. In Occuarance , Formation, Health Effects and Control of Disinfection By-Products Am Chem Soc In Press.

Plewa MJ, Wagner ED, Richardson SD, Thruston Jr AD, Woo YT, McKague AB. 2004b. Chemical and biological characterization of newly discovered iodoacid drinking water disinfection byproducts. Environ Sci Technol 38(18):4713-4722.

Pourmoghaddas H, Stevens AA. 1995. Relationship between trihalomethanes and haloacetic acids with total organic halogen during chlorination. Water Research 29(9):2059-2062.
Rahman MB, Cowie C, Driscoll T, Summerhayes RJ, Armstrong BK, Clements MS. 2014. Colon and rectal cancer incidence and water trihalomethane concentrations in New South Wales, Australia. BMC Cancer 14(1).
Richardson SD, Crumley FG, Plewa MJ, Wagner ED, Mize T, Ange P, Orlando R, Williamson L, Bartlett MG. 2007a. Chlorinated vs. chloraminated drinking water: Toxicity-based identification of disinfection by-products using ESI-MS and ESI-MS/MS. Abstracts of Papers of the American Chemical Society 233:572-572.
Richardson SD, Plewa MJ, Wagner ED, Schoeny R, DeMarini DM. 2007b. Occurrence, genotoxicity, and carcinogenicity of regulated and emerging disinfection by-products in drinking water: A review and roadmap for research. Mutation Research-Reviews in Mutation Research 636(1-3):178-242.
Richardson SD, Postigo C. 2012. Drinking water disinfection by-products. . Berlin, Germany: Springer.
Rivera-Núñez Z, Wright JM. 2013. Association of Brominated Trihalomethane and Haloacetic Acid Exposure with Fetal Growth and Preterm Delivery in Massachusetts. Journal of Occupational and Environmental Medicine 55(10):1125-1134.
Rodríguez E, Rivera I, Astorga S, Mendoza E, García F, Hernández-Echeagaray E. 2010. Uncoupling oxidative/energy metabolism with low sub chronic doses of 3-nitropropionic acid or iodoacetate in vivo produces striatal cell damage. International Journal of Biological Sciences 6(3):199-212.
Rook JJ. 1974. Formation of haloforms during chlorination of natural waters. *Water Treat Examination* 23:234-243.
Sale GJ, Randle PJ. 1981. Analysis of site occupancies in [32P]phosphorylated pyruvate dehydrogenase complexes by aspartyl-prolyl cleavage of tryptic phosphopeptides. Eur J Biochem 120(3):535-540.
Schmidt MM, Dringen R. 2009. Differential effects of iodoacetamide and iodoacetate on glycolysis and glutathione metabolism of cultured astrocytes. Frontiers in neuroenergetics 1:1-1.
Sirover MA. 1999. New insights into an old protein: the functional diversity of mammalian glyceraldehyde-3-phosphate dehydrogenase. Biochim Biophys Acta 13(2):159-184.
Stacpoole PW, Kerr DS, Barnes C, Bunch ST, Carney PR, Fennell EM, Felitsyn NM, Gilmore RL, Greer M, Henderson GN, Hutson AD, Neiberger RE, O'Brien RG, Perkins LA, Quisling RG, Shroads AL, Shuster JJ, Silverstein JH, Theriaque DW, Valenstein E. 2006. Controlled clinical trial of dichloroacetate for treatment of congenital lactic acidosis in children. Pediatrics 117(5):1519-1531.
Stacpoole PW, Moore GW, Kornhauser DM. 1978. Metabolic effects of dichloroacetate in patients with diabetes mellitus and hyperlipoproteinemia. N Engl J Med 298(10):526-530.
Stephens PE, Darlison MG, Lewis HM, Guest JR. 1983. The pyruvate dehydrogenase complex of Escherichia coli K12. Nucleotide sequence encoding the dihydrolipoamide acetyltransferase component. Eur J Biochem 133(3):481-489.
Stuart WK. 2009. The formation and control of emerging disinfection by-products of health concern. Philosophical Transactions of the Royal Society a-Mathematical Physical and Engineering Sciences 367(1904):4077-4095.

Sutendra G, Michelakis ED. 2013. Pyruvate dehydrogenase kinase as a novel therapeutic target in oncology. Front Oncol 3:38.
Szalai G, Rajeshwari, Krishnamurthy, Hajnoczky G. 1999. Apoptosis driven by IP3-linked mitochondrial calcium signals. EMBO Journal 18(22):6349-6361.
Teixido E, Pique E, Gonzalez-Linares J, Llobet JM, Gomez-Catalan J. 2015. Developmental effects and genotoxicity of 10 water disinfection by-products in zebrafish. J Water Health 13(1):54-66.
Tennant RW, Stasiewicz S, Eastin WC, Mennear JH, Spalding JW. 2001. The Tg.AC (v-Ha-ras) transgenic mouse: nature of the model. Toxicol Pathol 29 Suppl:51-59.
Texter FL, Radford SE, Laue ED, Perham RN, Miles JS, Guest JR. 1988. Site-directed mutagenesis and 1H NMR spectroscopy of an interdomain segment in the pyruvate dehydrogenase multienzyme complex of Escherichia coli. Biochemistry 27(1):289-296.
U. S. Environmental Protection Agency. 1979. National interim primary drinking water regulations:Total trihalomethanes. Fed Regist 44(228):68624.
U. S. Environmental Protection Agency. 1998. National Primary Drinking Water Regulations: Disinfectants and Disinfection Byproducts. 69390-69476 p.
U. S. Environmental Protection Agency. 2001. Environmental Protection Agency report on the toxicological review of chloroform; (CAS No. 67-66-3)
U. S. Environmental Protection Agency. 2006. National primary drinking water regulations: Stage 2 disinfectants and disinfection byproducts rule. Fed Regist 71(2):387-493.
U.S. Environmental Protection Agency. 1998. Quantification of Cancer Risk from Exposure of Chlorinated Drinking Water Washington,DC: Office of Water, Office of Science and Technology, Health and Ecological Criteria Division.
Van Metre PC, Mahler BJ. 2005. Trends in hydrophobic organic contaminants in urban and reference lake sediments across the United States, 1970-2001. Environ Sci Technol 39(15):5567-5574.
Van Metre PC, Mahler BJ. 2010. Contribution of PAHs from coal-tar pavement sealcoat and other sources to 40 U.S. lakes. Sci Total Environ 409(2):334-344.
Villanueva CM, Cantor KP, Grimalt JO, Malats N, Silverman D, Tardon A, Garcia-Closas R, Serra C, Carrato A, Castaño-Vinyals G, Marcos R, Rothman N, Real FX, Dosemeci M, Kogevinas M. 2007. Bladder cancer and exposure to water disinfection by-products through ingestion, bathing, showering, and swimming in pools. Am J Epidemiol 165(2):148-156.
Villanueva CM, Castano-Vinyals G, Moreno V, Carrasco-Turigas G, Aragones N, Boldo E, Ardanaz E, Toledo E, Altzibar JM, Zaldua I, Azpiroz L, Goni F, Tardon A, Molina AJ, Martin V, Lopez-Rojo C, Jimenez-Moleon JJ, Capelo R, Gomez-Acebo I, Peiro R, Ripoll M, Gracia-Lavedan E, Nieuwenhujsen MJ, Rantakokko P, Goslan EH, Pollan M, Kogevinas M. 2012. Concentrations and correlations of disinfection by-products in municipal drinking water from an exposure assessment perspective. Environ Res 114:1-11.
Waller K, Swan SH, DeLorenze G, Hopkins B. 1998. Trihalomethanes in drinking water and spontaneous abortion. Epidemiology 9(2):134-140.
Wang D, Xu Z, Zhao Y, Yan X, Shi J. 2011. Change of genotoxicity for raw and finished water: Role of purification processes. Chemosphere 83(1):14-20.

Wei X, Chen X, Wang X, Zheng W, Zhang D, Tian D, Jiang S, Ong CN, He G, Qu W. 2013a. Occurrence of Regulated and Emerging Iodinated DBPs in the Shanghai Drinking Water. PLoS ONE 8(3).

Wei X, Wang S, Zheng W, Wang X, Liu X, Jiang S, Pi J, Zheng Y, He G, Qu W. 2013b. Drinking water disinfection byproduct iodoacetic acid induces tumorigenic transformation of NIH3T3 cells. Environmental Science & Technology 47(11):5913-5920.

Wei XW, S.; Zheng, W.; Wang, X.; Liu, X.; Jiang, S.; He, G.; Zheng, Y.; Qu, W., . 2013. Tumorigenicity of drinking water disinfection byproduct iodoacetic acid in NIH3T3 cells. Envion Sci Technol Submitted.

Whitehouse S, Cooper RH, Randle PJ. 1974. Mechanism of activation of pyruvate dehydrogenase by dichloroacetate and other halogenated carboxylic acids. Biochemical Journal 141(3):761-774.

WHO. 2000. Environmental Health Criteria. Disinfectants and disinfectant by-products. Environmental Health Criteria Disinfectants and disinfectant by-products 216:i-xxvii, 1-499.

Wigley DB, Davies GJ, Dodson EJ, Maxwell A, Dodson G. 1991. Crystal structure of an N-terminal fragment of the DNA gyrase B protein. Nature 351(6328):624-629.

World Health Organization. 2011. Guidlines for Drinking Water Quality United Nations: Geneva, Switzerland. 541 p.

Xu KY, Zweier JL, Becker LC. 1995. Functional coupling between glycolysis and sarcoplasmic reticulum Ca2+ transport. Circ Res 77(1):88-97.

Yang Y, Van Metre PC, Mahler BJ, Wilson JT, Ligouis B, Razzaque MD, Schaeffer DJ, Werth CJ. 2010. Influence of coal-tar sealcoat and other carbonaceous materials on polycyclic aromatic hydrocarbon loading in an urban watershed. Environ Sci Technol 44(4):1217-1223.

Zhang SH, Miao DY, Liu AL, Zhang L, Wei W, Xie H, Lu WQ. 2010. Assessment of the cytotoxicity and genotoxicity of haloacetic acids using microplate-based cytotoxicity test and CHO/HGPRT gene mutation assay. Mutat Res 703(2):174-179.

CHAPTER 2

INVESTIGATE THE MOLECULAR TARGET OF THE MONOHALOACETIC ACID WATER DISINFECTION BY-PRODCUTS AND ITS TOXICITY MECHANISM

Preface

This research was published in the journal of Environmental and Molecular Mutagenesis: Dad, A.; Jeong, C. H.; Pals, J. A.; Wagner, E. D.; Plewa, M. J., Pyruvate remediation of cell stress and genotoxicity induced by haloacetic acid drinking water disinfection by-products. Environ. Mol. Mutagen. 2013, 54, (8), 629-637. With permission from Wiley and Sons. A. Dad is the first author of the paper.

2.1. INTRODUCTION

A preeminent public health accomplishment achieved during the last century was the disinfection of drinking water. Water treatment and distribution of disinfected water was an effective strategy in controlling waterborne diseases such as cholera, typhoid and dysentery (Cutler and Miller 2005). However, disinfection byproducts (DBPs) are inadvertently generated when chlorine or other disinfectants react with organic matter present in source water (Cutler and Miller 2005; Richardson 2011). Many DBPs are cytotoxic, genotoxic, mutagenic, carcinogenic and teratogenic (Richardson et al. 2007). Epidemiological studies demonstrated an association between lifetime exposures to DBPs and increased risk of bladder cancer (Villanueva et al. 2004; Villanueva et al. 2007; Costet et al. 2011; Kogevinas 2011), colorectal cancer (King et al. 2000; Rahman et al. 2010) and skin cancer (Karagas et al. 2008). The U.S. Environmental Protection Agency (U.S. EPA) estimated that between 2 and 17% of bladder cancer cases in the United States may be induced by DBPs (U. S. Environmental Protection Agency 1998). Epidemiological studies also demonstrated an association between disinfected drinking water and adverse pregnancy outcomes (Costet et al. 2012; Jeong et al. 2012; Righi et al. 2012).

Currently, over 600 DBPs have been identified and the spectrum of DBP chemical classes are influenced by the source water, water contaminants and the disinfectant used (Zhang et al. 2000; Hua and Reckhow 2007; Richardson 2011). In chlorinated water the second largest occurring DBP chemical class is the haloacetic acids (HAAs) (Krasner et al. 2006). The HAAs

are the most highly regulated DBPs. The U.S. EPA regulates chloroacetic acid (CAA), dichloroacetic acid, trichloroacetic acid, bromoacetic acid (BAA), and dibromoacetic acid to a total maximum contaminant level of 60 µg/L (U. S. Environmental Protection Agency 2006). At all water sites measured, the U.S. EPA Information Collection Rule recorded the mean and 90th percentile concentration for the 5 regulated HAAs (HAA5) as 23 µg/L and 47.5 µg/L, respectively (McGuire et al. 2002).

HAAs are alkylating agents and follow SN2 reactivity, which is primarily dependent on the carbon-halogen bond length and the bond dissociation energy. The α-carbon-halide (αC-X) bond length follows the pattern of C-I > C-Br > C-Cl, which implies that the greater the bond length, the lower the dissociation energy required to react with the target molecule (Plewa et al. 2004). Cytotoxic and genotoxic potencies induced by the monohaloacetic acids (monoHAAs) expressed the pattern of iodoacetic acid (IAA) > BAA >> CAA, which highly correlated to the SN2 reactivity, αC-X bond length and αC-X dissociation energy (Plewa et al. 2004).

HAAs are mutagenic in Salmonella typhimurium and Chinese hamster ovary (CHO) cells (Kargalioglu et al. 2002; Plewa et al. 2004; Zhang et al. 2010). They are cytotoxic and genotoxic in CHO cells (Plewa et al. 2010), non-transformed human cells (Attene-Ramos et al. 2010) and toxic in a variety of other bioassays (Richardson et al. 2007). The monoHAAs modulated the gene expression pathways of ATM, MAPK, p53, BRCA1, BRCA2, and ATR, in non-transformed human FHs 74-Int cells; these pathways are involved in stress response to DNA damage and regulate different stages in cell cycle progression or apoptosis (Attene-Ramos et al. 2010; Muellner et al. 2010). FHs 74-Int cells originated from a female fetus 3-4 months into gestation (Smith 1979). Recently, IAA induced malignant transformation in NIH/3T3 mouse embryonic fibroblast cells that progressed to highly aggressive fibrosarcomas when implanted in Balb/c nude mice (Wei et al. 2013). Under ex-vivo conditions, monoHAAs were teratogenic and induced dysmorphogenesis in 3-6 somite staged CD-1 mouse embryos and affected neural tube development, eye development and produced hypoplastic pharyngeal arches and anomalies in heart development (Hunter et al. 1996). F344 rats gavaged with a mixture of HAA5 during gestation resulted in pregnancy loss and eye malformation in surviving litters (Narotsky et al. 2011).

IAA induced toxicity in hippocampal neuronal cells by inhibiting the glycolytic enzyme glyceraldehyde-3-phosphate dehydrogenase (GAPDH), which led to hypoglycemia and the generation of reactive oxygen species (ROS) (Hernandez-Fonseca et al. 2008). IAA induced similar effects in hippocampal astrocytes (Kahlert and Reiser 2000). The direct role of monoHAA-mediated inhibition kinetics of GAPDH and their high correlation with many toxicity measurements was recently published by our laboratory (Pals et al. 2011).

Our working hypothesis is that GAPDH is inhibited by monoHAAs, which reduces the generation of pyruvate and ATP that is required for the tricarboxylic acid (TCA) cycle for the further production of ATP. We postulate that the unavailability of pyruvate causes mitochondrial stress leading to the generation of ROS and a reduction in cellular ATP levels, which may lead to cytotoxicity. The increased levels of ROS induce genomic DNA damage in HAA-treated cells. If this hypothesis is correct, then supplementing monoHAA-treated cells with exogenous pyruvate should restore cellular ATP levels and prevent or reduce genomic DNA damage. The objective of this research was to test this hypothesis. We measured the impact of the monoHAAs on ATP levels and the induction of genomic DNA damage with and without pyruvate supplementation.

2.2. MATERIALS AND METHODS

Reagents

General reagents were purchased from Fisher Scientific Co. (Itasca, IL) and Sigma Chemical Co. (St. Louis, MO). The sources and purities of the monoHAAs used in this research are listed in Table 2.1. Cell culture F12 medium and fetal bovine serum (FBS) were purchased from Fisher Scientific Co. Pyruvic acid was purchased from Acros Organics (NJ). Cell Titer-Glo reagent was purchased from Promega (Madison, WI). The monoHAAs were dissolved in dimethylsulfoxide (DMSO) and stored at −20°C in sealed sterile glass vials (Sulpelco, Bellefonte PA). Pyruvate was dissolved directly either in F12 or Hank's balanced salt solution (HBSS) according to the experimental design, while individual IAA, BAA and CAA stock solutions in DMSO (1M) were diluted in F12 medium or HBSS depending upon the experimental design.

Chinese Hamster Ovary Cells

CHO cell clone 11-4-8 was used (Wagner et al. 1998). Cells were grown in 100 mm glass petri plates with F12 medium containing 5% FBS, 1% glutamine and 1% antibiotic-antimycotic solution at 37°C in a humidified atmosphere of 5% CO_2.

ATP Analysis

Cellular ATP levels were determined after exposure to monoHAAs alone, pyruvic acid alone or monoHAAs plus pyruvic acid with a TUNE-SpectraMax Paradigm® Multi-Mode Microplate Detection Platform using Promega Cell Titer–Glo ATP reagents. The day before ATP analysis, 3×10^4 CHO cells/well were cultured in a 96 well opaque microplate in 200 µL of F12 plus 5% FBS. The next day, the cells were washed with 100 µL of HBSS and treated with concentrations of the monoHAAs with and without pyruvic acid in 50 µL HBSS (with 1.3 mM $CaCl_2$ and 1.1 mM $MgSO_4$). The microplate was covered with AlumnaSeal and incubated for 4 h at 37°C, 5% CO_2. Each experiment contained a concurrent negative control, a bioluminescence background control, pyruvic acid (10 mM), the monoHAAs, monoHAAs plus pyruvic acid and an ATP standard curve. After a 4 h incubation, the cells were washed with 100 µL of HBSS and supplemented with 10 mM pyruvate (for the pyruvate containing treatment groups), covered with AlumnaSeal and incubated for 30 min at 37°C, 5% CO_2 and then equilibrated to room temperature for 30 min. The ATP contents of the cells were measured according to the manufacturer's protocol using 50 µL of Cell Titer-Glo ATP reagents. Data were collected in an Excel spreadsheet and used in calculating pmols of ATP.

Protein Determination

Parallel ATP and protein analyses were performed. The day before the experiment, 3×10^4 CHO cells/well were cultured in a 96 well flat bottom clear microplate in 200 µL of F12 plus 5% FBS. The next day, cells were treated with the HAAs with and without pyruvate as discussed above for the ATP analysis. After treatment, the cells were lysed by adding 25 µL of Solulyse® cell homogenizing solution (Genlantis, San Diego, CA). The microplate was covered with sterile AlumnaSeal and put on a rocker platform (at 37°C) shaken for 5 min after which the plate was rotated and shaken for an additional 5 min. After cell lyses, 10 µL of the lysate from each well

was transferred into a new microplate; into each well was added 10 µL of an anti-foaming agent (Sigma 240, 0.01% v/v), 40 µL of Bradford solution (BioRad), and 140 µL of dH_2O for a final volume of 200 µL. A BioRad protein (BSA) standard was prepared on the same microplate, using 0.68 µg/µL of a BSA standard solution. The contents of each well were carefully mixed and incubated at room temperature for 20 min. The absorbance was read at 595 nm using a SpectraMax Molecular Device plate reader. The data were collected in an Excel spreadsheet and the mg of protein was calculated for each well.

Single Cell Gel Electrophoresis Assay

The alkaline single cell gel electrophoresis (SCGE) or Comet assay is a sensitive, quantitative method for the detection of genomic DNA damage in individual cells (Tice et al. 2000; Rundell et al. 2003). CHO cells were treated with a series of concentrations of IAA, BAA or CAA with and without pyruvic acid and the level of genomic DNA damage was measured. The SCGE microplate assay was performed as described by (Wagner and Plewa 2009). The day before treatment, 4×10^4 cells were cultured into each well of a 96 well microplate in 200 µl of F12 plus 5% FBS and incubated overnight. The following day, cells were washed twice with 100 µL of HBSS and treated with a series of concentrations of a monoHAA alone, pyruvic acid alone, and the monoHAA plus pyruvic acid in a total volume of 25 µL. The cells were covered with sterile AlumnaSeal and incubated for 4 h at 37°C in a humidified atmosphere of 5% CO_2. Each experiment had a concurrent negative control (F12 medium only) and a positive control (3.8 mM ethylmethanesulfonate). After treatment, the cells were washed with HBSS, harvested with a 0.05% trypsin +53 µM EDTA solution and incorporated into agarose microgels. For each concentration group, acute cytotoxicity was measured using the vital dye trypan blue (Phillips 1973). The microgels were electrophoresed and analyzed if the viability of the cell suspensions was >70%. The microgels were placed in lysing solution overnight at 4°C to remove cell membranes (2.5 M NaCl, 100 mM Na_2 EDTA, 10 mM Trisma base, 26 g of NaOH and 1% sodium lauryl sarcosinate, pH 10) with10% DMSO and 1% Triton X-100 added just prior to use. The microgels were rinsed twice with cold deionized water and the DNA was denatured for 20 min in electrophoresis buffer (1 mM Na_2EDTA and 300 mM NaOH, pH 13.5). The microgels were electrophoresed for 40 min at 25 V, 300 mA (0.72 V/cm) at 4°C. After electrophoreses, the microgels were neutralized with 400 mM Tris buffer (pH 7.5), dehydrated in methanol (4°C) and

dried for 5 min at 50°C. The microgels were stored in the dark at room temperature. To analyze the microgels they were first hydrated in deionized water for 30 min at 4°C, stained with 65 μL of 20 μg/mL ethidium bromide and rinsed in cold deionized water. After staining, a cover slip was applied onto the microgel and 25 randomly selected nuclei per microgel were analyzed under a Zeiss fluorescence microscope with the Comet IV imaging system (Perspective Instruments, Suffolk, UK). The data were automatically transferred to an Excel spreadsheet. For DNA damage the unit of measure for each microgel was the average % tail DNA, which is the amount of DNA that migrated into the gel from the nucleus. The mean % tail DNA values were calculated for the microgels in a treatment group and were analyzed with an ANOVA statistical test. If a significant F value of $P < 0.05$ was obtained, a Holm-Sidak pairwise comparison versus the control group analysis was conducted (power ≥ 0.8 at $\alpha = 0.05$).

Reactive Oxygen Species (ROS) Analysis in HAA-treated CHO Cells

A titer of 4×10^4 CHO cells were seeded into a 6 well plate in phenol free F12 plus 5% FBS medium with the final volume of 1 mL and incubated overnight at 37°C, 5% CO2. The next day, cells were washed with HBSS twice and treated with each monoHAA (50 μM IAA, 100 μM BAA, and 6 mM CAA) for 2 h with and without pyruvate in phenol free F12 medium. Every experiment included cells treated with 1 mL of phenol free F12 medium as a negative control and cells treated with 500 μM of H_2O_2 as a positive control. The wells with the treated cells were covered with AlumnaSeal and incubated for 2 h at 37 °C, 5% CO_2. After incubation, cells were washed with HBSS and treated with 15 μM of 2',7'dichlorofluorescein (H2DCF) for 20 min. After incubation, cells were washed with cold phosphate buffer solution (PBS). The ROS produced by monoHAAs oxidized the non-fluorescent substrate to a green florescent product. Cell membranes were permeable to esterified forms of H2DCF. Therefore, H2DCF entered into cells freely. Intracellular esterases deacetylate the H2DCF. Therefore, it was trapped intracellularly (Owusu-Ansah et al. 2008). The green florescence produced by the ROS induced oxidation of H2DCF into DCF was measured by florescence microscopy with FITC filter and the images were saved. These data tested the hypothesis that monoHAA mediated GAPDH inhibition generated ROS via pyruvate starvation.

2.3. RESULTS AND DISCUSSION

Five HAAs are regulated by the U.S.EPA; two of the five are BAA and CAA (U. S. Environmental Protection Agency 2006). MonoHAAs are cytotoxic, genotoxic, mutagenic and teratogenic (Richardson et al. 2007). This study extends our research on the molecular mechanism(s) of toxicity of these important DBPs by investigating the impact of monoHAAs on cellular ATP levels, their induction of genomic DNA damage and the attenuation of this DNA damage by pyruvate supplementation.

Previous studies demonstrated that IAA blocked glycolysis by inhibiting GAPDH that led to neurotoxicity (Matthews et al. 1997; Kahlert and Reiser 2000; Hernandez-Fonseca et al. 2008), ROS generation (Matthews et al. 1997; Hernandez-Fonseca et al. 2008), ATP depletion (Kahlert and Reiser 2000; Hernandez-Fonseca et al. 2008) and disruption of intracellular Ca^{2+} homeostasis (Kahlert and Reiser 2000; Chinopoulos and Adam-Vizi 2006). We recently demonstrated that the relative rates of monoHAA-induced GAPDH inhibition kinetics were highly correlated with many toxicity metrics (Pals et al. 2011). Central to its glycolytic function is a conserved cysteine residue in the active site of GAPDH. This cysteine serves as a nucleophile in the first catalytic step in the conversion of glyceraldehyde-3-phosphate to 1,3-bis-phosphoglycerate (Nakajima et al. 2007). The α-carbon of each monoHAA is a primary alkyl halide and an electrophile due to electron withdrawal from the carbon by the halogen substituent. IAA, BAA and CAA inhibit GAPDH when the α-carbon undergoes an S_N2 reaction with the nucleophilic thiol group on the catalytic cysteine residue. This results in a carboxymethylated cysteine which irreversibly inhibits the catalytic function of the enzyme. Our overall working hypothesis is that the monoHAAs inhibit GAPDH by alkylating the thiol group at the GAPDH active site. This leads to glycolytic ATP depletion and blocks the production of pyruvate that is a mitochondrial substrate for the TCA cycle (Tristan et al. 2011). Pyruvate starvation enhances mitochondrial stress, disrupts the TCA cycle and affects the generation of reducing power (NADH and $FADH_2$) within mitochondria during the TCA cycle. This deficiency in reducing power disturbs normal oxidative phosphorylation, which eventually generates ROS, depletes mitochondrial ATP and increases cytosolic Ca^{2+} concentration (Nakajima et al. 2007; Hernandez-Fonseca et al. 2008; Csordas and Hajnoczky 2009; Peng and Jou 2010). This proposed mechanism is supported in that IAA-induced mutagenicity in *Salmonella typhimurium*

and genotoxicity in CHO cells was repressed by the antioxidants catalase and butylated hydroxyanisole (Cemeli et al. 2006). We believe that ATP depletion and ROS generation are the principal forcing mechanisms for monoHAA-mediated toxicity (Schlisser et al. 2010; Pals et al. 2011).

Depletion of ATP by MonoHAAs

MonoHAAs inhibited GAPDH kinetics with a rank order of IAA > BAA >> CAA (Pals et al. 2011). We proposed that cells exposed to monoHAAs would express ATP depletion. To test this, CHO cells were treated with 25 and 40 μM IAA, 60 μM BAA and 6 mM CAA for 4 h in HBSS. The concentrations of each monoHAA were previously determined to be genotoxic in CHO cells without acute cytotoxicity (Komaki et al. 2009). The cellular ATP levels (as the average bioluminescence unit) for monoHAA-treated cells were significantly reduced as compared to the negative control. The ATP levels with CAA-treated cells were approximately the same as the blank (Figure 2.1). These data demonstrate that IAA, BAA and CAA significantly reduced cellular ATP levels; however, this experimental design could generate an artifact. Although, by observation, we did not detect CHO cell cytotoxicity after 4 h, we did not have a direct quantitative measurement of cell viability of the cell suspensions from which these ATP measurements were generated.

Pyruvate Supplementation and ATP Levels in monoHAA-Treated Cells

To avoid the artifacts that may be associated with the direct ATP measurements alone the experimental designs were refined and expanded to include protein analyses. We determined the minimum concentration of each monoHAA in HBSS (with 1.3 mM $CaCl_2$ and 1.1 mM $MgSO_4$) that induced a significant reduction in cellular ATP levels. The lowest non-cytotoxic concentrations of IAA, BAA and CAA that induced a significant reduction in ATP levels as compared to each concurrent negative control was 3 μM, 6 μM, and 1 mM, respectively (Figure 2.2). Using these concentrations of IAA, BAA and CAA, we conducted parallel experiments to determine the absolute amount of ATP and the total protein content of each cell suspension within each treatment group. Each monoHAA treatment had a negative control, a blank control, a pyruvate control, a monoHAA treatment and a monoHAA plus 10 mM pyruvate treatment. The number of replicate clones for the IAA treatment group was 40 while for BAA and CAA the

number of replicate clones were 37 and 32, respectively. This experimental design allowed us to determine concentrations of ATP and protein for each CHO cell suspension for a precise measurement of ATP depletion and restoration. The concentration of ATP as pmol/mg protein for each monoHAA treatment group is presented in Table 2.2. Figure 2.3 illustrates cellular ATP levels (pmol ATP/mg protein) normalized as 100% for each concurrent negative control for each monoHAA treatment group. A reduction in ATP levels was observed with exposures to 3 μM IAA, 6 μM BAA and 1 mM CAA with levels of 18.7 %, 48.2 % and 50.8 %, respectively, of the concurrent negative controls. When monoHAA- treated cells were simultaneously treated with10 mM pyruvate a significant recovery of cellular ATP levels was measured. For IAA, ATP concentrations increased from 18.7 % to 45.0 % of the concurrent negative control. Similar responses were observed for BAA (48.2 % to 122.1 %) and CAA (50.8 % to 80.2 %) (Figure 2.3). These data support our hypothesis that a major pathway in the toxic mode of action by the monoHAAs is the irreversible inhibition of GAPDH and the subsequent reduction of cellular ATP levels and a blockage in the generation of pyruvate from glucose.

From these ATP measurements an interesting and familiar pattern of response emerged. Comparing the monoHAAs, the CHO cells treated with IAA expressed the greatest reduction in cellular ATP levels (0.54 %) per pmol IAA as compared to the negative control. For the BAA and CAA treatment groups, the reduction in cellular ATP levels per pmol monoHAA was 0.15% for BAA and approximately 0.001% for CAA (Table 2.2). The monoHAA-mediated ATP depletion followed a rank order of IAA > BAA >> CAA. This pattern and magnitude of ATP depletion directly correlated with the αC-X bond length and relative alkylation potential of each monoHAA and was inversely correlated with the αC-X bond dissociation energy (Table 2.3). ATP depletion was highly correlated with the inhibition kinetics of GAPDH (Pals et al. 2011) (Table 2.4). Of importance is that ATP depletion by the monoHAAs (Table 2.5) are highly correlated with diverse measurements of toxicity including cytotoxicity, genotoxicity, mutagenicity and teratogenicity published in the literature over the past 17 years (Table 2.4).

Pyruvate Attenuation of MonoHAA-Induced Genotoxicity

The monoHAAs are direct-acting mutagens in *S. typhimurium* (Kargalioglu et al. 2002; Plewa et al. 2004) and in CHO cells (Zhang et al. 2010) and do not require monooxygenase-mediated metabolic activation for genotoxicity in CHO cells (Plewa et al. 2010). The

monoHAAs do not induce genomic damage via direct alkylation of DNA (Pals et al. 2011). We suggest that monoHAAs induce DNA damage by alkylating the thiol group of the cysteine residue in the active site of GAPDH (Jenkins and Tanner 2006). The resulting reduction in ATP and pyruvate levels leads to ROS generation (Matthews et al. 1997) and subsequent DNA damage (Kumagai et al. 2008). We postulated that if genomic DNA damage is linked to GAPDH inhibition then supplementing cells with exogenous pyruvate should lead to a reduction in genomic DNA damage. To test this hypothesis, CHO cells were treated with monoHAA concentrations that did not induce acute cytotoxicity but were strongly genotoxic in the SCGE assay (Table 2.5). We treated CHO cells with 25 μM IAA, 60 μM BAA or 6 mM CAA for 4 h with and without 10 mM pyruvate. Genomic DNA damage was measured by the SCGE assay. The mean % tail DNA values for the negative control and 10 mM pyruvate control were 2.80 and 2.79, respectively and were not statistically different (Table 2.5). All of the monoHAAs induced a significant level of DNA damage in CHO cells as compared to the negative controls. However, when 25 μM IAA was supplemented with pyruvate a significant reduction in the mean SCGE % tail DNA values was observed (IAA alone, 21.5 compared to IAA + pyruvate, 10.6). Similar reductions in genomic DNA damage with pyruvate supplementation were recorded for 60 μM BAA (BAA alone and BAA + pyruvate, 49.8 and 8.1 % tail DNA, respectively), and 6 mM CAA (CAA alone and CAA + pyruvate, 47.2 and 24.9 % tail DNA, respectively) (Table 2.5). When these data were normalized such that the concurrent monoHAA positive control equaled 100% of the observed DNA damage, pyruvate supplementation significantly repressed the induction of genomic DNA damage (Figure 2.4).

This proposed model for the toxicity of the monoHAAs has a unifying pattern of response (IAA > BAA >> CAA) that we identified a decade ago (Plewa et al. 2004). Although many iodinated DBPs are more toxic than their brominated and chlorinated analogues (Plewa et al. 2008; Plewa and Wagner 2009) the monoHAAs provide a class of substrates with a single variable (the single halogen atom bound to the α-carbon). Originally we believed that the monoHAAs induced genomic damage via direct alkylation of DNA; there was a high correlation among the alkylating potential, αC-X bond dissociation energy, cytotoxicity and genotoxicity in *S. typhimurium* and CHO cells (Table 2.4) (Plewa et al. 2004). These DBPs are direct-acting mutagens in that they do not require S9 microsomal activation in *S. typhimurium* (Plewa et al. 2004) or CHO cells (Zhang et al. 2010). However, we discovered that while the monoHAAs

induce DNA damage using the cellular SCGE assay (treatment of intact cells), the capacity to damage DNA was lost when analyzed with the acellular SCGE assay (treatment of nuclei) (Pals et al. 2011). We concluded that DNA was not the direct target of the monoHAAs. Previously CAA and IAA were demonstrated to inhibit GAPDH without affecting other glycolytic enzymes (Sakai et al. 2005; Hernandez-Fonseca et al. 2008). The linkage between GAPDH inhibition and the quantitative toxicity of the monoHAAs was established by the inhibition kinetics of GAPDH, which also expressed the pattern of IAA > BAA >> CAA. GAPDH inhibition kinetics were highly correlated with a host of toxicity metrics (Table 2.4) (Pals et al. 2011). From the present study we further define the role of GAPDH inhibition and the induction of toxicity. Cellular ATP depletion in monoHAA-treated cells followed the pattern of IAA > BAA >> CAA and was highly correlated with their S_N2 alkylating potential and with the induction of toxicity (Table 2.3). Pyruvate is a product of glycolysis; pyruvate supplementation restored ATP levels and reduced the genomic DNA damage in monoHAA-treated cells. These results strongly support our hypothesis that GAPDH inhibition and subsequent generation of ROS is linked with cytotoxicity, genotoxicity, teratogenicity, and neurotoxicity and may play a substantive role in neurodegenerative diseases such as Alzheimer's disease (Butterfield et al. 2010). The data presented here establish a comprehensive and testable model for the toxic mechanisms of the haloacetic acids, a major class of drinking water DBPs.

HAA Induced ROS Generation in CHO Cells

4×10^4 CHO cells were exposed to 500 μM H_2O_2 , 50 μM, and 100 μM IAA and a negative control in a 6 well plate. The CHO cells treated with IAA and H_2O_2 generated ROS. The H2DCFDA dye crossed the cell membrane and was hydrolyzed by cellular esterases into non-florescent DCFH. The ROS generated inside the cells oxidized the non-florescent DCFH into highly florescent molecules of DCF (Hafer et al. 2008). Therefore, cells treated with IAA and H_2O_2 were more florescent as compared to negative control (Figure 2.5). In order to investigate the antioxidant potential of pyruvate and its role in the monoHAA mediated genetic toxicity, these experiments will be repeated with the co-treatment of each monoHAA and pyruvate.

2.4. CONCLUSION

This study enhanced our understanding of the toxicity mechanisms of monoHAAs. The cellular rescue against the monoHAA-induced genomic DNA damage and increase in the cellular ATP level by exogenous pyruvate supplementation to the HAA-treated cells proved that the genotoxicity induced by these HAAs is due to disturbance in the cellular metabolism, generation of ROS, and cellular energy homeostasis.

2.5. TABLES AND FIGURES

Table 2.1. Monohaloacetic acid characteristics, sources and purities.

HAA [a]	CASN	MW (g/mol)	C–X [b]	Bond Length (Å) [c]	Dissociation Energy (kcal/mol) [d]	Source	Purity
IAA	64-69-7	185.95	C–I	2.14	57.4	Sigma-Aldrich	>99%
BAA	79-08-3	138.95	C–Br	1.93	65.9	Fluka	>99%
CAA	79-11-8	94.50	C–Cl	1.77	78.5	Fluka	>99%

[a] Abbreviations: HAA, haloacetic acids. IAA, iodoacetic acid; BAA, bromoacetic acid; CAA, chloroacetic acid. [b] α-Carbon-halogen bond. [c] C–X bond length summarized from (Loudon 1995).[d] C–X bond dissociation energy summarized from (Loudon 1995).

Table 2.2. Effect of the HAAs on ATP levels in CHO cells with and without pyruvate supplementation.			
HAA Group	Treatment Conditions	pmol ATP/mg Protein Mean Value ± SE	% Reduction per pmol HAA
IAA	Negative Control (IAA)	29788 ± 3197	NA
	10 mM Pyruvate	29476 ± 3575	NA
	3 µM IAA	5557 ± 274	0.54229
	3 µM IAA + Pyruvate	13411 ± 1105	NA
BAA	Negative Control (BAA)	18225 ± 1503	NA
	10 mM Pyruvate	29297 ± 2782	NA
	6 µM BAA	8786 ± 897	0.15136
	6 µM BAA + Pyruvate	24338 ± 2487	NA
CAA	Negative Control (CAA)	6814 ± 755	NA
	10 mM Pyruvate	23464 ± 2278	NA
	1 mM CAA	3463 ± 419	0.00098
	1 mM CAA + Pyruvate	5465 ± 589	NA

NA, not applicable.

Table 2.3. Pearson Product Moment Correlation analyses of HAA physiochemical parameters and the percent reduction of cellular ATP per pmol HAA in CHO cells.

Physicochemical Parameters	ELUMO (r) [a]	αC—X Bond Length (r) [b]	αC—X Dissociation Energy (r) [b]	Relative Alkylation Potential (S_N2) (r) [b]
ATP % Reduction per pmol HAA [c]	−0.986	0.985	−0.935	0.999
ELUMO		−1.000	0.981	−0.980
C—X Bond Length			−0.982	0.979
C—X Dissociation Energy				−0.922

[a] Calculated ELUMO (energy of the lowest unoccupied molecular orbital) summarized from (Richard and Hunter 1996). [b] Summarized from (Loudon 1995). [c] Calculated from data presented in this paper.

Table 2.4. Pearson Product Moment Correlation analyses of HAA toxicological parameters and the percent reduction of cellular ATP per pmol HAA in CHO cells.

HAA Toxico-logical Parameters	CHO cell cyto-toxic index (*r*)	CHO cell geno-toxic index (*r*)	FHs cell geno-toxic index (*r*)	*Salmonella* cytotoxic index (*r*)	*Salmonella* mutagenic potency (*r*)	CHO cell mutagen-icity index (*r*)	Mouse terato-genicity (*r*)	GAPDH inhibi-tion (*r*)
ATP % reduction per pmol HAA [a]	1.00	0.968	0.992	0.991	0.993	0.965	0.999	−0.986
CHO cell cytotoxic index [b]		0.976	0.996	0.995	0.996	0.956	0.998	−0.990
CHO cell genotoxic index [c]			0.992	0.993	0.991	0.868	0.959	−0.997
FHs cell genotoxic index [c]				1.00	1.00	0.925	0.987	−0.999
Salmonella cytotoxic index [d]					1.00	0.921	0.986	−0.999
Salmonella mutagenic potency [d]						0.926	0.988	−0.999
CHO cell mutagenicity index [e]							0.974	−0.906
Mouse terato-genicity [f]								−0.979
GAPDH inhibition kinetics [g]								1.00

[a] Calculated from data presented in this paper. [b] Derived as the reciprocal of the LC_{50} concentration (× constant to generate whole numbers), data from (Plewa et al. 2010). [c] Derived as the reciprocal of the SCGE genotoxic potency value (× constant to generate whole numbers), data from (Plewa et al. 2010; Pals et al. 2011). [d] Data from (Kargalioglu et al. 2002; Plewa et al. 2004). [e] Data from (Zhang et al. 2010). [f] Data from (Hunter et al. 1996). [g] The average rate of GAPDH inhibition per µM monoHAA concentration derived from the slope of the inhibition curves for each monoHAA (Pals et al. 2011).

Table 2.5. Induction of genomic SCGE DNA damage in CHO cells by HAAs with and without pyruvate supplementation.			
Treatment Groups	Number of Microgels	Mean SCGE % Tail DNA Value (±SE)	ANOVA Test Statistic $F_{7, 81} = 74.4$; $P \leq 0.001$
Negative Control (a)	18	2.80 ± 1.33	a
10 mM Pyruvate Control (b)	10	2.79 ± 1.03	a vs. b ($P = 0.998$)
25 µM IAA (c)	12	21.5 ± 2.07	c vs. a ($P \leq 0.001$)
25 µM IAA +10 mM Pyruvate (d)	10	10.6 ± 3.50	d vs. c ($P \leq 0.001$)
60 µM BAA (e)	10	49.8 ± 3.17	e vs. a ($P \leq 0.001$)
60 µM BAA +10 mM Pyruvate (f)	10	8.09 ± 1.13	f vs. e ($P \leq 0.001$)
6 mM CAA (g)	8	47.2 ± 3.79	g vs. a ($P \leq 0.001$)
6 mM CAA +10 mM Pyruvate (h)	11	24.9 ± 1.98	h vs. g ($P \leq 0.001$)

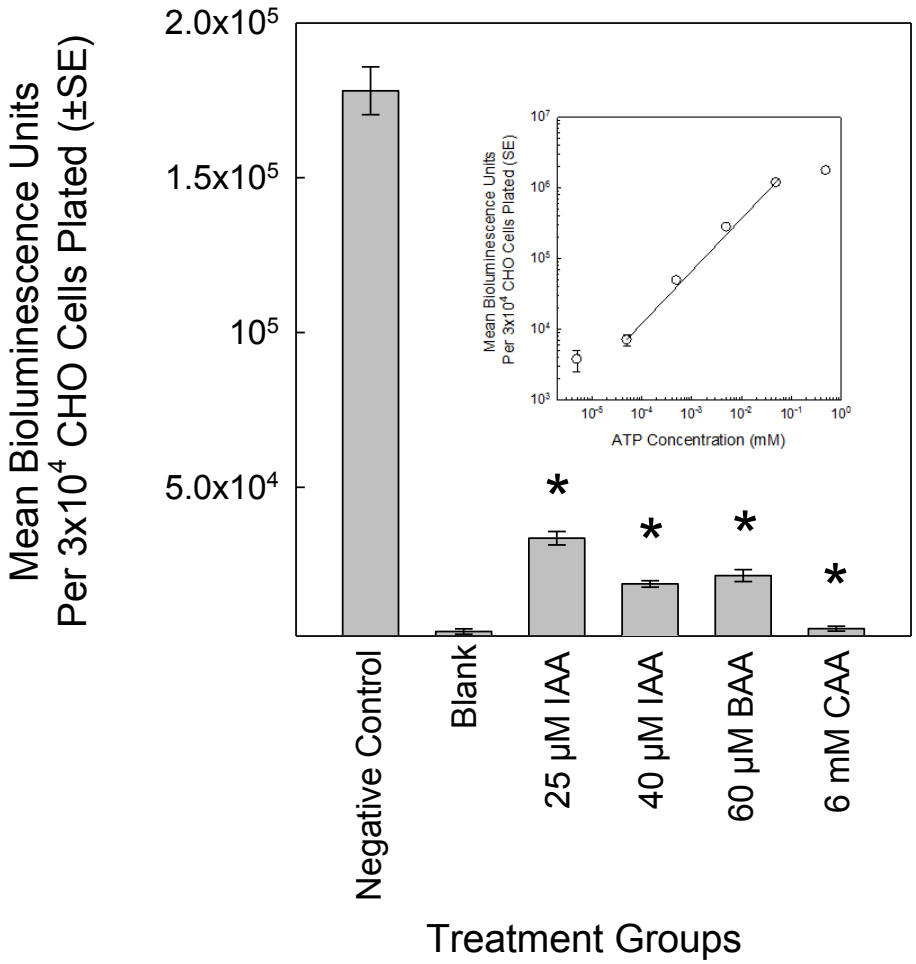

Figure 2.1. Impact of monoHAA exposure on the cellular ATP levels as measured using relative bioluminescence units. The * indicates a significant difference from the negative control. The insert is a ATP standard curve.

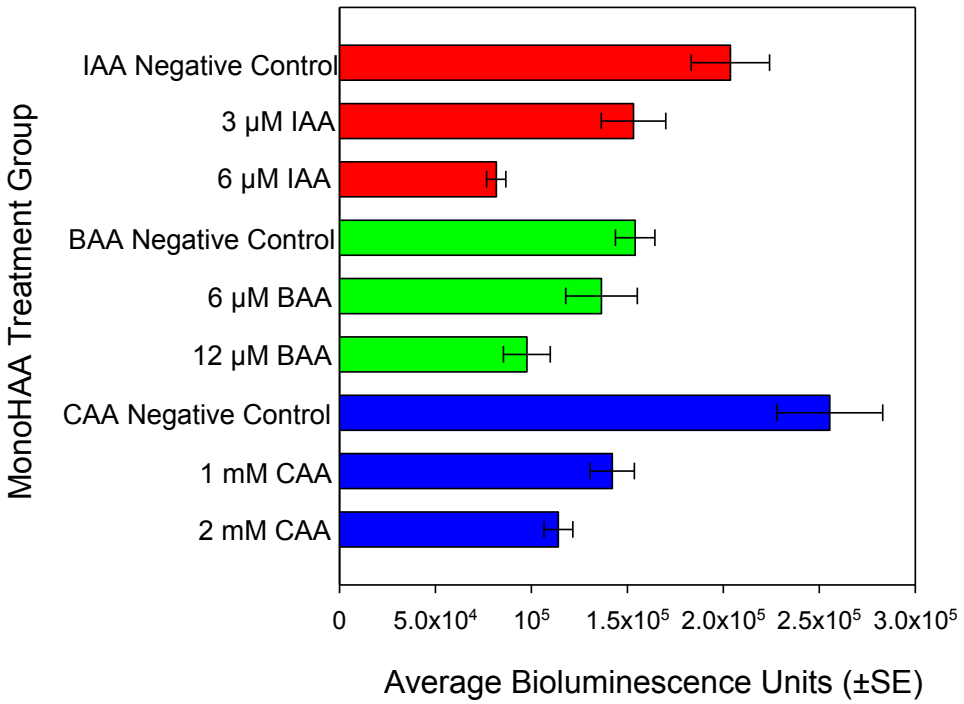

Figure 2.2. Reduction of ATP levels measured as bioluminescence units in CHO cells after exposure to monoHAAs. All monoHAA treatments induced a significant reduction in ATP levels as compared to the concurrent negative controls.

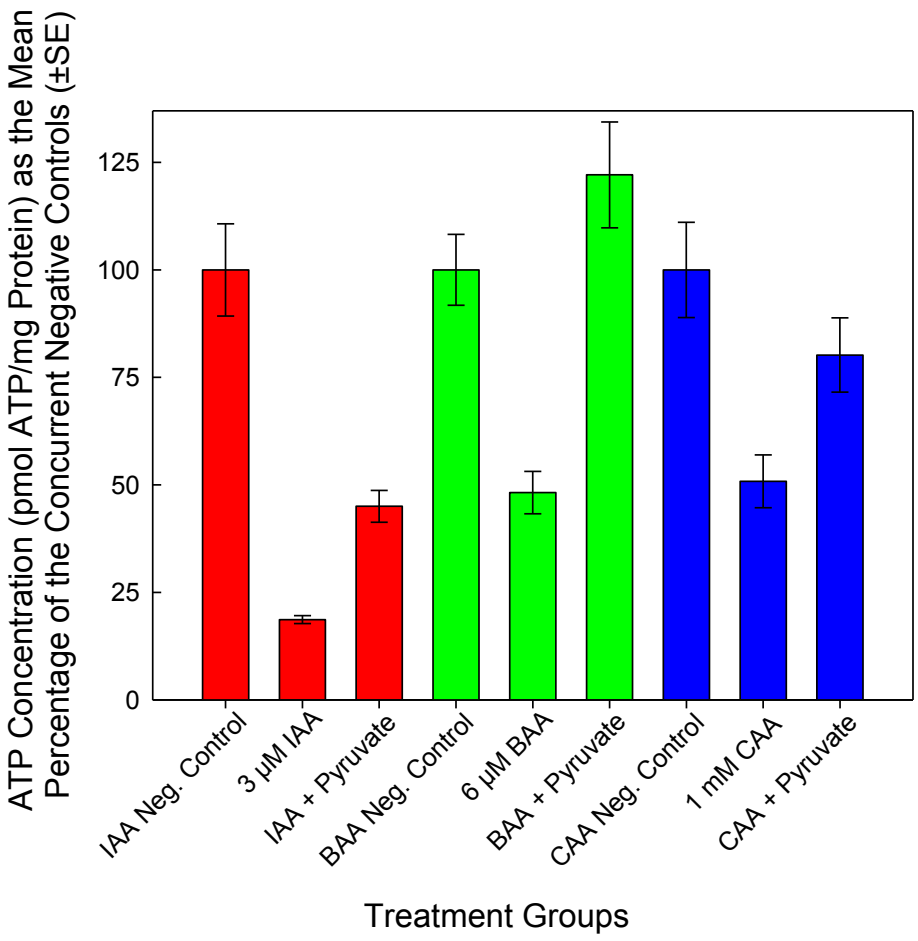

Figure 2.3. Effect of pyruvate supplementation on ATP content of the monoHAAs treated cells.

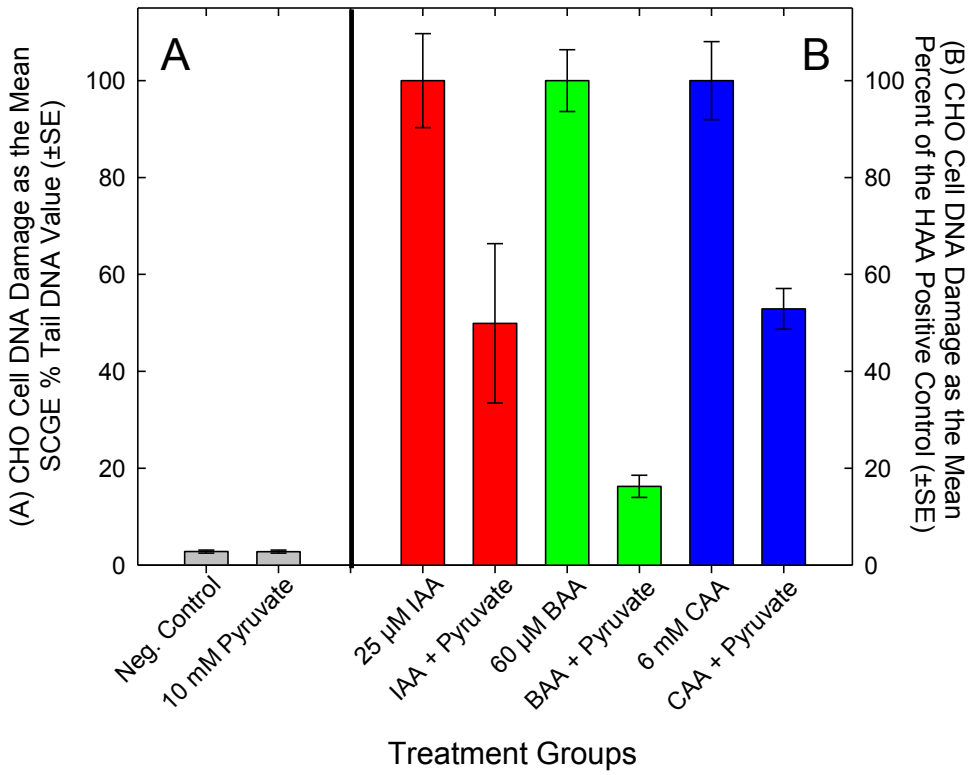

Figure 2.4. Reduction of monoHAA-induced genomic DNA damage by pyruvate supplementation. (A) The SCGE % tail DNA values for the negative control and for 10mM pyruvate. (B) MonoHAA-induced DNA damage normalized as 100% for the positive controls and the reduction in DNA damage with pyruvate supplementation.

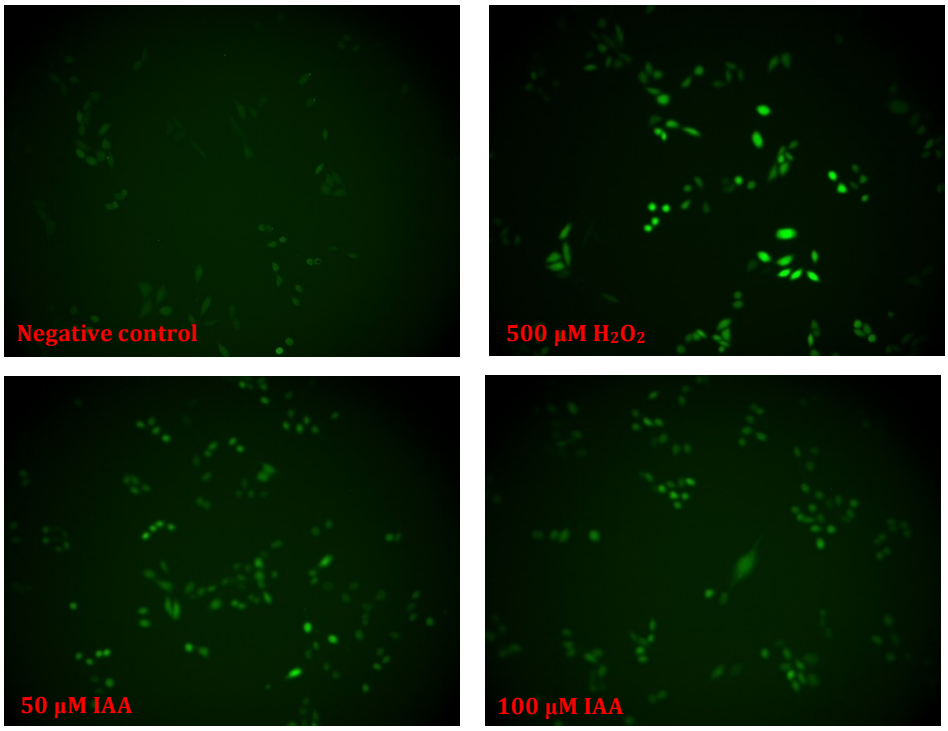

Figure 2.5. IAA and H_2O_2 generated more ROS as compared to the negative control that oxidized the H_2DCFDA dye and produced florescence in the cells.

2.6. REFERENCES

Attene-Ramos MS, Wagner ED, Plewa MJ. 2010. Comparative human cell toxicogenomic analysis of monohaloacetic acid drinking water disinfection byproducts. Environ Sci Technol 44(19):7206-7212.

Butterfield DA, Hardas SS, Lange MLB. 2010. Oxidatively modified glyceraldehyde-3-phosphate dehydrogenase (GAPDH) and Alzheimer's disease: many pathways to neurodegeneration. J Alzheimers Disease 20(2):369-393.

Cemeli E, Wagner ED, Anderson D, Richardson SD, Plewa MJ. 2006. Modulation of the cytotoxicity and genotoxicity of the drinking water disinfection byproduct iodoacetic acid by suppressors of oxidative stress. Environ Sci Technol 40(6):1878-1883.

Chinopoulos C, Adam-Vizi V. 2006. Calcium, mitochondria and oxidative stress in neuronal pathology. Novel aspects of an enduring theme. FEBS J 273(3):433-450.

Costet N, Garlantezec R, Monfort C, Rouget F, Gagniere B, Chevrier C, Cordier S. 2012. Environmental and urinary markers of prenatal exposure to drinking water disinfection by-products, fetal growth, and duration of gestation in the PELAGIE birth cohort (Brittany, France, 2002-2006). Am J Epidemiol 175(4):263-275.

Costet N, Villanueva CM, Jaakkola JJ, Kogevinas M, Cantor KP, King WD, Lynch CF, Nieuwenhuijsen MJ, Cordier S. 2011. Water disinfection by-products and bladder cancer: is there a European specificity? A pooled and meta-analysis of European case-control studies. Occup Environ Med 68(5):379-385.

Csordas G, Hajnoczky G. 2009. SR/ER-mitochondrial local communication: calcium and ROS. Biochim Biophys Acta 1787(11):1352-1362.

Cutler D, Miller G. 2005. The role of public health improvements in health advances: The twentieth-century United States. Demography 42(1):1-22.

Hafer K, Iwamoto KS, Schiestl RH. 2008. Refinement of the dichlorofluorescein assay for flow cytometric measurement of reactive oxygen species in irradiated and bystander cell populations. Radiat Res 169(4):460-468.

Hernandez-Fonseca K, Cardenas-Rodriguez N, Pedraza-Chaverri J, Massieu L. 2008. Calcium-dependent production of reactive oxygen species is involved in neuronal damage induced during glycolysis inhibition in cultured hippocampal neurons. J Neurosci Res 86(8):1768-1780.

Hua GH, Reckhow DA. 2007. Comparison of disinfection byproduct formation from chlorine and alternative disinfectants. Water Res 41(8):1667-1678.

Hunter ES, Rogers EH, Schmid JE, Richard A. 1996. Comparative effects of haloacetic acids in whole embryo culture. Teratology 54(2):57-64.

Jenkins JL, Tanner JJ. 2006. High-resolution structure of human D-glyceraldehyde-3-phosphate dehydrogenase. Acta Cryst 62:290-301.

Jeong CH, Wagner ED, Siebert VR, Anduri S, Richardson SD, Daiber EJ, McKague AB, Kogevinas M, Villanueva CM, Goslan EH, Luo W, Isabelle LM, Pankow JF, Grazuleviciene R, Cordier S, Edwards SC, Righi E, Nieuwenhuijsen MJ, Plewa MJ. 2012. The occurrence and toxicity of disinfection byproducts in European drinking waters in relation with the HIWATE epidemiology study. Envion Sci Technol 46(21):12120-12128.

Kahlert S, Reiser G. 2000. Requirement of glycolytic and mitochondrial energy supply for loading of $Ca^{(2+)}$ stores and InsP(3)-mediated $Ca^{(2+)}$ signaling in rat hippocampus astrocytes. J Neurosci Res 61(4):409-420.

Karagas MR, Villanueva CM, Nieuwenhuijsen M, Weisel CP, Cantor KP, Kogevinas M. 2008. Disinfection byproducts in drinking water and skin cancer? A hypothesis. Cancer Causes Control 19(5):547-548.

Kargalioglu Y, McMillan BJ, Minear RA, Plewa MJ. 2002. Analysis of the cytotoxicity and mutagenicity of drinking water disinfection by-products in *Salmonella typhimurium*. Teratogen Carcinogen Mutagen 22(2):113-128.

King WD, Marrett LD, Woolcott CG. 2000. Case-control study of colon and rectal cancers and chlorination by-products in treated water. Cancer Epidemiol Biomarkers Prev 9(8):813-818.

Kogevinas M. 2011. Epidemiological approaches in the investigation of environmental causes of cancer: the case of dioxins and water disinfection by-products. Environ Health 10 Suppl 1:S3.

Komaki Y, Pals J, Wagner ED, Marinas BJ, Plewa MJ. 2009. Comparative DNA damage and repair kinetics study in mammalian cells by chloro-, bromo,- and iodoacetic acid. Environmental Mutagen Society 40th Annual Meeting. St. Louis, MO: Wiley-Blackwell.

Krasner SW, Weinberg HS, Richardson SD, Pastor SJ, Chinn R, Sclimenti MJ, Onstad GD, Thruston AD, Jr. 2006. The occurrence of a new generation of disinfection by-products. Environ Sci Technol 40(23):7175-7185.

Kumagai S, Narasaki R, Hasumi K. 2008. Glucose-dependent active ATP depletion by koningic acid kills high-glycolytic cells. Biochem Biophys Res Commun 365(2):362-368.

Loudon GM. 1995. Organic Chemistry. 3rd edition. Redwood, CA: Benjamin/Cummings Publ. Co.

Matthews RT, Ferrante RJ, Jenkins BG, Browne SE, Goetz K, Berger S, Chen IY, Beal MF. 1997. Iodoacetate produces striatal excitotoxic lesions. J Neurochem 69(1):285-289.

McGuire MJ, McLain JL, Obolensky A. 2002. Information Collection Rule Data Analysis. Denver, CO: American Water Works Association Research Foundation and AWWA.

Muellner MG, Attene-Ramos MS, Hudson ME, Wagner ED, Plewa MJ. 2010. Human cell toxicogenomic analysis of bromoacetic acid: a regulated drinking water disinfection by-product. Environ Mol Mutagen 51:205-214.

Nakajima H, Amano W, Fujita A, Fukuhara A, Azuma YT, Hata F, Inui T, Takeuchi T. 2007. The active site cysteine of the proapoptotic protein glyceraldehyde-3-phosphate dehydrogenase is essential in oxidative stress-induced aggregation and cell death. J Biol Chem 282(36):26562-26574.

Narotsky MG, Best DS, McDonald A, Godin EA, Hunter ES, 3rd, Simmons JE. 2011. Pregnancy loss and eye malformations in offspring of F344 rats following gestational exposure to mixtures of regulated trihalomethanes and haloacetic acids. Reprod Toxicol 31(1):59-65.

Owusu-Ansah E, Yavari A, Banerjee U. 2008. A protocol for _in vivo_ detection of reactive oxygen species.

Pals J, Ang J, Wagner ED, Plewa MJ. 2011. Biological mechanism for the toxicity of haloacetic acid drinking water disinfection byproducts. Envion Sci Technol 45:5791–5797.

Peng TI, Jou MJ. 2010. Oxidative stress caused by mitochondrial calcium overload. Ann NY Acad Sci 1201:183-188.

Phillips HJ. 1973. Dye exclusion tests for cell viability. In: Kruse PF, Patterson MJ, editors. Tissue Culture: Methods and Applications. New York: Academic Press. p 406.
Plewa MJ, Simmons JE, Richardson SD, Wagner ED. 2010. Mammalian cell cytotoxicity and genotoxicity of the haloacetic acids, a major class of drinking water disinfection by-products. Environ Mol Mutagen 51:871-878.
Plewa MJ, Wagner ED. 2009. Mammalian Cell Cytotoxicity and Genotoxicity of Disinfection By-Products. Denver, CO: Water Research Foundation. 134 p.
Plewa MJ, Wagner ED, Muellner MG, Hsu KM, Richardson SD. 2008. Comparative mammalian cell toxicity of N-DBPs and C-DBPs. In: Karanfil T, Krasner SW, Westerhoff P, Xie Y, editors. Occurrence, formation, health effects and control of disinfection by-products in drinking water. Washington, D.C.: American Chemical Society. p 36-50.
Plewa MJ, Wagner ED, Richardson SD, Thruston AD, Jr., Woo YT, McKague AB. 2004. Chemical and biological characterization of newly discovered iodoacid drinking water disinfection byproducts. Environ Sci Technol 38(18):4713-4722.
Rahman MB, Driscoll T, Cowie C, Armstrong BK. 2010. Disinfection by-products in drinking water and colorectal cancer: a meta-analysis. Int J Epidemiol 39(3):733-745.
Richard AM, Hunter ES, 3rd. 1996. Quantitative structure-activity relationships for the developmental toxicity of haloacetic acids in mammalian whole embryo culture. Teratology 53(6):352-360.
Richardson SD. 2011. Disinfection by-products: formation and occurrence in drinking water. In: Nriagu JO, editor. Encyclopedia of Environmental Health. Burlington: Elsevier. p 110-136.
Richardson SD, Plewa MJ, Wagner ED, Schoeny R, DeMarini DM. 2007. Occurrence, genotoxicity, and carcinogenicity of regulated and emerging disinfection by-products in drinking water: A review and roadmap for research. Mutat Res 636:178-242.
Righi E, Bechtold P, Tortorici D, Lauriola P, Calzolari E, Astolfi G, Nieuwenhuijsen MJ, Fantuzzi G, Aggazzotti G. 2012. Trihalomethanes, chlorite, chlorate in drinking water and risk of congenital anomalies: A population-based case-control study in Northern Italy. Environ Res 116:66-73.
Rundell MS, Wagner ED, Plewa MJ. 2003. The comet assay: genotoxic damage or nuclear fragmentation? Environ Mol Mutagen 42(2):61-67.
Sakai A, Shimizu H, Kono K, Furuya E. 2005. Monochloroacetic acid inhibits liver gluconeogenesis by inactivating glyceraldehyde-3-phosphate dehydrogenase. Chem Res Toxicol 18(2):277-282.
Schlisser AE, Yan J, Hales BF. 2010. Teratogen-induced oxidative stress targets glyceraldehyde-3-phosphate dehydrogenase in the organogenesis stage mouse embryo. Toxicol Sci 118(2):686-695.
Smith HS. 1979. In vitro properties of epithelial cell lines established from human carcinomas and nonmalignant tissue. J Natl Cancer Inst 62(2):225-230.
Tice RR, Agurell E, Anderson D, Burlinson B, Hartmann A, Kobayashi H, Miyamae Y, Rojas E, Ryu JC, Sasaki YF. 2000. Single cell gel/comet assay: guidelines for in vitro and in vivo genetic toxicology testing. Environ Mol Mutagen 35(3):206-221.
Tristan C, Shahani N, Sedlak TW, Sawa A. 2011. The diverse functions of GAPDH: Views from different subcellular compartments. Cellular Signalling 23(2):317-323.

U. S. Environmental Protection Agency. 1998. Quantification of Cancer Risk from Exposure of Chlorinated Drinking Water. Washington, DC: Office of Water, Office of Science and Technology, Health and Ecological Criteria Division.

U. S. Environmental Protection Agency. 2006. National primary drinking water regulations: Stage 2 disinfectants and disinfection byproducts rule. Fed Reg 71(2):387-493.

Villanueva CM, Cantor KP, Cordier S, Jaakkola JJ, King WD, Lynch CF, Porru S, Kogevinas M. 2004. Disinfection byproducts and bladder cancer: a pooled analysis. Epidemiology 15(3):357-367.

Villanueva CM, Cantor KP, Grimalt JO, Malats N, Silverman D, Tardon A, Garcia-Closas R, Serra C, Carrato A, Castano-Vinyals G, Marcos R, Rothman N, Real FX, Dosemeci M, Kogevinas M. 2007. Bladder cancer and exposure to water disinfection by-products through ingestion, bathing, showering, and swimming in pools. Am J Epidemiol 165(2):148-156.

Wagner ED, Plewa MJ. 2009. Microplate-based comet assay. In: Dhawan A, Anderson D, editors. The Comet Assay in Toxicology. London: Royal Society of Chemistry. p 79-97.

Wagner ED, Rayburn AL, Anderson D, Plewa MJ. 1998. Analysis of mutagens with single cell gel electrophoresis, flow cytometry, and forward mutation assays in an isolated clone of Chinese hamster ovary cells. Environ Mol Mutagen 32(4):360-368.

Wei X, Wang S, Zheng W, Wang X, Liu X, Jiang S, He G, Zheng Y, Qu W. 2013. Tumorigenicity of drinking water disinfection byproduct iodoacetic acid in NIH3T3 cells. Envion Sci Technol In Press.

Zhang SH, Miao DY, Liu AL, Zhang L, Wei W, Xie H, Lu WQ. 2010. Assessment of the cytotoxicity and genotoxicity of haloacetic acids using microplate-based cytotoxicity test and CHO/HGPRT gene mutation assay. Mutat Res 703(2):174-179.

Zhang X, Echigo S, Minear RA, Plewa MJ. 2000. Characterization and comparison of disinfection by-products of four major disinfectants. In: Barrett SE, Krasner SW, Amy GL, editors. Natural Organic Matter and Disinfection By-Products: Characterization and Control in Drinking Water. Washington, D.C.: American Chemical Society. p 299-314.

CHAPTER 3

HALOACETIC ACIDS WATER DISINFECTION BY-PRODUCTS DISTURB CELLULAR GLYCOLYTIC AND MITOCHONDRIAL METABOLISM

3.1. INTRODUCTION

Disinfection of drinking water was a preeminent public health achievement of the 20th century, which significantly reduced the outbreak of water-borne diseases like cholera, typhoid and dysentery (Cutler and Miller 2005). Disinfectants are powerful oxidants; disinfectants not only kill pathogenic microorganisms but also inadvertently generate disinfection by-products (DBPs) (Richardson et al. 2002). DBPs are formed when chemical disinfectants (chlorine, chlorine dioxide, chloramine, or ozone) react with organic precursors, natural organic matter (NOM), and inorganic precursors such as Br^- and I^-. Disinfectants oxidize organic and inorganic precursors, which are then reactive with additional chlorine or chloramine and act as halogen substituents to produce DBPs (Stuart 2009). Currently over 600 DBPs have been chemically identified (Richardson et al. 2007) and the spectrum of DBPs in water is influenced by the type of disinfectants used, the concentration of disinfectants, reaction time, NOM concentration as dissolved organic carbon (DOC), pH, and temperature (Krasner 2009). In chlorinated water, the second largest DBP chemical class is the haloacetic acids (HAAs) (Krasner et al. 2006; Stuart 2009). HAAs are the most highly regulated DBPs. The U.S. Environmental Protection Agency (U.S.EPA) regulates five HAAs (chloroacetic acid (CAA), dichloroacetic acid (DCA), trichloroacetic acid (TCA), bromoacetic acid (BAA), and dibromoacetic acid (DBA)) to a total maximum contaminant level of 60 μg/L (U. S. Environmental Protection Agency 2006).

DBPs are cytotoxic, mutagenic, genotoxic, carcinogenic and teratogenic (Plewa et al. 2002; Villanueva et al. 2007; Narotsky et al. 2011). DBP exposure was associated with increased risk of bladder, and colorectal cancer (Villanueva et al. 2007). U. S. EPA estimated that 2-17% of bladder cancer cases in the U.S. might be induced by DBPs (U. S. Environmental Protection Agency 1998). Furthermore, DBPs in chlorinated drinking water were associated with spontaneous abortion in 5144 pregnant women (Waller et al. 1998) and other pregnancy outcomes. In *in vivo* studies, HAAs (DCA, TCA, and DBA) induced hepatocellular adenomas and hepatocellular carcinomas in B6C3F1 mice and F344 rats (U. S. Environmental Protection Agency 2008) and DCA, DBA, and bromochloroacetic acid (BCA) altered intestinal microflora

and metabolism in rats, which could also have an effect on bioactivation of promutagens or procarcinogen (George et al. 2000). Moreover, iodoacetic acid (IAA) induced malignant transformation in NIH/3T3 mouse embryonic fibroblast cells and when implanted in Balb/c nude mice, developed into highly aggressive fibrosarcomas (Wei 2013). Gestational exposure of mixture of HAA5 resulted in pregnancy loss and eye malformation in rats (Narotsky et al. 2011). Under *ex vivo* conditions, monoHAAs were teratogenic and induced dysmorphogenesis in CD-1 mouse embryos and affected neural tube development, eye development and produced anomalies in heart development (Hunter et al. 1996). Under *in vitro* conditions, HAAs were cytotoxic and genotoxic in Chinese hamster ovary (CHO) cells (Plewa et al. 2010), mutagenic in *Salmonella typhimurium* and CHO cells (Kargalioglu et al. 2002; Plewa et al. 2004; Zhang et al. 2010), cytotoxic and genotoxic in nontransformed human cells (Attene-Ramos et al. 2010), and teratogenic in mice (Andrews et al. 2004). The above-mentioned studies show that HAAs are cytotoxic, genotoxic, mutagenic, teratogenic and carcinogenic yet the molecular mode of toxicity mechanism of these HAAs is not well understood (Pals et al. 2011; Dad et al. 2013).

HAAs are S_N2 alkylating agents (Plewa et al. 2004). The S_N2 reactivity of monoHAAs is dependent on the α-carbon-halide (αC-X) bond length and bond dissociation energy. The αC-X bond length follows the pattern of C-I > C-Br >> C-Cl, which has an inverse relation with the bond dissociation energy (Plewa et al. 2004). The genotoxic, cytotoxic and mutagenic potencies expressed a high correlation with the S_N2 reactivity and also followed a pattern of IAA > BAA >> CAA (Plewa et al. 2004). We demonstrated that monoHAAs do not directly damage DNA (Pals et al. 2010) but inhibit the glyceroldehyde 3-phosphate dehydrogenase (GAPDH) probably by alkylating the sulfhydryl group of the cysteine residue in the active site of GAPDH and renders it inactive (Pals et al. 2011). For the monoHAAs GAPDH is a molecular target. GAPDH is a pivotal enzyme in glycolysis and produce mitochondrial substrate in the form of pyruvate from glucose. The unavailability or scarcity of pyruvate induces mitochondrial stress by affecting its ability to produce reducing power (NADH) through the tricarboxylic acid (TCA) cycle and causes a reduction of cellular ATP levels. Due to mitochondrial stress and the scarcity of reducing power reactive oxygen species (ROS) are produced. ROS can damage biological macromolecules such as DNA (Jena 2012). Treating cells with exogenous pyruvate overcame the monoHAA –mediated reduction in cellular ATP and reduced the genomic DNA damage

(Dad et al. 2013). We hypothesized that di-, and triHAAs may follow the same toxicity pathway by inhibiting GAPDH and reducing the ATP contents of the cells.

DCA was used as a treatment in patients with lactic acidosis especially, in patients with pyruvate dehydrogenase (PDH) deficiency (Fouque et al. 2003), DCA is also used as a chemotherapeutic agent because it reverses the Warburg effect (Dhar and Lippard 2009) by activating PDH through inhibiting PDH kinase (Whitehouse et al. 1974; Kerbey et al. 1976; Fouque et al. 2003; Itoh et al. 2003). In oncology, in mitochondria, the phenomenon of the cellular energy production predominantly by a high rate of glycolysis followed by lactic acid fermentation by the cytosol rather than by a low rate of glycolysis followed by oxidative phosphorylation is known as the Warburg effect (Wikipedia).

The pyruvate dehydrogenase complex (PDC) is a multi-enzyme complex, a member of the α-ketoacid dehydrogenase complex family (De Marcucci and Lindsay 1985) and catalyzes the conversion of pyruvate, NAD^+, and coenzyme-A into acetyl-CoA, NADH and CO_2 in the presence of thiamine pyrophosphate and Mg^{+2} (Tymoczko et al. 2013). Mammalian PDC has multiple copies of 6 different components; they are (i) pyruvate dehydrogenase (E1), (ii) dihydrolipoamide acetyltransferase (E2), (iii) dihydrolipoamide dehydrogenase (E3), (iv) E1 specific kinases, (v) phospho-E1 phosphotase and (vi) X protein (De Marcucci and Lindsay 1985; Jilka et al. 1986). E1, E2, and E3 are the major catalytic components, which are responsible for the stepwise decarboxylation and dehydrogenation of pyruvate into acetyl- CoA (Patel and Roche 1990).

The E1 component of PDC is a tetramer ($\alpha_2\beta_2$), which has two thiamine pyrophosphate (TPP) binding sites. TPP is required for the first step of pyruvate decarboxylation, which involves TPP-dependent decarboxylation of pyruvate to hydroxyl TPP. This reaction leaves an acetyl group, which links to the lipomide group of E2. The $E_1\alpha$ component of the tetrameric E1 component of the PDC is inactivated/phosphorylated by pyruvate dehydrogenase kinase (PDK) enzyme and activated/dephosphorylated by a specific phosphatase enzyme. The dephosphorylation of these sites by phospho-E1-phosphotase leads to the activation of the enzyme (Frey et al. 1989; Patel and Roche 1990). E2 is responsible for the generation of acetyl-CoA by transferring the acetyl group from acetyl-lipoyl to CoA. E2 has different structural domains, which are different in different organisms. Human E2 has 2 lipoyl domians presented

as L1 and L2. The E2B or subunit-binding domain is responsible for binding E1 and E3. The inner domain (E-I), catalyzes the transacetylation reaction and self association to form the dodecahedral structure, which contain 60 subunits. The E2 component also plays a crucial role in the activation and inactivation of the pyruvate dehydrogenase by providing a binding site to the PDK and phospho-E1-phosphotase enzymes (Patel and Roche 1990; Patel and Korotchkina 2003). The third main component of the PDC is E3, which transfers electrons from dihydrolipoamide to NAD^+. It is a homodimer and each polypeptide noncovalently binds to a molecule of FAD (Patel and Roche 1990).

Pyruvate dehydrogenase kinase (PDK) plays an important role in regulating the PDC. PDK has four isoforms and exhibit tissue specific expression; PDK1 is detected in heart, pancreatic islets, and skeletal muscles; PDK2 is expressed in all tissues; PDK3 is present in testes, kidney, and pancreatic islets. Phosphorylation of E1p by PDK occurs at three different serine residues (S264: site 1, S271: site 2, and S203: site 3). Among the three conserved phosphorylation sites, site 1 is the most rapidly phosphorylated site where site 3 is the slowest phosphorylated site (Sale and Randle 1981; Korotchkina and Patel 1995). Structural studies of the PDKs showed that all the four isoforms of PDKs phosphorylate sites 1 and 2, but only PDK1 modifies site 3 (Korotchkina and Patel 2001).

The rat PDK2 structure revealed that these proteins have two distinct domains; the N-terminal domain and the C-terminal domain; the C-terminal domain is an α/β structure with a 5 stranded β sheet. These enzymes also have four conserved motifs (N-G1-,G2-, and G3-boxes), which build a unique ATP-binding fold. The ATP-binding fold has a structure known as the "ATP lid". The conformational changes in ATP-lid are linked with the ATP hydrolysis and protein-protein interaction (Wigley et al. 1991; Ban et al. 1999). The binding of the PDKs to the L2 domain of the E2p subunit of the PDC activates PDK activity, but this activation of different PDK isoforms occurs in a different fashion (Kato et al. 2005). The L2 domain of the E2 component of the PDC plays an important role in regulation of the PDC by inducing allosteric changes in the PDK enzyme. The crystal structure of PDK3 with and without L2 binding showed that L2 binding affects the ATP lid confirmation and regulates the activation of PDK. PDK3 without L2 binding had the ATP lid in the ordered form, which had high affinity for ADP binding and rendered PDK3 inactive. Where PDK3 with L2 binding had the ATP lid in a

disordered form, the low affinity for ADP of the disordered ATP lid led to the release of ADP, which resulted in the removal of PDK inhibition caused by bound ADP and resulted in L2-induced PDK3 activity (Kato et al. 2005).

PDK2 structure with dichloroacetic acid (DCA) revealed that DCA binds to the N-terminal domain of PDK2. The E2P/E3BP scaffold-free activity showed that DCA reduced PDK1 and PDK3 activity in a similar fashion to 4% and 17%, respectively (Kato et al. 2007). L2 binding promotes the opening of the active-site cleft and destabilizes the ATP lid facilitating ADP dissociation in the PDK3-L2 complex, rendered PDK active(Kato et al. 2005). Kinetic studies demonstrated that the exposure to DCA prevented the ADP dissociation from the active-site cleft resulting in PDK inhibition. ADP binding to PDK reduces the affinity of this enzyme for L2 binding by 3-fold; the presence of DCA and ADP synergistically decreases the affinity of the PDK for L2 by 130-fold as compared to ADP alone and eventually affects the L2-induced activation of the PDK. The inhibition of the PDK by DCA-induced allosteric change keeps the PDC in its active state and accelerates the tricarboxylic acid (TCA) cycle (Kato et al. 2007).

DCA induced apoptosis in the tumor cells by reversing the Warburg effect (Bonnet et al. 2007). DCA activated PDC by inhibiting PDK and shifting the glycolytic-based metabolism to mitochondria in tumor cells. Bonnet et al showed that DCA decreased the mitochondrial membrane potential ($\Delta\Psi m$) by activating TCA cycle, generating more protons by mitochondria, and by decreasing cytosolic Ca^{++} concentration. The decrease in $\Delta\Psi m$ also induced mitochondrial transition pore (MTP) opening. The opening of MTP activated the release of cytochrome-C, which is required for the caspase activation and apoptosis induction. DCA induced activation of mitochondrial metabolism and it activated complex-I induced ROS generation. The complex-I induced ROS generation upregulated the K^+ channel Kv1.5 expression and decreased K^+ concentration, which augmented the activation of apoptosis in tumor cells. DCA lowered the plasma lactate, alanine, cholesterol, and glucose levels in adult, noninsulin-dependent diabetic patients (Stacpoole et al. 1978). DCA also reduced lactic acidosis in patients with pyruvate dehydrogenase deficiency (Stacpoole et al. 2006). DCA generated oncolysis in attenuated oncolytic measles virus Edmonston strain (MV-Edm) caused glioblastoma cells by inhibiting aerobic glycolysis. DCA enhanced the MV-Edm replication (increasing bioenergetic consumption) and inhibited glycolysis (decreasing bioenergetics

production), which, in combination, accelerated bioenergetics exhaustion caused necrotic cell death (Li et al. 2015).

Cellular Ca^{+2} concentration plays a major role in regulating mitochondrial metabolism. Browning et al reported that DCA inhibited the phosphorylation of intra-mitochondrial PDH ά-subunit in a concentration-dependent manner, which was accompanied by PDH activation and pyruvate supported calcium accumulation. PDH activity and pyruvate-supported calcium accumulation showed similar dependence on pyruvate concentration of 40 μM and 30 μM, respectively (Browning et al. 1981). In concert with above information, ruthenium red inhibited the uniporter and stopped the calcium uptake by mitochondria and in turn inhibited the PDH activity (McCormack and England 1983). These studies indicated that pyruvate supported calcium transportation in mitochondria and pyruvate dehydrogenase activation are coupled activities and play a major role in cellular calcium homeostasis and ATP production. Moreover, the cellular ATP/ADP ratio also plays a significant role in regulating PDK, PDC and overall mitochondrial metabolism (J.M. et al. 2002).

My central hypothesis is that increased activation of PDH activity by the HAAs accelerates pyruvate transport in mitochondria, which is coupled with Ca^{+2} influx and enhanced oxidative decarboxylation of pyruvate into acetyl CoA, this will produce more reducing power in the form of NADH. The NADH will be further utilized by oxidative phosphorylation to produce more ATP. The accelerated TCA cycle due to PDC activation and enhanced NADH formation will utilize more O_2 as a final electron acceptor, which may lead to hypoxia and eventually ROS production. In order to generate more pyruvate, required by mitochondria due to HAA- induced activation, the cells will consume more glucose and will accelerate the release of pyruvate, lactate and alanine from cells (Evans and Stacpoole 1982), this process will disturb the glucose homeostasis and may lead to toxicity. The chronic exposure to diHAAs and triHAAs through drinking water may be involved with hypolactatemia, disturbed glucose homeostasis and hepatotoxicity in humans especially sensitive populations e.g. featuses.

The objectives of this research are (i) measure GAPDH inhibition in HAA-treated cells (ii) determine the effect of HAA-treatment in CHO cells on PDC activity, and (iii) measure the impact of HAA exposure on cellular ATP levels.

3.2. MATERIALS AND METHODS

Reagents

General reagents were purchased from Fisher Scientific Co. (Itasca, IL) and Sigma Chemical Co. (St. Louis, MO). DBA, DCA, TBA, TCA, and, CAA were purchased from Fluka, IAA and BAA were purchased from Sigma Chemical Co. (St. Louis, MO), DBCA was from Radian international, DBCA from Cerilliant, and BCA from U. S. EPA. Cell culture F12 medium and fetal bovine serum (FBS) were purchased from Fisher Scientific Co. Cell Titer-Glo reagent was purchased from Promega (Madison, WI). The Pyruvate Dehydrogenase (PDH) Activity Colorimetric Assay Kit was purchased from BioVision (San Fransisco, CA). Glyceraldehyde-3-phosphate was purchased from Sigma-Aldrich (St. Louis, MO).

HAAs were dissolved in dimethylsulfoxide (DMSO) and stored at −20°C in sealed sterile glass vials (Sulpelco, Bellefonte PA). HAAs were diluted in Hank's balanced salt solution (HBSS).

Chinese Hamster Ovary (CHO) Cells

CHO cell strain AS52 (derived from K1) clone 11-4-8 was used in all experiments (Wagner et al. 1998). Cells were grown in 100 mm glass petri plates with F12 medium containing 5% FBS, 1% glutamine and 1% antibiotic-antimycotic solution at 37°C in a humidified atmosphere of 5% CO_2.

Glycerladehyde-3-Phosphate Dehydrogenase (GAPDH) Enzyme kinetics Analysis

CHO cells were grown in F12, 5% FBS medium on 60 mm plastic cell culture plates. The medium was removed and the cells were washed 3× with 2 mL of cold phosphate-buffered saline (PBS) and once with 2 mL of cold buffer K (1 mM Tris-HCl, 1 mM EDTA, 1 mM $MgCl_2$, pH 7.6). Then the cells were tumefied with buffer K for 2 min at room temperature. After treatment with buffer K, cells were homogenized with a sterilized cell scraper. The cell homogenate was collected in microfuge tubes and centrifuged at 16,100 ×g for 3 min at room temperature to remove cellular debris. A reaction mixture (0.1 M Tris-HCl (pH 8.5) containing 5 mM KH_2PO_4, 20 mM NaF, 1.7 mM $NaAsO_2$, and 1 mM NAD) was prepared. The supernatant fluid (CHO cell

homogenate) was analyzed for GAPDH activity. The reaction mixture was dispensed in tubes with 854 µL per tube. To the reaction mixture, added 220 µL of the 5× solution of the test agent and then added 22 µL of the cell homogenate, vortexed, and incubated for 2 min. This reaction mixture of 996.3 µL was transferred to a cuvette and served as a blank. After the blanked reading, 3.7 µL of 1 mM glyceraldyde-3-phospate (G3P) was added to the mixture to initiate the reaction. The increase in absorption at 340 nm every 10 s for a total of 60 s was recorded using a Beckman DU7400 UV-vis spectrophotometer. The absorbance signal for NADH formation at 340 nm was used to determine GAPDH activity. Each experiment included a negative control and different concentrations of the HAAs included in the experiment with three replicates for each concentration. Absorbance values were plotted against time for each individual experiment and linear regression was conducted. Rates were calculated using the slope of the regression. GAPDH activity rates were calculated as µMol NADH/min/µg protein. Data were normalized to the concurrent negative control for each experiment. The data from multiple experiments were combined and statistical significance was calculated using an ANOVA test.

ATP Analysis and Protein Determination

Cellular ATP levels of control and HAA-treated cells were measured as pmol ATP/mg protein using the Promega Cell Titer-Glo reagent in a 96-well microplate assay with a TUNE-SpectraMax Paradigm® Multi-Mode Microplate Detection Platform. The day before ATP analysis, 3×10^4 CHO cells/well were cultured in a 96 well opaque microplate in 200 µL of F12 plus 5% FBS. The next day, the cells were washed with 100 µL of HBSS and treated with concentrations of the HAAs in 50 µL HBSS (with 1.3 mM $CaCl_2$ and 1.1 mM $MgSO_4$). The microplate was covered with AlumnaSeal and incubated for 4 h at 37°C, 5% CO_2. Each experiment contained a concurrent negative control, a bioluminescence background control, HAAs, and an ATP standard curve. After 4 h incubation, the cells were washed with 100 µL of HBSS and equilibrated to room temperature for 30 min. The ATP contents of the cells were measured according to the manufacturer's protocol using 50 µL of Cell Titer-Glo ATP reagents. Data were collected in an Excel spreadsheet and used in calculating pmols of ATP.

Protein Determination

Parallel ATP and protein analyses were performed. The day before the experiment, 3×10^4 CHO cells/well were cultured in a 96 well flat bottom clear microplate in 200 µL of F12 plus 5% FBS. The next day, cells were treated with the HAAs as discussed above for the ATP analysis. After treatment, the cells were lysed by adding 25 µL of Solulyse® cell homogenizing solution (Genlantis, San Diego, CA). The microplate was covered with sterile AlumnaSeal and put on a rocker platform (at 37°C) shaken for 5 min after which the plate was rotated and shaken for an additional 5 min. After cell lyses, 10 µL of the lysate from each well was transferred into a new microplate; into each well was added 10 µL of an anti-foaming agent (Sigma 240, 0.01% v/v), 40 µL of Bradford solution (BioRad), and 140 µL of dH_2O for a final volume of 200 µL. A BioRad protein (BSA) standard was prepared on the same microplate, using 0.68 µg/µL of a BSA standard solution. The contents of each well were carefully mixed and incubated at room temperature for 20 min. The absorbance was read at 595 nm using a SpectraMax Molecular Device plate reader. The data were collected in an Excel spreadsheet and the mg of protein was calculated for each well.

Pyruvate Dehydrogenase (PDH) Enzyme Kinetics Analysis

PDH enzyme activity was measured in HAA-treated CHO cells using BioVison PDH colorimetric assay kit with a TUNE-SpectraMax Paradigm® Multi-Mode Microplate Detection Platform. CHO cells at 3×10^6 cells/ mL with 2 mL/well in a 6-well plate were cultured in F12 5% FBS medium and incubated overnight at 37°C, 5% CO_2 in a tissue culture incubator. The following day, medium was aspirated and the cells were washed with 2 mL HBSS twice. After washing, the cells were treated with monoHAAs (3 µM IAA, 15 µM BAA, 300 µM CAA), diHAAs (900 µM DBA, 900 µM BCA, 50 µM DCA), and triHAAs (300 µM TCA, 300 µM CDBA, 500 µM TBA, 900 µM BDCA) in HBSS plus 1.3 mM $CaCl_2$ and 0.5 mM $MgCl_2$ and incubated at 37°C, 5% CO_2 for 4 h. After incubation, the cells were washed with HBSS once and harvested with 500 µL trypsin / well. The harvested cells from different wells with the same test agent and same concentrations were collected in a single tube and centrifuged at 16,100 ×g for 1 min. After centrifugation, cell pellets were washed with 500 µL HBSS and homogenized in 200 µL PDH buffer/tube using a Fisherbrand Motorized Tissue Grinder. Homogenates were incubated on ice for 10 min. Meanwhile, reaction mixture was prepared according to the

manufacturer's protocol. Each experiment had a series of control that included a negative control, NADH standard curve, positive control, and a background control. After incubation on ice, the homogenates were centrifuged at 10,000 × g for 5 min at 4°C. 50 µL of the supernatant for each treatment group were transferred to a 96-well microplate. 50 µL of the reaction mixture was added to each well and absorbance was measured immediately at 450 nm in kinetic mode for 60 min at 10 min interval at 37 °C. Each treatment group had three replicates in every experiment and every experiment was repeated at least three times. The data were collected in excel sheet and blank corrected. NADH standard curve was calculated and used to determine the PDH activity as nmol NADH/min/mL using formula given below**.**

$$\text{Sample Pyruvate Dehydrogenase Activity} = B/(\Delta T \times V) \times D = \text{nmol/min/mL}$$

Where: B = NADH amount from standard curve (nmol)

ΔT = reaction time (min)

V = Sample volume added into the reaction well (ml)

D = Dilution factor

The amount of protein was measured in each sample using the Bradford assay and nmol NADH/min/mg protein was calculated. To determine significance differences among the different HAAs an ANOVA test statistics was employed.

3.3. RESULTS AND DISCUSSION

Pyruvate dehydrogenase plays a pivotal role in mitochondrial metabolism. Pyruvate dehydrogenase is present in the form of a multienzyme complex and converts pyruvate, NAD^+ and coenzyme-A into acetyl-CoA, NADH, and CO_2 in the presence of thiamine pyrophosphate (TPP) and Mg^{+2} and links glycolysis to the TCA cycle (Tymoczko et al. 2013). Mammalian pyruvate dehydrogenase complex (PDC) has multiple copies of 6 different components but the three major components are (i) pyruvate dehydrogenase (E1), (ii) dihydrolipoamide acetyltransferase (E2), (iii) dihydrolipoamide dehydrogenase (E3) (De Marcucci and Lindsay 1985; Jilka et al. 1986). E1, E2, and E3 are the major catalytic components, which are responsible for the stepwise decarboxylation and dehydrogenation of pyruvate into acetyl- CoA (Patel and Roche 1990). The activity of PDC is regulated by different metabolic precursors such

as ATP/ADP, NADH/NAD, and Acetyl-CoA/CoA ratios (Kerbey et al. 1976) . Other than the different precursor's ratios, pyruvate dehydrogenase kinase (PDK) and phospho-E1-phosphatase are also involved in the regulation of PDC (Whitehouse et al. 1974; Kato et al. 2005). The $E_1\alpha$ component of the tetrameric E1 component of the PDC is inactivated/phosphorylated by pyruvate dehydrogenase kinase (PDK) enzyme and activated/dephosphorylated by a specific phosphatase enzyme. The dephosphorylation of these sites by phospho-E1-phosphotase leads to the activation of the enzyme (Frey et al. 1989; Patel and Roche 1990).

In humans, PDH deficiency disease is X-linked (Lissens et al. 2000); it reduces mitochondrial function and is associated with different abnormalities. It results in 2 forms of abnormality: a metabolic form (lactic acidosis) and a neurological form (neurodevelopment delay and hypotonia) (Patel et al. 2012). Studies showed that PDH is also involved in the oncogene-induced senescence (Bonnet et al. 2007; Kaplon et al. 2013); activation of PDH enhances pyruvate utilization and increases respiration and redox stress (Bonnet et al. 2007).

Studies showed that DCA inhibited pyruvate dehydrogenase kinase by inducing allosteric changes in it and activated PDC activity (Kato et al. 2005). DCA was used to activate the PDC activity in different diseased states based on PDH deficiency (Stacpoole et al. 1978; Li et al. 2015). However, monoHAAs were involved in the blockage of glycolysis due to monoHAA-induced GAPDH inhibition (Pals et al. 2011). Previous studies revealed that monoHAAs induced their cytotoxicity and genotoxicity by generating oxidative stress (Pals et al. 2013). The HAA-generated ROS induced toxicity was based on the inhibition of GAPDH (Kahlert and Reiser 2000; Pals et al. 2011), ATP depletion, pyruvate remediation of cell stress and genotoxicity, and rescue against genotoxicity by antioxidants (Cemeli et al. 2006; Dad et al. 2013). However, the differences among the toxicity mechanisms of mono-, di-, and triHAAs are still unknown. We postulate that di-, and triHAAs are inhibiting PDK and activate PDC leading to increased cellular ATP levels. Where monoHAAs are the strongest inhibitors of GAPDH and greatly reduce ATP levels leading to ATP/ADP ratio disruption and require cells to accelerate TCA cycle by increasing PDC activity. To test this hypothesis we analyzed the effect of all HAAs on GAPDH kinetics, cellular energy level and PDC activity.

Effect of HAAs on GAPDH Kinetics

CHO cells were grown to confluence in a 60 mm plastic petri-plate in F12 5% FBS and then homogenized. GAPDH kinetic study was performed on homogenates treated with HAAs for 2 min. Results showed that monoHAAs were the strongest inhibitors of GAPDH, which agrees with the previous study (Pals et al. 2011). Figure 3.1 presents the percent reduction in GAPDH activity by 1 μM HAA. These data demonstrated that monoHAAs are the strongest inhibitors of GAPDH as comparaed to di-, and triHAAs. Among monoHAAs, IAA was the strongest inhibitor of GAPDH followed by BAA and then CAA. However, di-, and triHAAs were weaker inhibitors of GAPDH. Figure 3.2 illustrates the percent reduction by 1 μmol BAA, DBA, and TBA as representative of the mono-, di-, and triHAAs. Data for the GAPDH kinetic study from BAA, DBA, and TCA treated cells showed that monoHAAs were the strongest inhibitors of GAPDH as 1 μmol of BAA reduced GAPDH activity by 478.3% , where DBA reduced the activity by 37.5% and TBA reduced the activity by 21%. These data suggest that monoHAAs are the strongest inhibitors of GAPDH, where di-, and triHAAs are the weaker inhibitors of GAPDH. GAPDH is a pivotal enzyme in glycolysis and plays a crucial role in cellular energy homeostasis. Our data showed that HAAs are the inhibitors of GAPDH; to study the association between GAPDH inhibition and ATP depletion; we also studied the effect of HAAs on the cellular ATP levels.

The Effect of HAAs on ATP Levels in Chinese Hamster Ovary Cells

CHO cells were treated with HAAs for 4 h in HBSS (with 1.3 mM $CaCl_2$ and 1.1 mM $MgSO_4$) using different concentrations. The concentrations used in this experiment were based on the genotoxicity and cytotoxicity data of HAAs determined previously (Plewa et al. 2010) (Figure 3.3). To test for a significant difference between the effect of an HAA on the cellular ATP levels and its concurrent negative control a t-test analysis was performed, which is presented in Table 3.1. Results showed that monoHAAs greatly reduced the ATP levels as compared to the "concurrent negative control" and as compared to di-, and triHAAs. Figure 3.3 illustrates the effect of HAAs on ATP levels as pmol ATP/mg protein normalized against 100% for each concurrent negative control for each HAA treatment group. All HAAs except TCA induced significant alterations of cellular ATP levels. The reduction in ATP levels by di-, and triHAAs was also expected, as they were also the weak inhibitors of GAPDH. However, some of

the triHAAs (TBA, CDBA, DCBA) induced a significant increase on cellular ATP levels. An interesting trend was found in the ATP levels and the number of halogens attached (Table 3.1 and Figure 3.3-3.4). MonoHAAs induced the greatest reduction in ATP levels, where diHAAs induced a moderate reduction with higher concentration ranges. TriHAAs induced a significant increase in ATP levels except for TCA. MonoHAAs and diHAAs decreased the ATP levels by 59.1% and 27.1% as compared to the negative control, respectively. Where the average ATP levels as the percent of the negative control for triHAAs was 120%, meaning that triHAAs increased the cellular ATP (Figure 3.4). The unexpected increase in ATP levels by triHAAs suggested that these HAAs may have other targets involved in ATP regulation pathways. Previous studies demonstrated that DCA and TCA inhibited PDK (Whitehouse et al. 1974; Kato et al. 2005) and elevated the active/phosphorylated proportion of PDC (Whitehouse et al. 1974). The decorboxylation of pyruvate into acetyl-CoA by PDC links glycolysis to the TCA cycle and is a rate-limiting step as the pyruvate decarboxylation by PDC provides substrate (acetyl-CoA) for the TCA cycle (Tymoczko et al. 2013). Kerby et al showed that 1 mM DCA increased the active proportion of PDC in rat heart by inhibiting PDK and also showed that there was an inverse relation between NADH/NAD^+, ATP/ADP, and acetyl-CoA/CoA and active proportion of PDC with a few exceptions (Kerbey et al. 1976). The GAPDH inhibition kinetics data showed that Di-, and triHAAs were relatively weaker inhibitors of GAPDH and triHAAs increased ATP levels where diHAAs induced a moderate reduction in ATP levels. MonoHAAs were the strongest inhibitors of GAPDH and greatly reduced ATP contents. From previous studies, we also know that TCA cycle and oxidative phosphorylation are the pivotal steps in the cellular energy homeostasis. Since TCA is dependent on PDC for its substrate, PDC regulation plays an important role in overall energy homeostasis. PDC is either regulated by different metabolite ratios such as the NADH/NAD^+, ATP/ADP, and acetyl-CoA/CoA, and also by PDK (Kerbey et al. 1976; Kato et al. 2005). It would be interesting to see the effect of these HAAs on the overall PDC activity and the difference among the mode of actions of these HAAs on PDC activity modulation.

Effect of HAAs on Pyruvate Dehydrogenase Complex Activity

Data in Figure 3.1-3.3 demonstrated that monoHAAs were the strongest inhibitors of GAPDH and greatly reduced the ATP contents of the cells. However, di-, and triHAAs were

relatively weaker inhibitors of GAPDH and triHAAs unexpectedly increased the ATP contents of cells as compared to the negative control. PDC activity is regulated by different cellular metabolite ratios e.g. $NADH/NAD^{+}$, ATP/ADP, and acetyl-CoA/CoA, and also by PDH phosphorylation state, which is controlled by PDK; based on these data and the PDC activity regulation mechanisms, we hypothesize that monoHAAs activate PDC activity by reducing ATP contents of the cells due to the strong GAPDH inhibition leading to ATP/ADP ratio disruption, which requires cells to activate PDC activity and eventually TCA cycle to produce more energy and maintain the ATP/ADP. However, di-, and triHAAs are the weaker inhibitors of GAPDH and increase the ATP contents of the cells; we hypothesize that di-, and triHAAs increase the ATP contents of the cells due to PDK inhibition, which leads to increased PDC activity and elevated levels of ATP contents. To test this hypothesis, PDC activity was measured in CHO cells cultured in F12 5% FBS medium using different concentrations of HAAs. Concentrations, which gave best response, were used for further experiments. PDC kinetics activity was measured for 60 min at 10 min interval and the final data were recorded as nmol NADH/min/mg protein. We found that most of the HAAs except BCA and BDCA increased the PDC activity. The Data demonstrated that monoHAAs greatly increased the PDC activity as compared to di-, and triHAAs. Among monoHAAs , IAA had the highest increase in PDC activity, which was 369.5% of the negative control followed by BAA (308.1%) and then by CAA (193.8%) (Table.3.2). Previous studies and our current GAPDH kinetics study and ATP data showed that IAA is the strongest inhibitor of GAPDH and greatly reduces ATP levels followed by BAA and then CAA (Pals et al. 2011; Dad et al. 2013). Previous studies also demonstrated that there was an inverse relation between $NADH/NAD^{+}$, ATP/ADP, and acetyl-CoA/CoA and active proportion of PDC (Kerbey et al. 1976). Therefore, an increase in the PDC activity by monoHAAs corroborated with findings from previous studies and showed an inverse relation with ATP/ADP ratio. The pattern (IAA > BAA >> CAA) found in PDC activity increase was also correlated with the pattern found in other HAA toxicity potentials (Pals et al. 2011; Dad et al. 2013) Among diHAAs , DCA increased PDC activity to 135.4% of the negative control and DBA increased the activity to 184.30% of the negative control (Table 3.2). However, BCA did not increase PDC activity and had no significant effect on PDC activity. Similarly, triHAAs also increased the PDC activity except CDBA and BDCA. Among triHAAs, TBA increased PDC activity to 255.2% of the negative control where, TCA increased the PDC activity to 148.3% of

the negative control. However, BDCA significantly decreased the PDC activity to 35.4% as compared to the negative control while CDBA had no significant effect on PDC activity. The significant increase or decrease by HAAs in PDC activity as compared to negative control is presented in the Figure 3.5. These data demonstrated that increased PDH activity by monoHAAs was due to disturbances in the metabolite ratios (ATP/ADP, NADH/$NAD^{+)}$ induced by GAPDH inhibition while di-, and triHAAs were the weaker inhibitors of GAPDH and had no drastic reduction in the ATP levels (Figure 3.3) , which suggests that increased PDC activity by di-, and triHAAs was due to the inhibition of PDK . We also saw a significant increase in PDC activity by DCA 50 μM and TCA 300μM (Figure 3.5), which conforms to previous studies (Whitehouse et al. 1974; Kato et al. 2005). Concentrations based on genotoxicity potential were used for the initial ATP study but those concentrations were different than what we used for PDC activity to achieve better resolution of the assays. We repeated the ATP study with the same concentrations that were explored in the PDC activity study to determine if this relationship between the PDC activity under HAA's effect and its role in cellular energy homeostasis could be replicated. We observed exactly the same pattern for the HAA effect on ATP alterations as it was found in PDC activity study in HAA-treated cells. ATP data (Table 3.3) showed that all the monoHAAs significantly reduced the ATP contents of the cells and we found an inverse relation between the ATP content and PDC activity under the monoHAA effect. Among the diHAAs, DCA significantly increased cellualr ATP content to 207.4% as compared to negative control (Table 3.3). 50 μM DCA significantly increased the PDC activity as well (Figure 3.5). Therefore, increase in PDC activity and changes in energy homeostasis by DCA is not due to changes in the metabolite ratios induced by GAPDH inhibition but due to allosteric changes induced in PDK by DCA, leading to inhibition of PDK and activation of PDC, which also agrees with previous studies (Kerbey et al. 1976; Kato et al. 2005). Other di-, and triHAAs such as DBA, TBA, and TCA increased ATP contents to 128.5%, 114.4%, and 128.1% respectively. However, BCA and CDBA had no significant effect on cellular ATP contents like its effect on PDC activity, where DCBA significantly decreased the ATP contents to 37.7% as compared to negative control (Table 3.3). The significant increase or decrease in the ATP contents of HAA-treated cells is shown in Figure 3.6.

3.4. CONCLUSION

The GAPDH kinetics study, cellular ATP contents analysis, and PDC activity under the effect of HAAs demonstrated that mono-, di-, and triHAAs are affecting the cellular metabolism by disrupting the cellular energy homeostasis. However, there are some differences among their modes of action. MonoHAAs induce toxicity by inhibiting GAPDH and reducing the ATP contents of the cells. Disturbances in different cellular metabolite ratios such as ATP/ADP, and NADH/NAD, under the monoHAA-effect, require cells to activate the TCA cycle and rescue cells against the monoHAA-induced metabolites scarcity by activating the PDC activity, which also signifies an inverse relationship between the different metabolite ratios and PDC activity. Where di-, and triHAAs are the weak inhibitors of GAPDH and disrupt cellular energy homeostasis by inhibiting PDK, which leads to PDC activation, TCA cycle acceleration, and eventually cellular ATP levels elevation. Our results supported our hypothesis and demonstrated that monoHAAs induce their toxicity by indirectly affecting mitochondrial metabolism due to GAPDH inhibition where, di-, and triHAAs have a direct effect on mitochondrial metabolism by inhibiting PDK enzyme and activating PDC.

3.5. TABLES AND FIGURES

Table 3.1. Effects of the HAAs on ATP levels compared to its concurrent negative control in CHO cells and t-test statistical analysis calculated with the LUM as the % of negative control.

HAA Group	Average LUM (RLU ± SE)	Average LUM as the % of control (± SE)	*t*	*P*
CAA control	4142.4 ± 185.6	100.00 ± 4.48	10.820	<0.001
CAA 700 µM	1386.9 ± 174.4	33.48 ± 4.21		
BAA control	5195.4 ± 222.9	100.00 ± 4.29	10.943	<0.001
BAA 15 µM	2585.0 ± 94.5	49.76 ± 1.82		
IAA control	4856.3 ± 309.2	100.00 ± 6.37	8.529	<0.001
IAA 4 µM	1917.0 ± 152.2	39.47 ± 3.13		
DCAA control	4708.8 ± 90.4	100.00 ± 1.92	3.133	0.003
DCAA 2000 µM	4296.0 ± 96.0	103.71 ± 2.04		
DBAA control	5270.1 ± 93.7	100.00 ± 1.78	14.270	<0.001
DBAA 700 µM	3707.1 ± 56.6	70.34 ± 1.07		
BCAA control	6309.8 ± 177.4	100.00 ± 2.81	9.545	<0.001
BCAA 700 µM	4147.8 ± 136.2	66.16 ± 2.16		
TCAA control	4760.9 ± 226.3	100.00 ± 4.75	-0.749	0.456
TCAA 2000 µM	4969.6 ± 164.5	104.38 ± 3.46		
TBAA control	4220.3 ± 208.5	100.00 ± 4.94	-3.830	<0.001
TBAA 1000 µM	5168.1 ± 133.3	122.46 ± 3.16		
BDCAA control	4852.3 ± 82.8	100.00 ± 1.71	-5.453	<0.001
BDCAA 2000 µM	5883.6 ± 165.8	121.25 ± 3.42		
DBCAA control	4771.7 ± 191.4	100.00 ± 4.01	-4.473	<0.001
DBCAA 1000 µM	6044.0 ± 210.4	126.66 ± 4.41		

Table 3.1. (Continued)

Abbreviations: HAA, haloacetic acid; CAA, chloroacetic acid; BAA, bromoacetic acid; IAA, iodoacetic acid; DCAA, dichloroacetic acid; DBAA, dibromoacetic acid; BCAA, bromochloroacetic acid; TCAA, trichloroacetic acid; TBAA, tribromoacetic acid; BDCAA, bromodichloroacetic acid; DBCAA, dibormochloroacetic acid; LUM, luminescence; RLU, relative light unit; SE, standard error.

Table: 3.2. Effect of HAAs on percent alteration of pyruvate dehydrogenase complex activity as nmol NADH/min/mg protein

Treatment Group	Treatment Concentration (μM)	nmol NADH/min/mg protein as % of negative control	±SE
Negative Control	-	100.01	4.34
IAA	3	369.50	20.34
BAA	15	308.12	41.65
CAA	300	193.79	11.71
DCA	50	135.40	8.46
BCA	900	74.23	16.52
DBA	900	184.30	7.90
TBA	500	255.21	43.64
TCA	300	148.31	4.76
CDBA	300	107.18	5.67
BDCA	900	35.44	8.91

Table:3.3. Effect of HAAs on percent alteration of ATP as pmol ATP/mg protein as compared to negative control.

Treatment Group	Treatment Concentration (μM)	pmolATP/mg protein as % of negative control	±SE
Negative Control	-	100	6.20
IAA	3	28.08	3.76
BAA	15	14.29	5.00
CAA	300	52.18	5.31
DCA	50	207.38	15.72
BCA	900	73.30	4.81
DBA	900	128.55	10.27
TBA	500	114.35	11.26
TCA	300	128.05	6.90
CDBA	300	108.37	6.57
BDCA	900	37.71	2.41

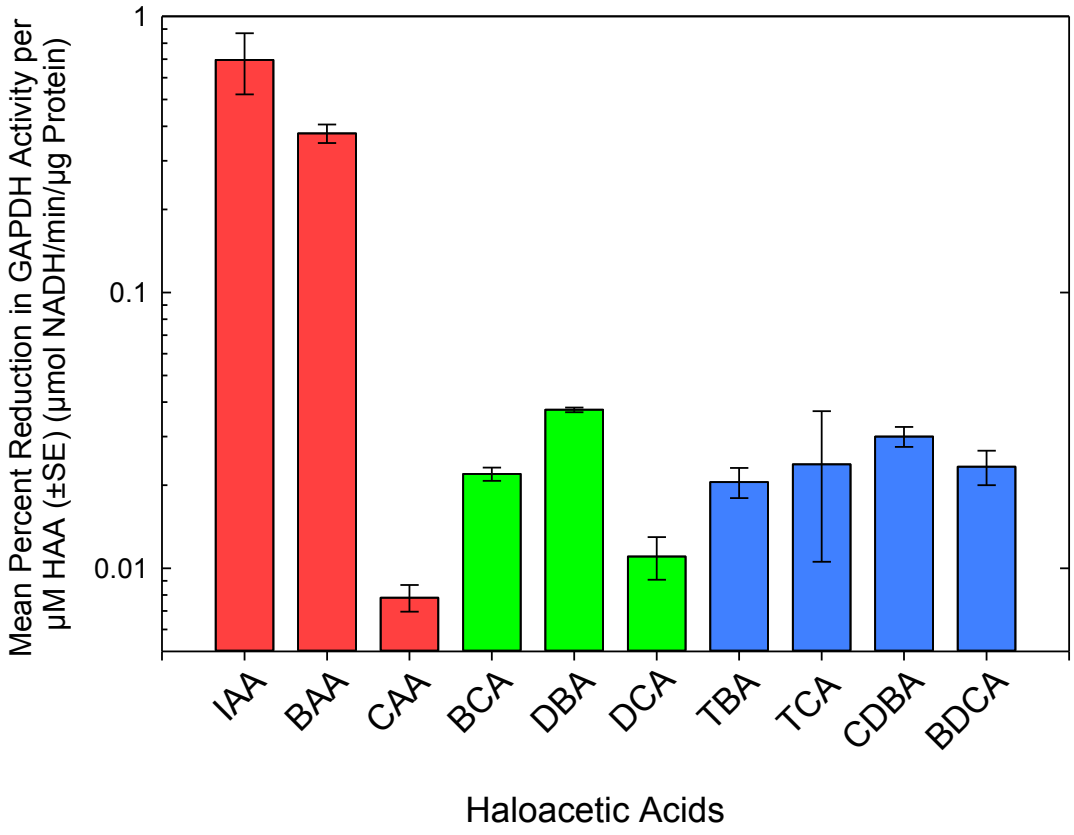

Figure 3.1. Percent reduction in GAPDH activity by 1µM of each HAA. MonoHAAs were the strongest inhibitors of GAPDH activity, where di-, and triHAAs were the weaker inhibitors of GAPDH.

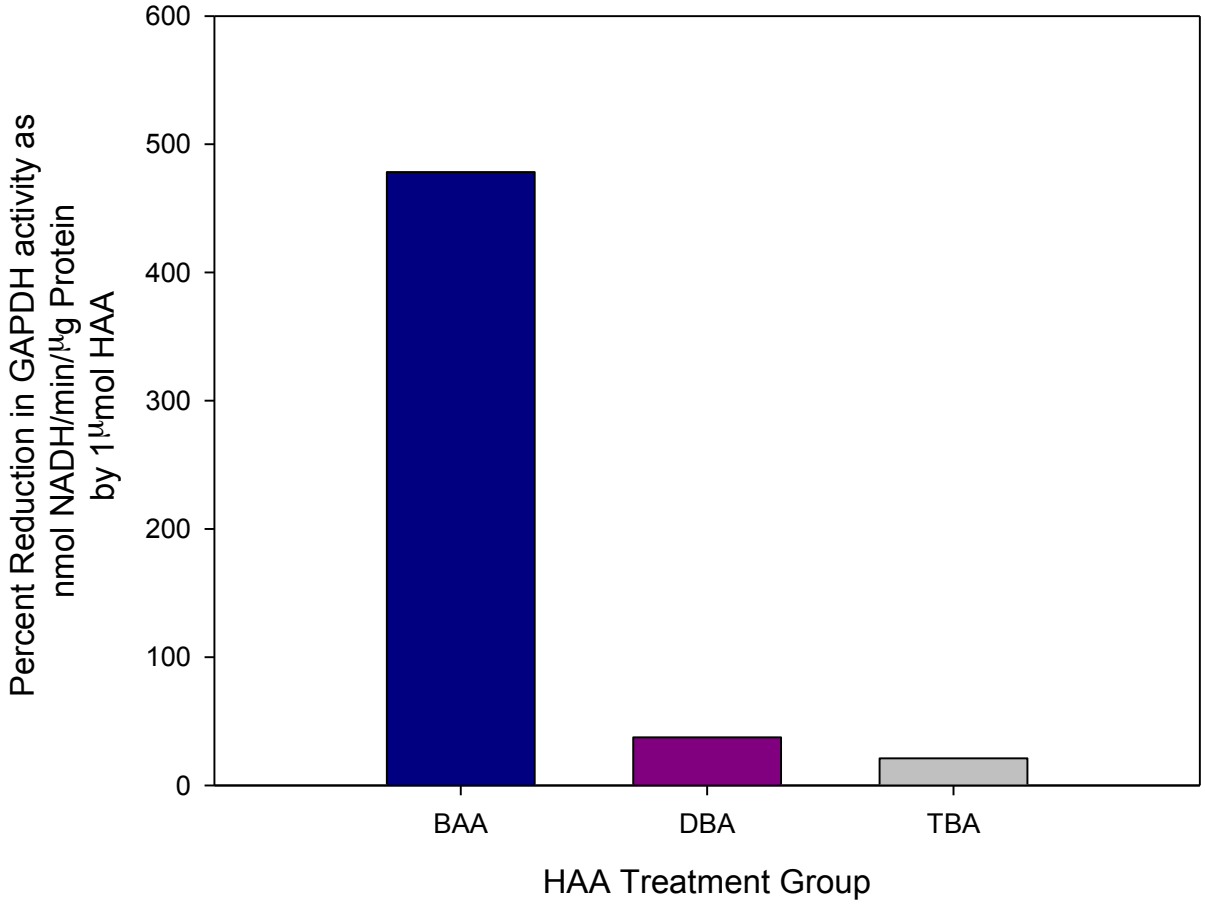

Figure 3.2. BAA, DBA, and TBA as representatives of mono-, di-, and triHAAs with its effect on GAPDH activity as percent reduction in GAPDH activty/nmol NADH/min/µg protein by 1 µmol of the given HAAs.

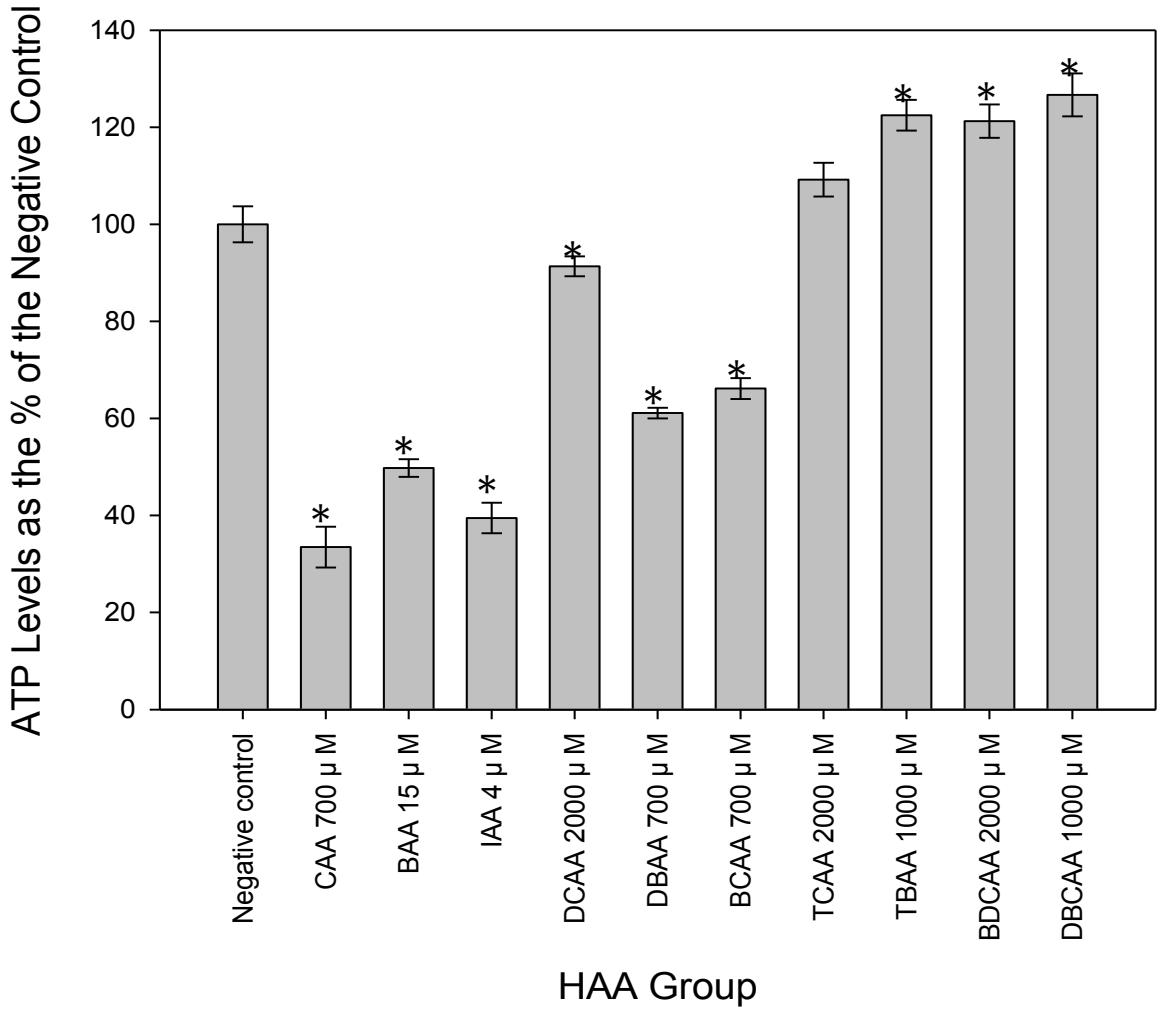

Figure 3.3. Effect of HAA-exposure on the ATP contents of the cells. ATP levels for each treatment group are normalized against the negative control/100%. The * indicates a statistically significant difference from their concurrent negative control.

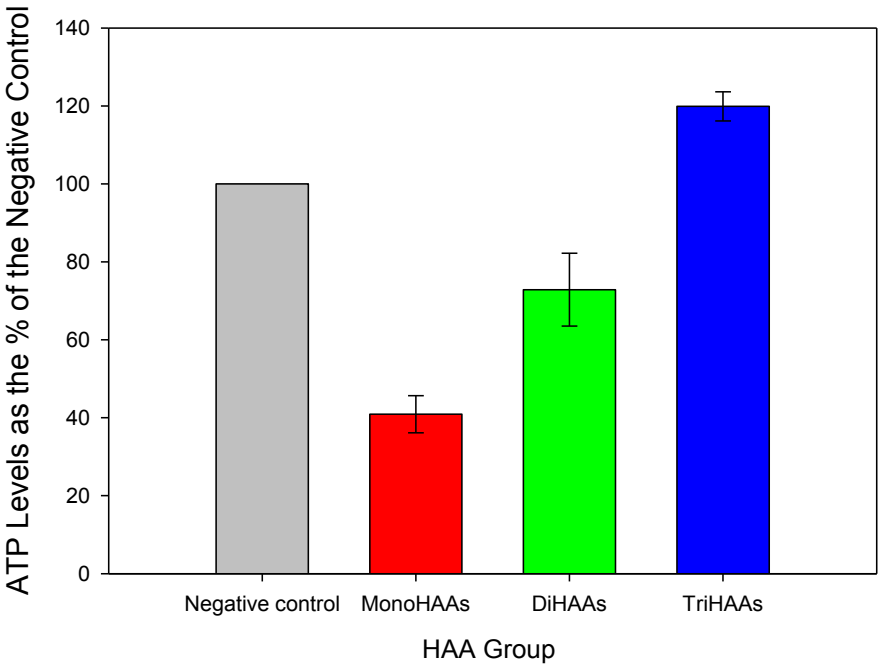

Figure 3.4. Average ATP data catagorized in three groups based on number of halogens present in each HAA treatment group. ATP levels were normalized against each concurrent negative control.

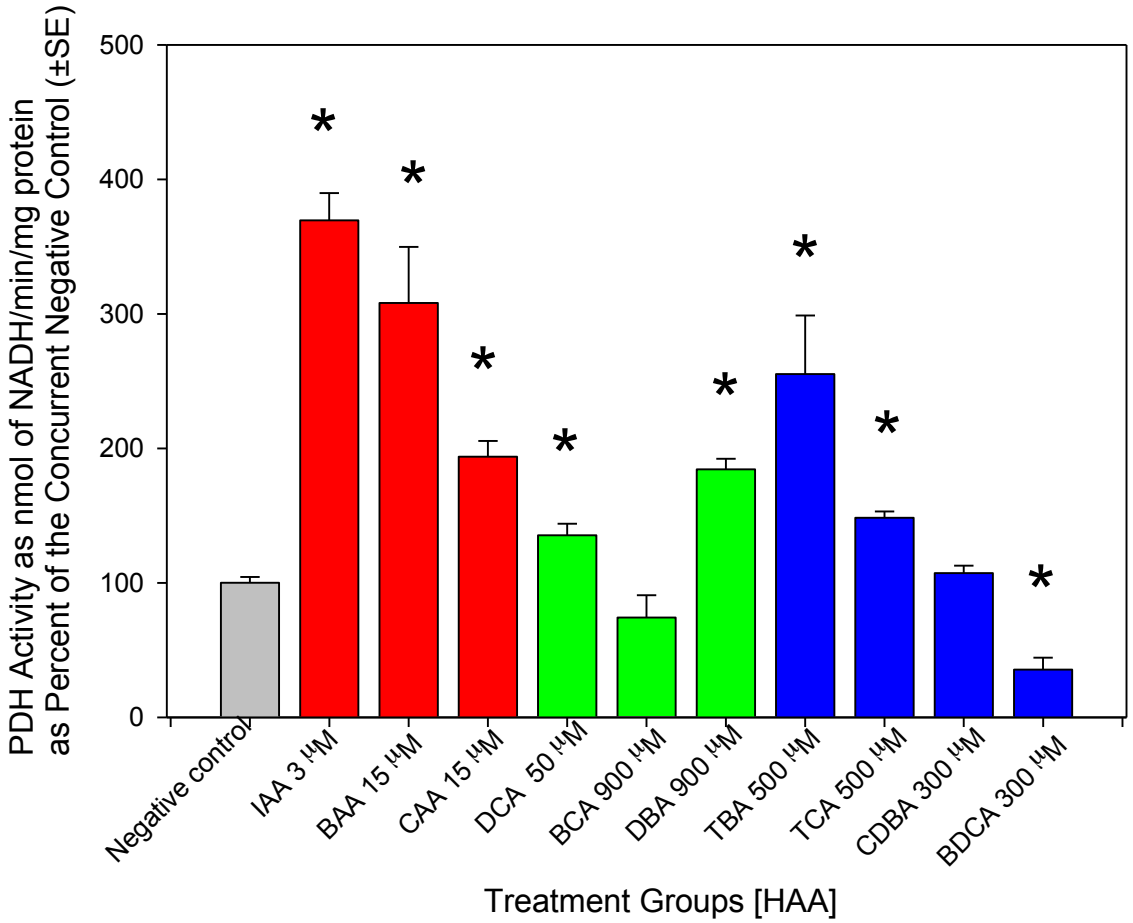

Figure 3.5. Effect of HAAs on CHO PDC activity (nmolNADH/min/mg protein). PDC activity for each HAA treatment group was normalized against each concurrent negative control/100% and the negative control shown here is the average of all the negative control groups. The * indicates a statistically significant difference from their concurrent negative control.

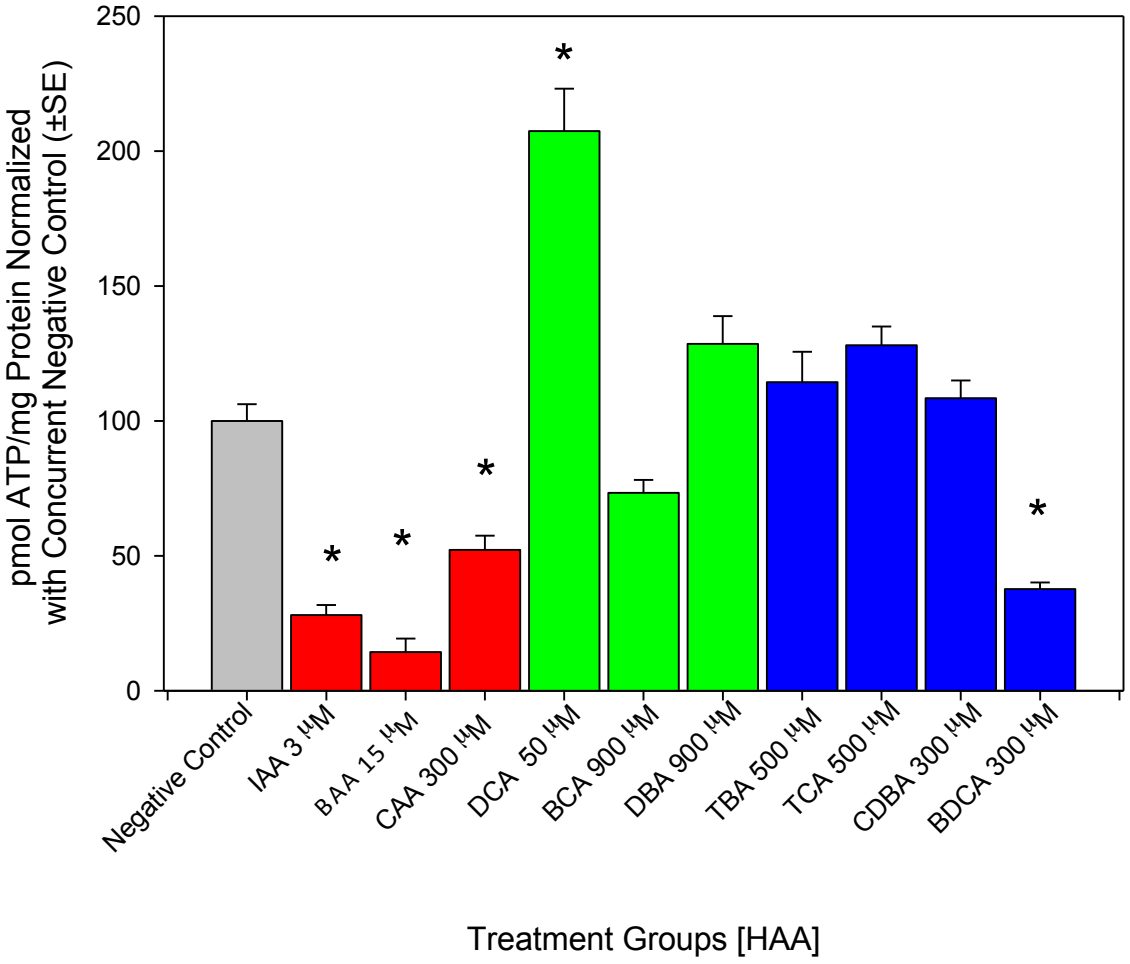

Figure 3.6. Effect of HAAs on cellular ATP levels (pmol ATP/mg protein). ATP levels for each HAA treatment group was normalized against each concurrent negative control and the negative control shown here is the average of all the negative control groups. The * indicates a statistically significant difference from the negative control.

3.6. REFERENCES

Andrews JE, Nichols HP, Schmid JE, Mole LM, Hunter ES, 3rd, Klinefelter GR. 2004. Developmental toxicity of mixtures: the water disinfection by-products dichloro-, dibromo- and bromochloro acetic acid in rat embryo culture. Reprod Toxicol 19(1):111-116.

Attene-Ramos MS, Nava GM, Muellner MG, Wagner ED, Plewa MJ, Gaskins HR. 2010. DNA damage and toxicogenomic analyses of hydrogen sulfide in human intestinal epithelial FHs 74 Int cells. Environ Mol Mutagen 51(4):304-314.

Ban C, Junop M, Yang W. 1999. Transformation of MutL by ATP binding and hydrolysis: a switch in DNA mismatch repair. Cell 97(1):85-97.

Bonnet S, Archer SL, Allalunis-Turner J, Haromy A, Beaulieu C, Thompson R, Lee CT, Lopaschuk GD, Puttagunta L, Bonnet S, Harry G, Hashimoto K, Porter CJ, Andrade MA, Thebaud B, Michelakis ED. 2007. A Mitochondria-K+ Channel Axis Is Suppressed in Cancer and Its Normalization Promotes Apoptosis and Inhibits Cancer Growth. Cancer Cell 11(1):37-51.

Browning M, Baudry M, Bennett WF, Lynch G. 1981. Phosphorylation-mediated changes in pyruvate dehydrogenase activity influence pyruvate-supported calcium accumulation by brain mitochondria. J Neurochem 36(6):1932-1940.

Cemeli E, Wagner ED, Anderson D, Richardson SD, Plewa MJ. 2006. Modulation of the cytotoxicity and genotoxicity of the drinking water disinfection byproduct lodoacetic acid by suppressors of oxidative stress. Environ Sci Technol 40(6):1878-1883.

Cutler D, Miller G. 2005. The role of public health improvements in health advances: The twentieth-century United States. Demography 42(1):1-22.

Dad A, Jeong CH, Pals JA, Wagner ED, Plewa MJ. 2013. Pyruvate remediation of cell stress and genotoxicity induced by haloacetic acid drinking water disinfection by-products. Environ Mol Mutagen 54(8):629-637.

De Marcucci O, Lindsay JG. 1985. Component X. An immunologically distinct polypeptide associated with mammalian pyruvate dehydrogenase multi-enzyme complex. European Journal of Biochemistry 149(3):641-648.

Dhar S, Lippard SJ. 2009. Mitaplatin, a potent fusion of cisplatin and the orphan drug dichloroacetate. Proc Natl Acad Sci U S A 106(52):22199-22204.

Evans OB, Stacpoole PW. 1982. Prolonged hypolactatemia and increased total pyruvate dehydrogenase activity by dichloroacetate. Biochem Pharmacol 31(7):1295-1300.

Fouque Fo, Brivet M, Boutron A, Vequaud C, Marsac Cc, Zabot M-Trs, Benelli C. 2003. Differential Effect of DCA Treatment on the Pyruvate Dehydrogenase Complex in Patients with Severe PDHC Deficiency. Pediatr Res 53(5):793-799.

Frey PA, Flournoy DS, Gruys K, Yang YS. 1989. Intermediates in reductive transacetylation catalyzed by pyruvate dehydrogenase complex. Annals of the New York Academy of Sciences 573:21-35.

George SE, Nelson GM, Swank AE, Brooks LR, Bailey K, George M, DeAngelo A. 2000. The disinfection by-products dichloro-, dibromo-, and bromochloroacetic acid impact intestinal microflora and metabolism in Fischer 344 rats upon exposure in drinking water. Toxicol Sci 56(2):282-289.

Health Canada. 2008. Guidelines for Canadian Drinking Water Quality: Guideline Technical Document — Haloacetic Acids.

Hunter ES, 3rd, Rogers EH, Schmid JE, Richard A. 1996. Comparative effects of haloacetic acids in whole embryo culture. Teratology 54(2):57-64.
Itoh Y, Esaki T, Shimoji K, Cook M, Law MJ, Kaufman E, Sokoloff L. 2003. Dichloroacetate effects on glucose and lactate oxidation by neurons and astroglia in vitro and on glucose utilization by brain in vivo. Proc Natl Acad Sci U S A 100(8):4879-4884.
J.M. B, J.L. T, L. S. 2002. Entry to the Citric Acid Cycle and Metabolism Through It Are Controlled. Biochemistry. 5th ed. New York: W H Freeman.
Jena NR. 2012. DNA damage by reactive species: Mechanisms, mutation and repair. J Biosci 37(3):503-517.
Jilka JM, Rahmatullah M, Kazemi M, Roche TE. 1986. Properties of a newly characterized protein of the bovine kidney pyruvate dehydrogenase complex. J Biol Chem 261(4):1858-1867.
Kahlert S, Reiser G. 2000. Requirement of glycolytic and mitochondrial energy supply for loading of Ca2+ stores and InsP(3)-mediated Ca2+ signaling in rat hippocampus astrocytes. J Neurosci Res 61(4):409-420.
Kaplon J, Zheng L, Meissl K, Chaneton B, Selivanov VA, Mackay G, van der Burg SH, Verdegaal EM, Cascante M, Shlomi T, Gottlieb E, Peeper DS. 2013. A key role for mitochondrial gatekeeper pyruvate dehydrogenase in oncogene-induced senescence. Nature 498(7452):109-112.
Kargalioglu Y, McMillan BJ, Minear RA, Plewa MJ. 2002. Analysis of the cytotoxicity and mutagenicity of drinking water disinfection by-products in Salmonella typhimurium. Teratog Carcinog Mutagen 22(2):113-128.
Kato M, Chuang JL, Tso SC, Wynn RM, Chuang DT. 2005. Crystal structure of pyruvate dehydrogenase kinase 3 bound to lipoyl domain 2 of human pyruvate dehydrogenase complex. Embo j 24(10):1763-1774.
Kato M, Li J, Chuang JL, Chuang DT. 2007. Distinct structural mechanisms for inhibition of pyruvate dehydrogenase kinase isoforms by AZD7545, dichloroacetate, and radicicol. Structure 15(8):992-1004.
Kerbey AL, Randle PJ, Cooper RH, Whitehouse S, Pask HT, Denton RM. 1976. Regulation of pyruvate dehydrogenase in rat heart. Mechanism of regulation of proportions of dephosphorylated and phosphorylated enzyme by oxidation of fatty acids and ketone bodies and of effects of diabetes: role of coenzyme A, acetyl-coenzyme A and reduced and oxidized nicotinamide-adenine dinucleotide. Biochem J 154(2):327-348.
Korotchkina LG, Patel MS. 1995. Mutagenesis studies of the phosphorylation sites of recombinant human pyruvate dehydrogenase. Site-specific regulation. J Biol Chem 270(24):14297-14304.
Korotchkina LG, Patel MS. 2001. Site specificity of four pyruvate dehydrogenase kinase isoenzymes toward the three phosphorylation sites of human pyruvate dehydrogenase. J Biol Chem 276(40):37223-37229.
Krasner SW. 2009. The formation and control of emerging disinfection by-products of health concern. Philos Trans A Math Phys Eng Sci 367(1904):4077-4095.
Krasner SW, Weinberg HS, Richardson SD, Pastor SJ, Chinn R, Sclimenti MJ, Onstad GD, Thruston Jr AD. 2006. Occurrence of a new generation of disinfection byproducts. Environ Sci Technol 40(23):7175-7185.

Li C, Meng G, Su L, Chen A, Xia M, Xu C, Yu D, Jiang A, Wei J. 2015. Dichloroacetate blocks aerobic glycolytic adaptation to attenuated measles virus and promotes viral replication leading to enhanced oncolysis in glioblastoma. Oncotarget 6(3):1544-1555.

Lissens W, De Meirleir L, Seneca S, Liebaers I, Brown GK, Brown RM, Ito M, Naito E, Kuroda Y, Kerr DS, Wexler ID, Patel MS, Robinson BH, Seyda A. 2000. Mutations in the X-linked pyruvate dehydrogenase (E1) alpha subunit gene (PDHA1) in patients with a pyruvate dehydrogenase complex deficiency. Hum Mutat 15(3):209-219.

McCormack JG, England PJ. 1983. Ruthenium Red inhibits the activation of pyruvate dehydrogenase caused by positive inotropic agents in the perfused rat heart. Biochemical Journal 214(2):581-585.

Narotsky MG, Best DS, McDonald A, Godin EA, Hunter ES, 3rd, Simmons JE. 2011. Pregnancy loss and eye malformations in offspring of F344 rats following gestational exposure to mixtures of regulated trihalomethanes and haloacetic acids. Reprod Toxicol 31(1):59-65.

Pals J, Ang J, Ramos MA, Marinas B, Wagner E, Plewa MJ. 2010. Investigating the Mechanism of DNA Damage Induced by Three Haloacetic Acid Drinking Water Disinfection ByProducts. Environmental and Molecular Mutagenesis 51(7):718-718.

Pals J, Attene-Ramos MS, Xia M, Wagner ED, Plewa MJ. 2013. Human cell toxicogenomic analysis linking reactive oxygen species to the toxicity of monohaloacetic acid drinking water disinfection byproducts. Environmental Science and Technology 47(21):12514-12523.

Pals JA, Ang JK, Wagner ED, Plewa MJ. 2011. Biological mechanism for the toxicity of haloacetic acid drinking water disinfection byproducts. Environ SciTechnol 45(13):5791-5797.

Patel KP, O'Brien TW, Subramony SH, Shuster J, Stacpoole PW. 2012. The spectrum of pyruvate dehydrogenase complex deficiency: clinical, biochemical and genetic features in 371 patients. Mol Genet Metab 105(1):34-43.

Patel MS, Korotchkina LG. 2003. The Biochemistry of the Pyruvate Dehydrogenase Complex. Biochemistry & Molecular Biology Education 31(1):5-15.

Patel MS, Roche TE. 1990. Molecular biology and biochemistry of pyruvate dehydrogenase complexes. FASEB J 4(14):3224-3233.

Plewa MJ, Kargalioglu Y, Vankerk D, Minear RA, Wagner ED. 2002. Mammalian cell cytotoxicity and genotoxicity analysis of drinking water disinfection by-products. Environmental and Molecular Mutagenesis 40(2):134-142.

Plewa MJ, Simmons JE, Richardson SD, Wagner ED. 2010. Mammalian cell cytotoxicity and genotoxicity of the haloacetic acids, a major class of drinking water disinfection by-products. Environ Mol Mutagen 51(8-9):871-878.

Plewa MJ, Wagner ED, Richardson SD, Thruston Jr AD, Woo YT, McKague AB. 2004. Chemical and biological characterization of newly discovered iodoacid drinking water disinfection byproducts. Environ Sci Technol 38(18):4713-4722.

Richardson SD, Plewa MJ, Wagner ED, Schoeny R, DeMarini DM. 2007. Occurrence, genotoxicity, and carcinogenicity of regulated and emerging disinfection by-products in drinking water: A review and roadmap for research. Mutation Research-Reviews in Mutation Research 636(1-3):178-242.

Richardson SD, Simmons JE, Rice G. 2002. Disinfection byproducts: The next generation. Environmental Science and Technology 36(9):198A-205A.

Sale GJ, Randle PJ. 1981. Analysis of site occupancies in [32P]phosphorylated pyruvate dehydrogenase complexes by aspartyl-prolyl cleavage of tryptic phosphopeptides. Eur J Biochem 120(3):535-540.

Stacpoole PW, Kerr DS, Barnes C, Bunch ST, Carney PR, Fennell EM, Felitsyn NM, Gilmore RL, Greer M, Henderson GN, Hutson AD, Neiberger RE, O'Brien RG, Perkins LA, Quisling RG, Shroads AL, Shuster JJ, Silverstein JH, Theriaque DW, Valenstein E. 2006. Controlled clinical trial of dichloroacetate for treatment of congenital lactic acidosis in children. Pediatrics 117(5):1519-1531.

Stacpoole PW, Moore GW, Kornhauser DM. 1978. Metabolic effects of dichloroacetate in patients with diabetes mellitus and hyperlipoproteinemia. N Engl J Med 298(10):526-530.

Stuart WK. 2009. The formation and control of emerging disinfection by-products of health concern. Philosophical Transactions of the Royal Society A: Mathematical, Physical & Engineering Sciences 367(1904):4077-4095.

Tymoczko JL, Berg JM, Stryer L. 2013. Biochemistry; a short course. 2nd ed. Houndmills, Basingstoke RG21 6XS, England: W. H. Freeman and Company p683.

U. S. Environmental Protection Agency. 2006. National Primary Drinking Water Regulations; Stage 2 Disinfectants and Disinfection Byproducts Rule. Fed Reg 71(2):387-493.

U. S. Environmental Protection Agency. 1998. National Primary Drinking Water Regulations: Disinfectants and Disinfection Byproducts. 69390-69476 p.

Villanueva CM, Cantor KP, Grimalt JO, Malats N, Silverman D, Tardon A, Garcia-Closas R, Serra C, Carrato A, Castaño-Vinyals G, Marcos R, Rothman N, Real FX, Dosemeci M, Kogevinas M. 2007. Bladder cancer and exposure to water disinfection by-products through ingestion, bathing, showering, and swimming in pools. Am J Epidemiol 165(2):148-156.

Wagner ED, Rayburn AL, Anderson D, Plewa MJ. 1998. Analysis of mutagens with single cell gel electrophoresis, flow cytometry, and forward mutation assays in an isolated clone of Chinese hamster ovary cells. Environ Mol Mutagen 32(4):360-368.

Waller K, Swan SH, DeLorenze G, Hopkins B. 1998. Trihalomethanes in drinking water and spontaneous abortion. Epidemiology 9(2):134-140.

Wei XW, S.; Zheng, W.; Wang, X.; Liu, X.; Jiang, S.; He, G.; Zheng, Y.; Qu, W., . 2013. Tumorigenicity of drinking water disinfection byproduct iodoacetic acid in NIH3T3 cells. Envion Sci Technol Submitted.

Whitehouse S, Cooper RH, Randle PJ. 1974. Mechanism of activation of pyruvate dehydrogenase by dichloroacetate and other halogenated carboxylic acids. Biochemical Journal 141(3):761-774.

Wigley DB, Davies GJ, Dodson EJ, Maxwell A, Dodson G. 1991. Crystal structure of an N-terminal fragment of the DNA gyrase B protein. Nature 351(6328):624-629.

Wikipedia. https://en.wikipedia.org/wiki/Warburg_effect.

Zhang SH, Miao DY, Liu AL, Zhang L, Wei W, Xie H, Lu WQ. 2010. Assessment of the cytotoxicity and genotoxicity of haloacetic acids using microplate-based cytotoxicity test and CHO/HGPRT gene mutation assay. Mutat Res 703(2):174-179.

CHAPTER 4

TOXICITY OF DBPs GENERATED AFTER CHLORINATION OF WASTE WATER EFFLUENTS

4.1. INTRODUCTION

Domestic wastewaters have different pathogenic microorganisms such as viruses, enteric bacteria and protozoa. The wastewater use is associated with potential health risks through direct (drinking and every day domestic use) and indirect (irrigation) use, if the wastewater treatment process was not managed properly. Therefore, wastewaters are treated with different chemical disinfectants to control the potential health risks associated with wastewater contaminants (Food and Agriculture Organization of the United Nations). Different chemical disinfectants such as chlorine, chlorine dioxide, ozone, and chloramine are used to inactivate the pathogenic microorganisms (Krasner 2009). The most prevalent chemical disinfectant is chlorine in both Kingdom of Saudi Arabia (KSA) and USA. Chlorine can be supplied in different forms such as chlorine gas, hypochlorite solution and other chlorine compounds in solid or liquid form. Chlorine disinfection of the wastewaters not only destroys the pathogens at the time of treatment but chlorine residue in the wastewater effluents prolong this oxidation and destruction of the pathogenic cells even after the treatment time. However, chlorine residue in water is very toxic to aquatic life even if it is present at a very low concentration; it also produces some unwanted toxic water disinfection by-products due to oxidation of some organic material present in the wastewaters (U. S. Environmental Protection Agency 1999). In this study, the target waters are wastewater effluents containing ammonia and nitrogenous organic matter. Ammonia and organic nitrogen presence in excess with respect to the chlorine dose result in a very fast conversion of the free chlorine into monochloramine and organic chloramines. Chloramines then react with both inorganic and organic constituents in water forming a large number of disinfection byproducts (DBPs). Relevant reactions to this study involving inorganic species are the oxidation of iodide ion (I^-) by monochloramine (NH_2Cl) to form hypoiodous acid (HOI) (Bichsel and von Gunten 1999).

In this study, the cytotoxicity and genotoxicity potentials of the chlorinated and chloraminated wastewater effluents extracts, extracted through XAD-8 and XAD-4 were analyzed using in vitro CHO cells assays.

4.2. MATERIALS AND METHODS

XAD Resins

XAD-8 with acrylic ester composition, 250 angstrom pore diameter, 140 m^2/g of the specific surface area was used. Similarly XAD-4 with styrene divinylbenzene composition, 50 angstroms pore diameter, 750 m^2/g of specific surface area was used.

Wastewater Samples

Dr. Julien Le Roux shipped 10 mL of each of the concentrated organic extracts of the wastewater (WW) samples from King Abdullah University of Science and Technology to Dr. Plewa's laboratory at the University of Illinois in May 2014. The samples were derived from two experiments. The XAD-8/XAD-4 experimental design for the extraction of the organic fractions for each wastewater sample is illustrated in Figure 4.1.

Extraction; Experiment Series 1

76 L of chloraminated wastewater was extracted over XAD-8 and XAD-4 resins (Figure 4.1). The organics were eluted from the XAD columns using spectroscopy-grade ethyl acetate. The ethyl acetate volume was reduced over vacuum evaporation on a rotary evaporator. The samples were concentrated to 10 mL in ethyl acetate and shipped to Dr. Plewa's laboratory.

Experiment Series 2

In this experiment the toxicity of the organics concentrated from chlorinated wastewater (HOCl) or chloraminated (NH_2Cl) wastewater were compared. In addition, the spent wastewater (the wastewater that passed through each column) was further analyzed by liquid-liquid extraction using methyl tertiary butyl ether (MTBE) and concentrated using a rota-vaporator. This provided a measure of the residual toxicity that was retained in the wastewater after XAD extraction and provided a measure of the efficiency of XAD to isolate toxic agents in wastewater.

CHO Cell Chronic Cytotoxicity Analyses

Preparation and Storage of KAUST Wastewater Samples

The organic materials in the wastewater effluent samples that were concentrated over XAD-8 or XAD-4 were eluted in ethyl acetate and received from Drs. Jean-Philippe Croue and Julien Le Roux, logged into a spreadsheet file and stored at −20°C. The samples were solvent exchanged into dimethylsulfoxide (DMSO) at a concentration in that the organic material from 1 L of effluent was concentrated into 10 µL of DMSO (10^5× concentration) and stored in Teflon-sealed sample vials at −20°C.

CHO Cell Cytotoxicity Assay Protocol

The CHO cell microplate chronic cytotoxicity assay measures the reduction in cell density as a function of the concentration of the test agent over a 72 h period (Plewa et al. 2002; Plewa and Wagner 2009). A 96-well flat-bottomed microplate was used to evaluate a series of concentrations of wastewater effluent organic extracts. One column of eight microplate wells served as the blank control consisting of 200 µL of F12 + 5% fetal bovine serum (FBS) medium only. The concurrent negative control column consisted of eight wells with 3×10^3 CHO cells plus F12 +FBS medium. The remaining wells within the experiment contained 3×10^3 CHO cells, F12 +FBS and a known volume of water concentrate in a total of 200 µL. The wells were covered with a sheet of sterile Alumna Seal™. The microplate was placed on a rocking platform at 37°C for two 5 min-periods (turning the plate 90° after the first 5 min). This ensures an even distribution of cells across the bottom of the microplate wells. The cells were incubated for 72 h at 37°C at 5% CO_2. After the treatment time, the medium from each well was aspirated, the cells fixed in methanol for 10 min and stained for 10 min with a 1% crystal violet solution in 50% methanol. The microplate was washed, and 50 µL of DMSO/methanol (3:1 v/v) was added to each well, and the plate incubated at room temperature for 10 min. The microplate was analyzed at 595 nm with a Spectramax microplate reader; the absorbency of each well was recorded and stored on a spreadsheet file. This assay was calibrated and there is a direct relationship between the absorbency of the crystal violet dye associated with the cell and the number of viable cells.(Plewa et al. 2002)

The averaged absorbency of the blank wells was subtracted from the absorbency data from each microplate well. The mean blank-corrected absorbency value of the negative control

was set at 100%. The absorbency for each treatment group well was converted into a percentage of the negative control. This procedure normalizes the data, maintains the variance and allows for the combination of data from multiple microplates. The data were used to generate a concentration-response curve for each test agent. Regression analysis was applied to each test agent concentration-response curve, which was used to calculate the LC_{50}. The LC_{50} is the calculated concentration of test agent that induced a cell density that was 50% of the negative control. The original absorbency data, the blank-corrected data and the conversion to the percent of the negative control values were saved on the spreadsheet for each test agent analyzed. In general we analyzed 16-24 replicate clones for the negative controls and 4-6 replicate clones per concentration of the test agent with 10 concentrations of the test material. This provided the data with a high statistical power $(1-\beta) > 0.8$ ($\alpha = 0.05$) when an analysis of variance statistical test was conducted. Prior to conducting the complete chronic cytotoxicity assay, we conducted a screening assay. In the screening assay a serial dilution of the concentrated organic extract was prepared in F12 +FBS medium and one clone was analyzed per concentration. A screening assay provided a range of concentrations in which a more complete experimental design can be generated with replicate experiments.

CHO Cell Acute Genotoxicity Analyses

The single cell gel electrophoresis (SCGE) assay quantitatively measures the level of genomic DNA damage that was induced by the KAUST wastewater samples. The SCGE, or Comet, assay is a sensitive, quantitative method for the detection of genomic DNA damage in individual cells. (Tice et al. 2000; Rundell et al. 2003) The SCGE microplate assay was performed as previously published. (Wagner and Plewa 2009)

CHO Cell SCGE Assay Protocol

The day before treatment, 4×10^4 cells were cultured into each well of a 96-well microplate in 200 µL of F12 medium plus 5% FBS and incubated overnight. The following day, cells were washed twice with 100 µL of Hank's Balanced Salt Solution (HBSS) and treated with a series of concentrations of each water sample in a total volume of 25 µL. The cells were covered with sterile AlumnaSeal and incubated for 4 h at 37°C in a humidified atmosphere of 5% CO_2. Each experiment had a concurrent negative control (F12 medium only) and a positive control (3.8 mM ethylmethanesulfonate). After treatment, the cells were washed with HBSS

buffer, harvested with a 0.05% trypsin, 153 μM EDTA solution and incorporated into agarose microgels. For each concentration group, acute cytotoxicity was measured using the vital dye trypan blue. (Phillips 1973) The microgels were electrophoresed and analyzed if the viability of the cell suspensions was >70%. The microgels were placed in lysing solution overnight at 4°C to remove cell membranes (2.5 M NaCl, 100 mM Na_2EDTA, 10 mM Trizma base, 26 g of NaOH and 1% sodium lauryl sarcosinate, pH 10) with 10% DMSO and 1% Triton X-100 added just prior to use. The microgels were rinsed twice with cold deionized water and the DNA was denatured for 20 min in electrophoresis buffer (1 mM Na_2EDTA and 300 mM NaOH, pH 13.5). The microgels were electrophoresed for 40 min at 25 V, 300 mA (0.72 V/cm) at 4°C. After electrophoresis, the microgels were neutralized with 400 mM Tris buffer (pH 7.5), dehydrated in methanol (4°C) and dried for 5 min at 50°C. The microgels were stored in the dark at room temperature. To analyze the microgels, they were first hydrated in deionized water for 30 min at 4°C, stained with 65 μL of 20 μg/mL ethidium bromide and rinsed in cold deionized water. After staining, a cover slip was applied onto the microgel and 25 randomly selected nuclei per microgel were analyzed under a Zeiss fluorescence microscope with the Comet IV imaging system (Perceptive Instruments, Suffolk, UK). The data were automatically transferred to an Excel spreadsheet. For DNA damage the unit of measure for each microgel was the average % tail DNA, which is the amount of DNA that migrated into the gel from the nucleus. The mean % tail DNA values were calculated for the microgels in a treatment group and were analyzed with an ANOVA statistical test. If a significant F value of $P \leq 0.05$ was obtained, a Holm-Sidak pairwise comparison versus the control group analysis was conducted (power $(1-\beta) \geq 0.8$ at $\alpha=0.05$).

4.3. RESULTS AND DISCUSSION

CHO Cell Cytotoxicity Concentration-Response Data

For each experiment we prepared a dilution series of each sample stock solution in F12 +5% FBS cell culture medium and from this solution we prepared a concentration series in which CHO cells were exposed to the samples in microplate wells (200 μL). After 72 h the microplates were developed and the results are presented in the following concentration response curves (Figures 4.2-4.9).

Determination of LC_{50} Values and Statistical Analyses of Chronic Cytotoxicity Data

Employing quantitative in vitro assays allows for high precision and high statistical power when analyzing a series of water samples. In order to compensate for "real world" lifetime exposures of large populations, the standard procedure for in vitro toxicity assays is to increase the concentration of agents during short treatment times (hours to days). Range-finding experiments define the concentration range in which a response signal is observed, followed by focused experiments to generate concentration-response curves. Each concentration-response curve is generated from repeated experiments and a descriptive metric, including a LC_{50} value, is calculated using non-linear regression analyses. Bootstrap statistic tables were generated and averaged LC_{50} or cytotoxic index values were generated in order to run an ANOVA test for significance (Efron 1987; Singh and Xie 2008). These short-term assays with their high resolution can be used in optimizing engineering processing to reduce toxic agents in treated waters. From the data generated by the cytotoxicity concentration-response curves, for each KAUST EfOM sample we calculated the LC_{50} value, the lowest significant concentration factor as compared to the concurrent negative control, and the cytotoxicity index value. These metrics are presented in Table 4.1. The LC_{50} value was calculated from the regression analyses for each curve and it represents the concentration factor that would induce a cell density of 50% as compared to the concurrent control. The lowest cytotoxic concentration factor was the lowest concentration factor that induced a statistically significant cytotoxic response and was determined by the ANOVA test statistic (Table 4.1). The CHO cell chronic cytotoxicity index (CTI) value was calculated as the reciprocal of the LC50 value $\times 10^3$ to generate unit-less whole numbers. A larger number indicates a greater cytotoxic potency of the KAUST EfOM sample (Figure 4.10).

Statistical analyses of the data generated in the cytotoxicity concentration-response experiments (Figures 4.2-4.9) are presented in Table 4.1.

CHO Cell Genotoxicity Concentration-Response Data

For each experiment we prepared a dilution series of each sample stock solution in F12 (without FBS) cell culture medium and from this solution we prepared a concentration series in which CHO cells were exposed to the samples in microplate wells (25 μL). After treatment and

analyses with fluorescent microscopy the data were stored in an Excel file. The SCGE results are presented in the following concentration response curves (Figures 4.11-4.18).

Determination of 50%Tail DNA Values and Statistical Analyses of Genotoxicity Data

The SCGE %Tail DNA value for each nucleus within each microgel was measured using the Comet IV software. These data were stored on a spreadsheet and the Mean %Tail DNA value for that microgel was calculated and transferred to a data spreadsheet. In addition the acute cytotoxicity of the treated cells was entered into the same data spreadsheet. Within the water sample concentrate concentration range that allowed for 70% or greater viable cells, a concentration-response curve was generated. The data were plotted and a regression analysis was used to fit the curve and the 50%Tail DNA value was calculated. This information is presented in Table 4.2. The data were transferred to the SigmaPlot 11 program spreadsheet for an ANOVA statistical test. The %Tail DNA values in the SCGE assay are not normally distributed and violate the requirements for analysis by parametric statistics. The mean %Tail DNA value for each microgel was determined as described above and the data were averaged amongst all of the microgels for each water sample concentrate concentration. Averaged median or mean values express a normal distribution according to the central limit theorem (Box et al. 1978). The averaged mean %Tail DNA values obtained from repeated experiments were analyzed with a one-way ANOVA test (Lovell and Omori 2008). If a significant F value of $P \leq 0.05$ was obtained, a Holm-Sidak multiple comparison versus the control group analysis was conducted. The power of the test statistic $(1-\beta)$ was maintained as ≥ 0.8 at $\alpha=0.05$. The lowest genotoxic concentration factor that induced a statistically significant genotoxic response is presented in Table 4.2.

The SCGE genotoxic index (GTI) value was determined as the reciprocal of the 50%Tail DNA value $\times 10^3$ to generate unit-less whole numbers. A larger GTI number indicates a greater genotoxic potency of the KAUST wastewater sample (Figure 4.19).

An ANOVA test was used to analyze the GTI values derived from the bootstrap statistics. If there was not a significant difference between the negative control and a specific wastewater sample, then a GTI value was entered as zero. To prepare the comparison table and statistical analyses of the GTI values, a series of six zero values were used as placeholders for those

KAUST wastewater samples that did not express a significant response within their concentration-response as compared to the concurrent negative control. This allowed these non-significant responders to be included in the comparison amongst all of the wastewater samples.

4.4. CONCLUSIONS

Conclusion from the CHO Cell Chronic Cytotoxicity Analyses

From the data derived from the cytotoxicity concentration-response curves (Figures 4.2-4.9), their statistical analyses and the ANOVA tests of the cytotoxicity index values (Figure 4.10) we conclude the following.

1. The wastewater XAD-8-isolated EfOM was more cytotoxic than the XAD-4 extracts of the same wastewaters. This suggests that halogenated hydrophobic acid fractions, aliphatic carboxylic acids, aromatic carboxylic acids, phenols and humic substances were more cytotoxic than those organic materials eluted from the XAD-4 resins.
2. The amount of cytotoxic material retained in the XAD-8 and XAD-4 extracted (spent) wastewater was very low. For NH_2Cl disinfection, the residual cytotoxicity of the organic material present in the spent wastewater was 1.4% of the summed cytotoxicity of the XAD-8 and XAD-4 isolated organics. With HOCl disinfection, the cytotoxicity of the residual organic material present in the spent wastewater was also 1.4% of the summed cytotoxicity of the XAD-8 and XAD-4 isolated organics.
3. There was no significant difference between the cytotoxic indices for the spent NH_2Cl and HOCl wastewaters. Thus the XAD-8 and XAD-4 extraction protocol was efficient in extracting the cytotoxic organic materials from the wastewaters.
4. The disinfectant used with the wastewaters had an effect on the resulting cytotoxicity of the XAD-8 extracted organic material. Within experiment 2, the HOCl XAD-8 extract was significantly more cytotoxic than the NH_2Cl XAD-8 extract. There was no significant difference between the XAD-4 extracts of HOCl and NH_2Cl treated wastewaters.

Conclusions from the CHO Cell Genotoxicity Analyses

From the data derived from the genotoxicity concentration-response curves (Figures 4.11- 4.18), their statistical analyses and the ANOVA tests of the genotoxicity index values (Figure 4.19) we conclude the following.

1. The wastewater XAD-8-isolated EfOM was more genotoxic than the XAD-4 extracts of the same wastewaters. This suggests that halogenated hydrophobic acid fractions, aliphatic carboxylic acids, aromatic carboxylic acids, phenols and humic substances were more potent inducers of genomic DNA damage than those organic materials eluted from the XAD-4 resins.
2. The organic material retained in the XAD-8 and XAD-4 extracted (spent) wastewater expressed no significant genotoxic response throughout the concentration factor range from 200× to 1,000×. There was no significant difference between the genotoxic indices for the spent NH_2Cl and HOCl wastewaters. Thus the XAD-8 and XAD-4 extraction protocol was efficient in extracting the genotoxic organic materials from the wastewaters.
3. The disinfectant used with the wastewaters had an effect on the resulting genotoxicity of the XAD-8 extracted organic material. Within experiment 2, and in contrast to the cytotoxicity data, the NH_2Cl XAD-8 extract was significantly more genotoxic than the HOCl XAD-8 extract.

4. XAD-4 extracted organics from the NH_2Cl treated wastewaters were significantly more genotoxic than those of the HOCl treated wastewaters.

These data indicate that the NH_2Cl EfOM extracted over XAD-8 or XAD-4 were more genotoxic than EfOM from HOCl treated wastewaters.

4.5. FIGURES AND TABLES

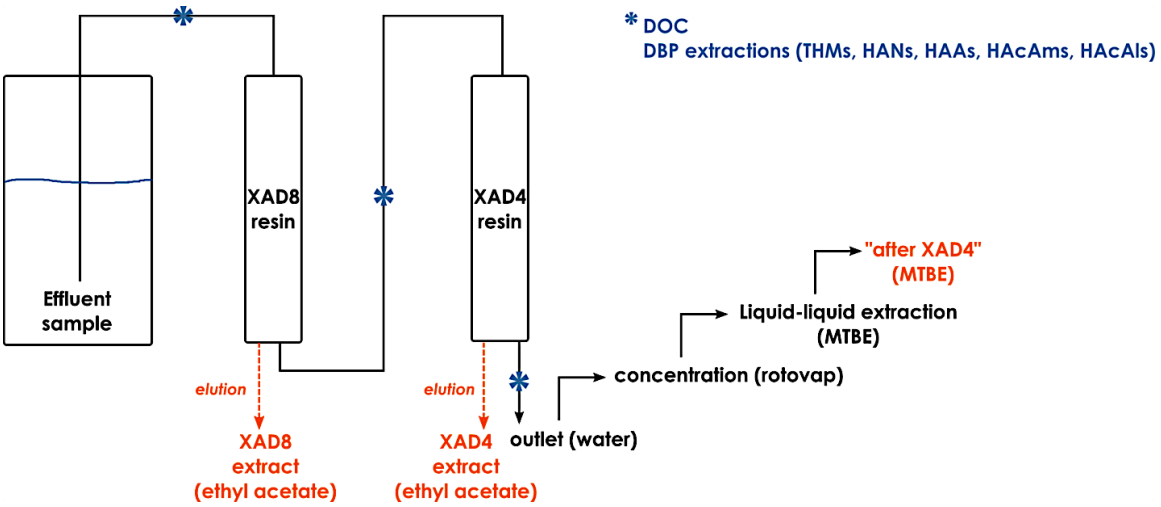

Figure 4.1. Experimental design for the extraction of the wastewater effluent organic fractions.

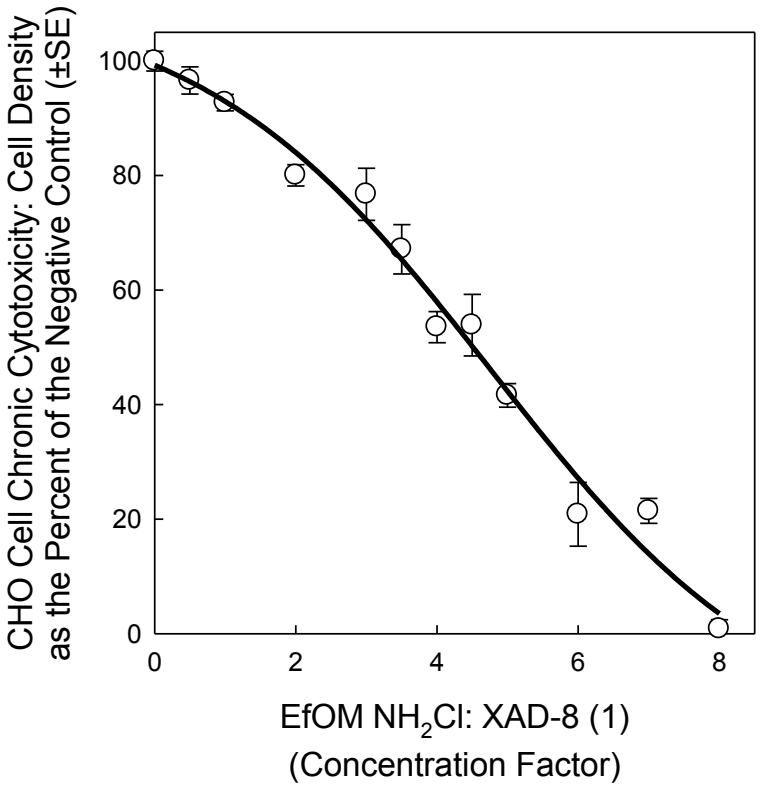

Figure 4.2. Experiment 1. CHO cell cytotoxicity concentration response curve for the chloraminated wastewater EfOM extracted over XAD-8 resin.

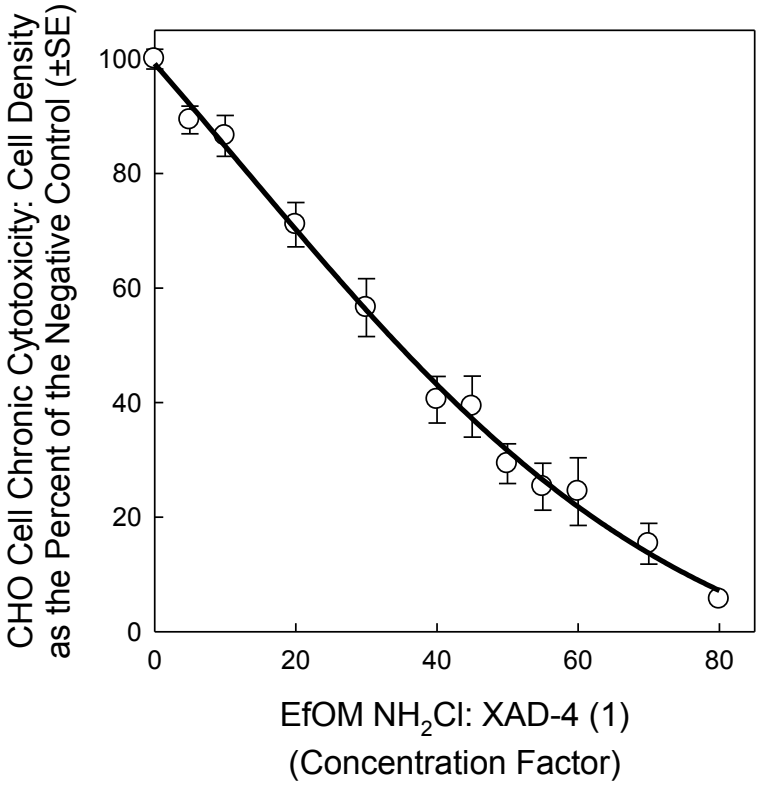

Figure 4.3. Experiment 1. CHO cell cytotoxicity concentration response curve for the chloraminated wastewater EfOM extracted over XAD-4 resin.

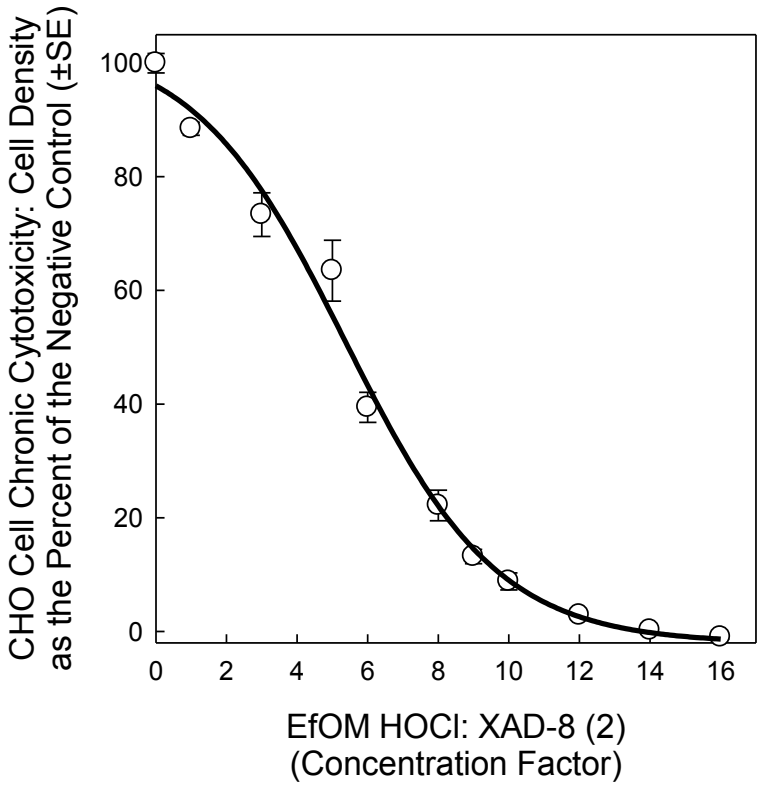

Figure 4.4. Experiment 2. CHO cell cytotoxicity concentration response curve for the chlorinated wastewater EfOM extracted over XAD-8 resin.

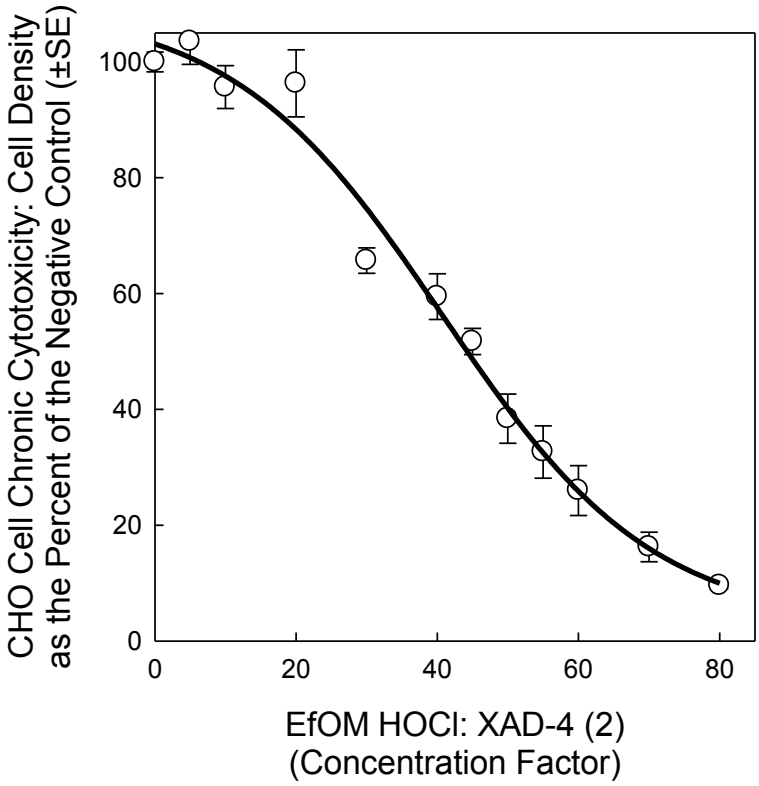

Figure 4.5. Experiment 2. CHO cell cytotoxicity concentration response curve for the chlorinated wastewater EfOM extracted over XAD-4 resin.

.

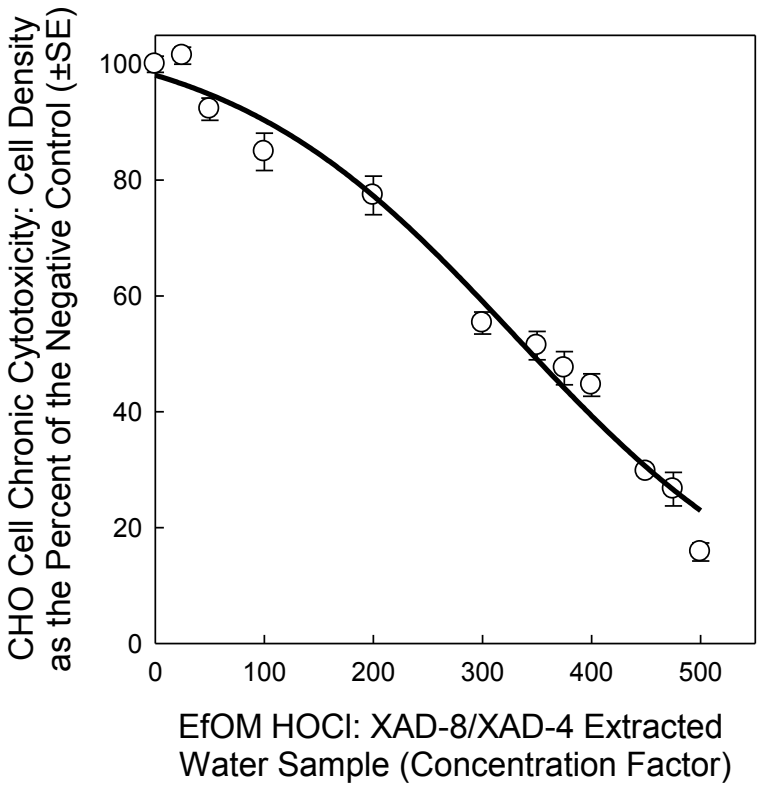

Figure 4.6. Experiment 2. CHO cell cytotoxicity concentration response curve for the chlorinated wastewater after extraction over XAD-8 and XAD-4 resins. The resulting wastewater after XAD extraction was reduced in volume by vacuum evaporation and the residual was liquid/liquid extracted with MTBE.

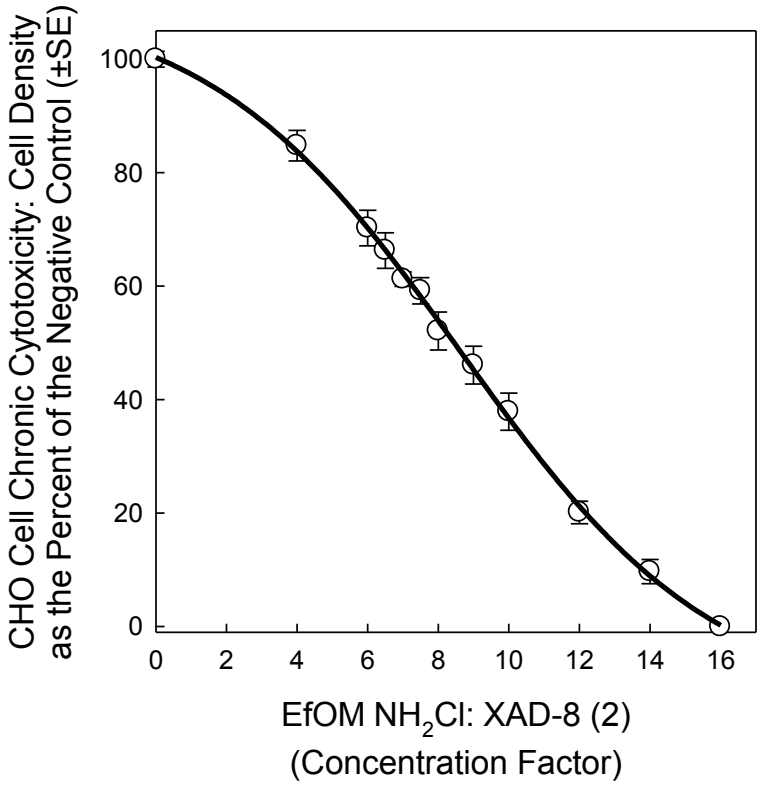

Figure 4.7. Experiment 2. CHO cell cytotoxicity concentration response curve for the chloraminated wastewater EfOM extracted over XAD-8 resin.

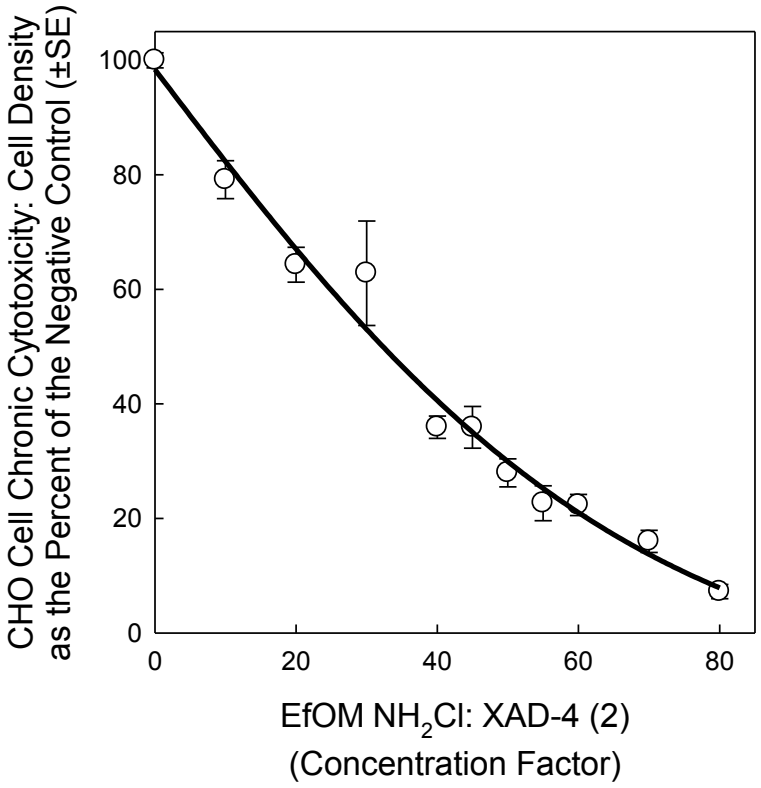

Figure 4.8. Experiment 2. CHO cell cytotoxicity concentration response curve for the chloraminated wastewater EfOM extracted over XAD-4 resin.

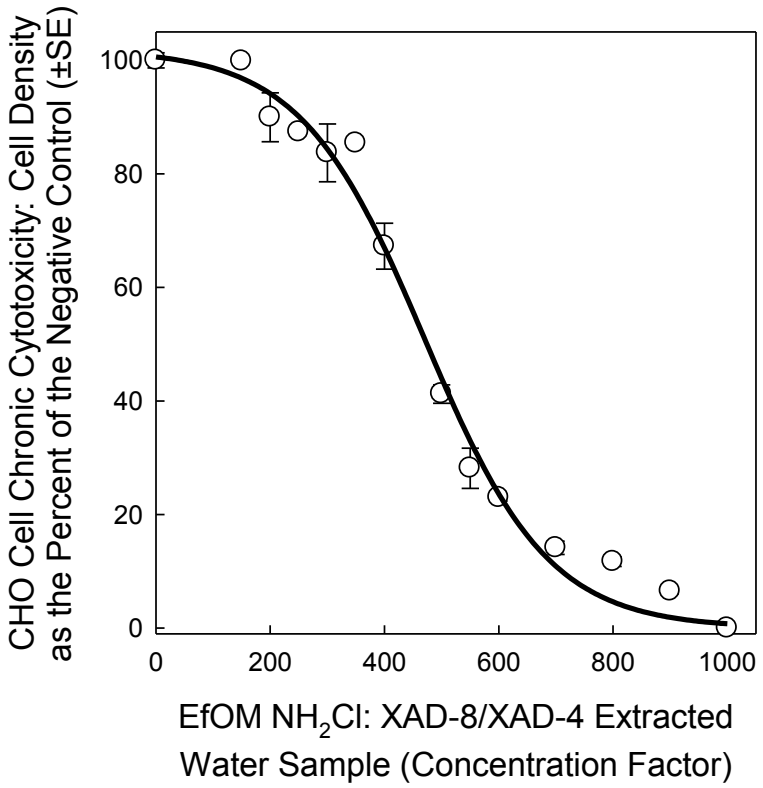

Figure 4.9. Experiment 2. CHO cell cytotoxicity concentration response curve for the chloraminated wastewater after extraction over XAD-8 and XAD-4 resins. The resulting wastewater after XAD extraction was reduced in volume by vacuum evaporation and the residual was liquid/liquid extracted with MTBE.

Table 4.1 Statistical analyses of the cytotoxicity data from the XAD-extracted wastewater samples				
WW EfOM Sample	LC_{50} Conc. Factor [a]	r^2 [b]	Lowest Cytotox. Conc. Factor [c]	ANOVA Test Statistic [d]
EfOM NH_2Cl: XAD-8 (1)	4.51	0.98	2	$F_{11,59} = 103.1$; $P \leq 0.001$
EfOM NH_2Cl: XAD-4 (1)	34.5	0.99	10	$F_{11,84} = 66.9$; $P \leq 0.001$
EfOM HOCl: XAD-8 (2)	5.45	0.99	1	$F_{10,47} = 193.0$; $P \leq 0.001$
EfOM HOCl: XAD-4 (2)	44.2	0.99	30	$F_{11,83} = 87.1$; $P \leq 0.001$
EfOM HOCl: XAD-8/XAD-4 Spent Water (2)	354	0.99	50	$F_{11,52} = 172.7$; $P \leq 0.001$
EfOM NH_2Cl: XAD-8 (2)	8.45	0.99	4	$F_{11,52} = 164.1$; $P \leq 0.001$
EfOM NH_2Cl: XAD-4 (2)	32.3	0.98	10	$F_{10,54} = 115.1$; $P \leq 0.001$
EfOM NH_2Cl: XAD-8/XAD-4 Spent Water (2)	470	0.99	200	$F_{13,41} = 195.6$; $P \leq 0.001$

[a] The LC_{50} value is the fold concentration factor of the wastewater sample, determined from a regression analysis of the data, that induced a cell density of 50% as compared to the concurrent negative controls. [b] r^2 is the coefficient of determination for the regression analysis upon which the LC_{50} value was calculated. [c] Lowest cytotoxic concentration was the lowest concentration factor of the wastewater sample in the concentration-response curve that induced a statistically significant reduction in cell density as compared to the concurrent negative controls. [d] The degrees of freedom for the between-groups and residual associated with the calculated *F*-test result and the resulting probability value.

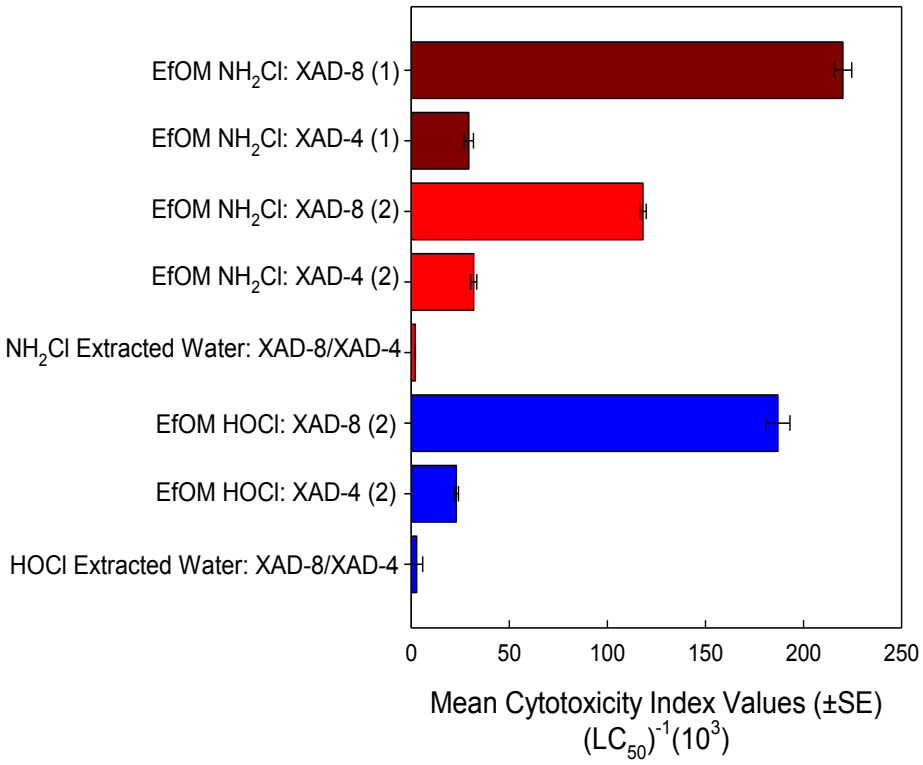

Figure 4.10. A comparison of the CHO cell cytotoxicity index values for each group in experiment 1 and experiment 2.

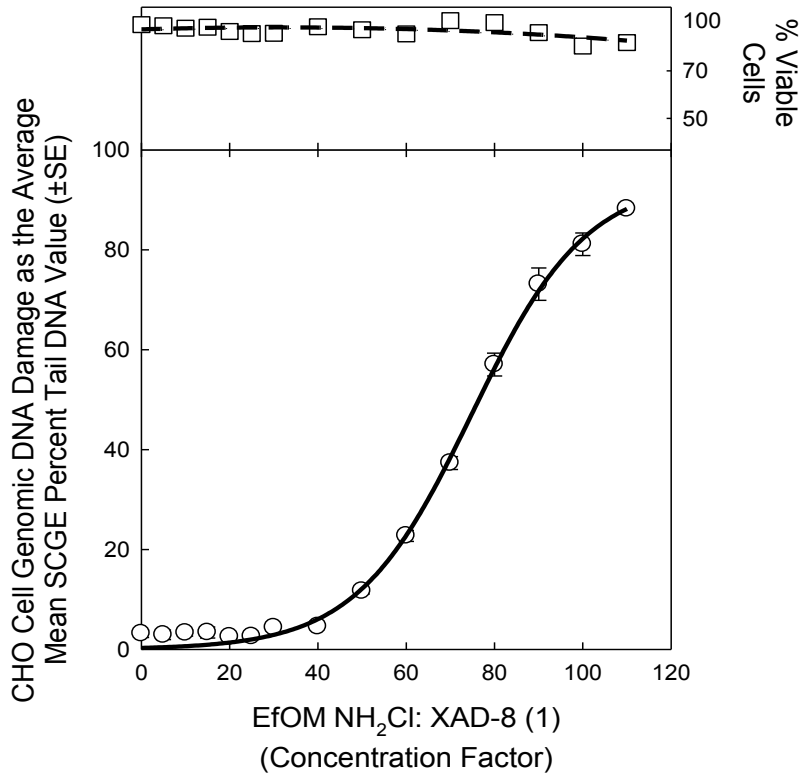

Figure 4.11. Experiment 1sample EfOM NH_2Cl extracted over XAD-8 illustrating its CHO cell SCGE genotoxicity concentration-response curve (bottom panel) and acute cytotoxicity (top panel).

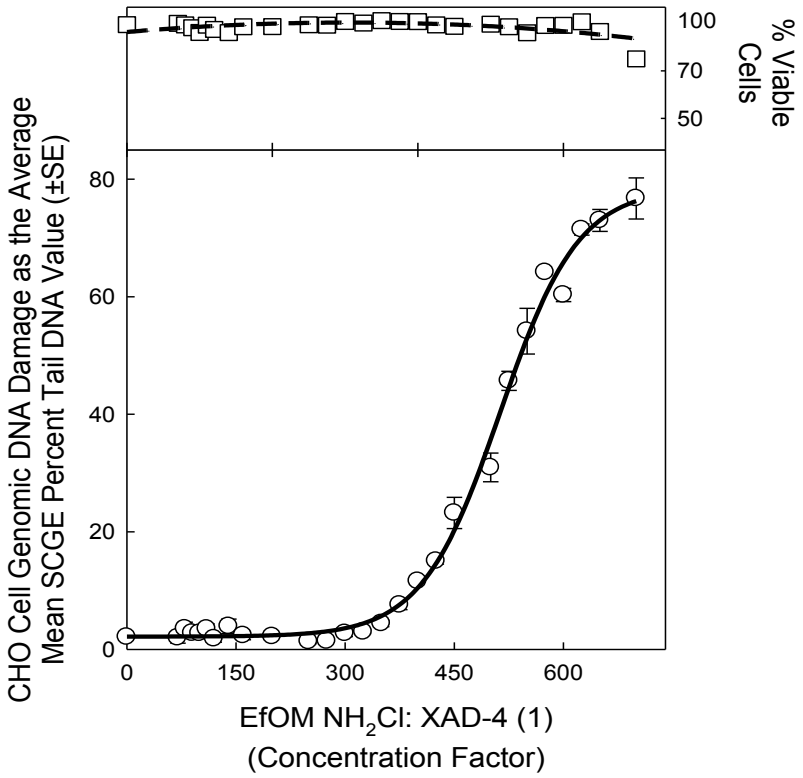

Figure 4.12. Experiment 1 sample EfOM NH_2Cl extracted over XAD-4 illustrating its CHO cell SCGE genotoxicity concentration-response curve (bottom panel) and acute cytotoxicity (top panel).

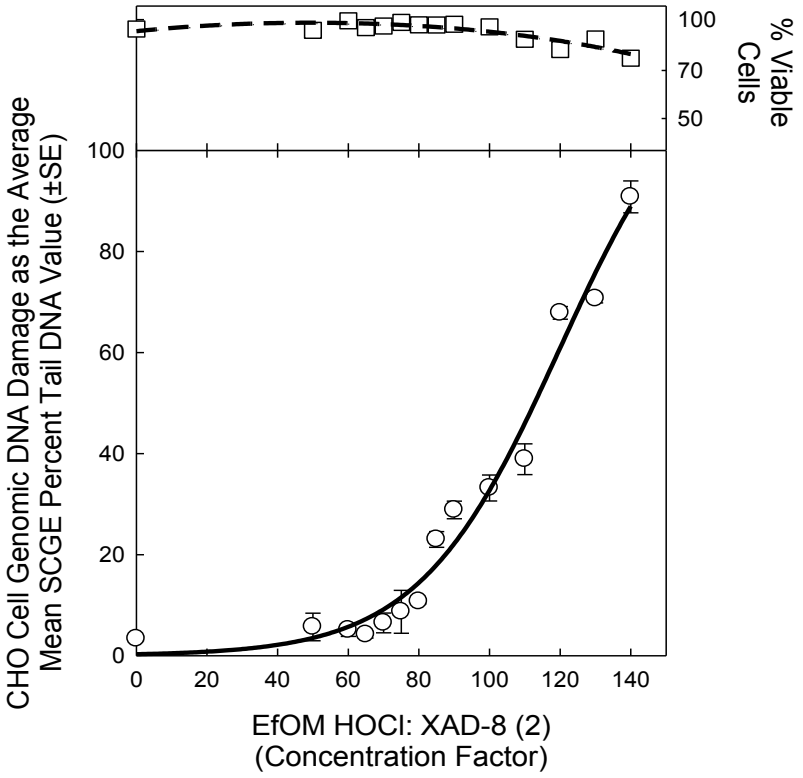

Figure 4.13. Experiment 2 sample EfOM HOCl extracted over XAD-8 illustrating its CHO cell SCGE genotoxicity concentration-response curve (bottom panel) and acute cytotoxicity (top panel).

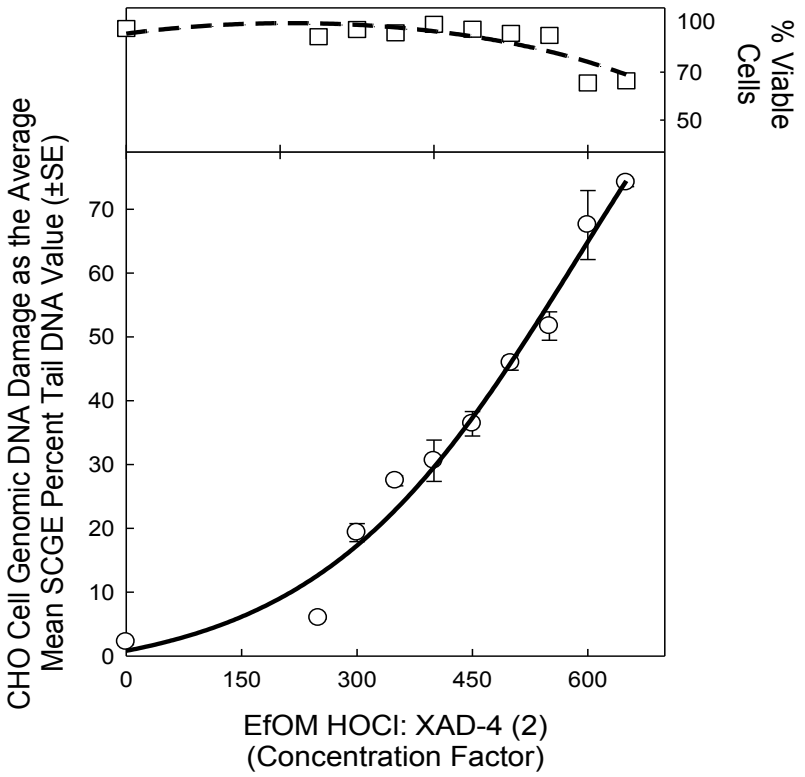

Figure 4.14. Experiment 2 sample EfOM HOCl extracted over XAD-4 illustrating its CHO cell SCGE genotoxicity concentration-response curve (bottom panel) and acute cytotoxicity (top panel).

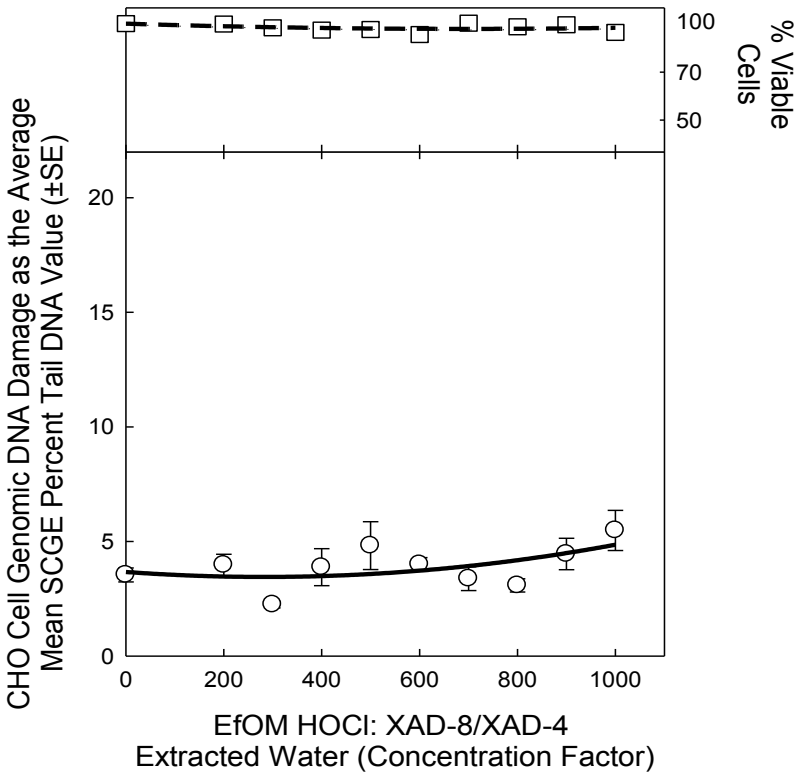

Figure 4.15. Experiment 2 CHO cell genotoxicity concentration response curve for the chlorinated wastewater after extraction over XAD-8 and XAD-4 resins (bottom panel). The resulting wastewater after XAD extraction was reduced in volume by vacuum evaporation and the residual was liquid/liquid extracted with MTBE. The acute cytotoxicity response is illustrated in the top panel.

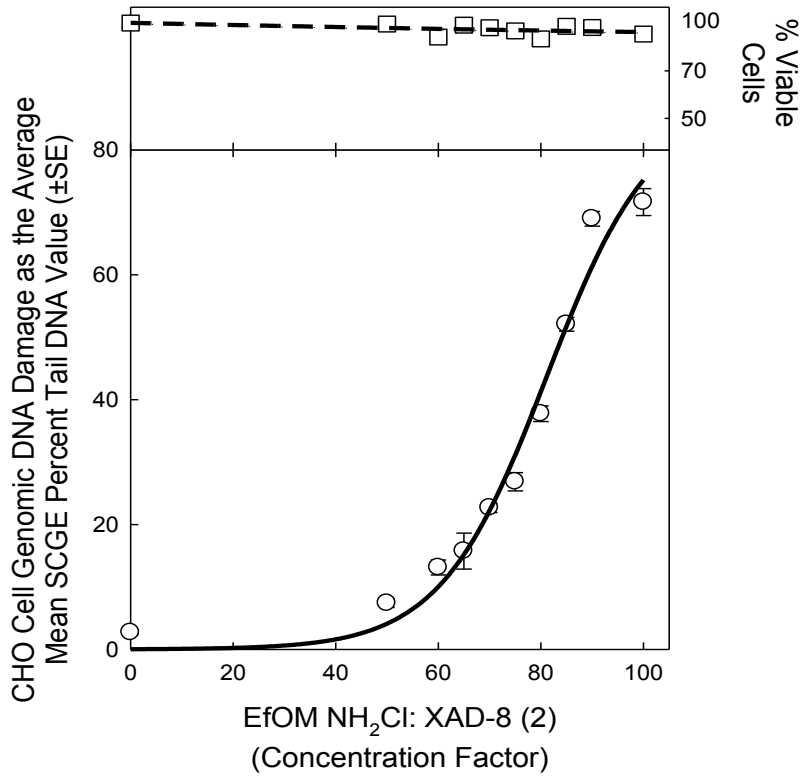

Figure 4.16. Experiment 2 sample EfOM NH_2Cl extracted over XAD-8 illustrating its CHO cell SCGE genotoxicity concentration-response curve (bottom panel) and acute cytotoxicity (top panel).

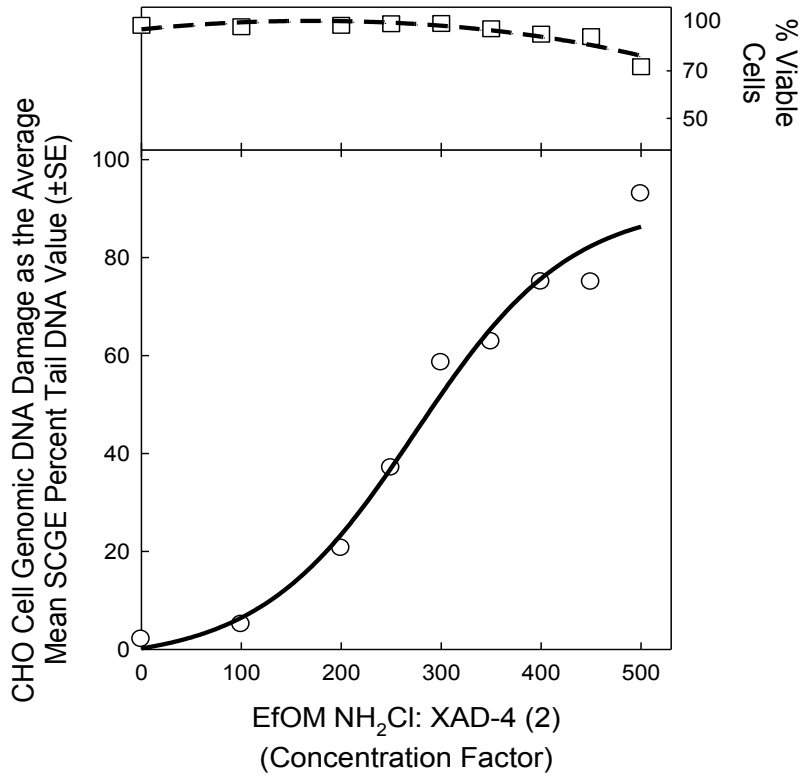

Figure 4.17. Experiment 2 sample EfOM NH_2Cl extracted over XAD-4 illustrating its CHO cell SCGE genotoxicity concentration-response curve (bottom panel) and acute cytotoxicity (top panel).

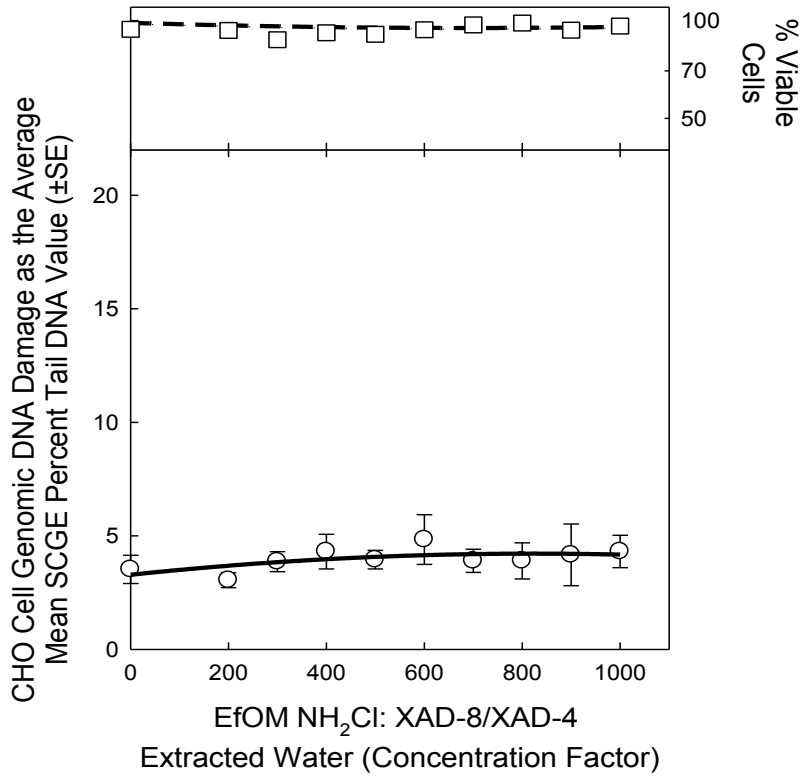

Figure 4.18. Experiment 2 CHO cell genotoxicity concentration response curve for the chloraminated wastewater after extraction over XAD-8 and XAD-4 resins (bottom panel). The resulting wastewater after XAD extraction was reduced in volume by vacuum evaporation and the residual was liquid/liquid extracted with MTBE. The acute cytotoxicity response is illustrated in the top panel.

Table 4.2 Statistical analyses of the genotoxicity data from the XAD-extracted wastewater samples				
WW EfOM Sample	50% TDNA Conc. Factor [a]	r^2 [b]	Lowest Genotox. Conc. Factor [c]	ANOVA Test Statistic [d]
EfOM NH_2Cl: XAD-8 (1)	76.4	0.99	50	$F_{14,37} = 195.1$; $P \leq 0.001$
EfOM NH_2Cl: XAD-4 (1)	541	0.99	400	$F_{26,53} = 133.8$; $P \leq 0.001$
EfOM HOCl: XAD-8 (2)	112.7	0.98	85	$F_{13,20} = 154.4$; $P \leq 0.001$
EfOM HOCl: XAD-4 (2)	522	0.98	300	$F_{11,83} = 89.9$; $P \leq 0.001$
EfOM HOCl: XAD-8/XAD-4 Spent Water (2)	NA [e]	NA	NS [f]	$F_{9,30} = 2.2$; $P = 0.051$
EfOM NH_2Cl: XAD-8 (2)	83.7	0.98	60	$F_{9,30} = 300.1$; $P \leq 0.001$
EfOM NH_2Cl: XAD-4 (2)	293	0.98	200	$F_{10,54} = 155.7$; $P \leq 0.001$
EfOM NH_2Cl: XAD-8/XAD-4 Spent Water (2)	NA	NA	NS	$F_{13,41} = 0.395$; $P = 0.928$

[a] The SCGE 50% Tail DNA value is the wastewater sample concentration factor determined from a regression analysis of the data that was calculated to induce a 50% SCGE Tail DNA value. [b] r^2 is the coefficient of determination for the regression analysis upon which the SCGE 50%Tail DNA value was calculated. [c] The lowest genotoxic concentration was the lowest concentration factor of the wastewater sample in the concentration-response curve that induced a statistically significant amount of genomic DNA damage as compared to the negative control. [d] The degrees of freedom for the between-groups and residual associated with the calculated *F*-test result and the resulting probability value. [e] NA = not applicable, [f] NS = not significant.

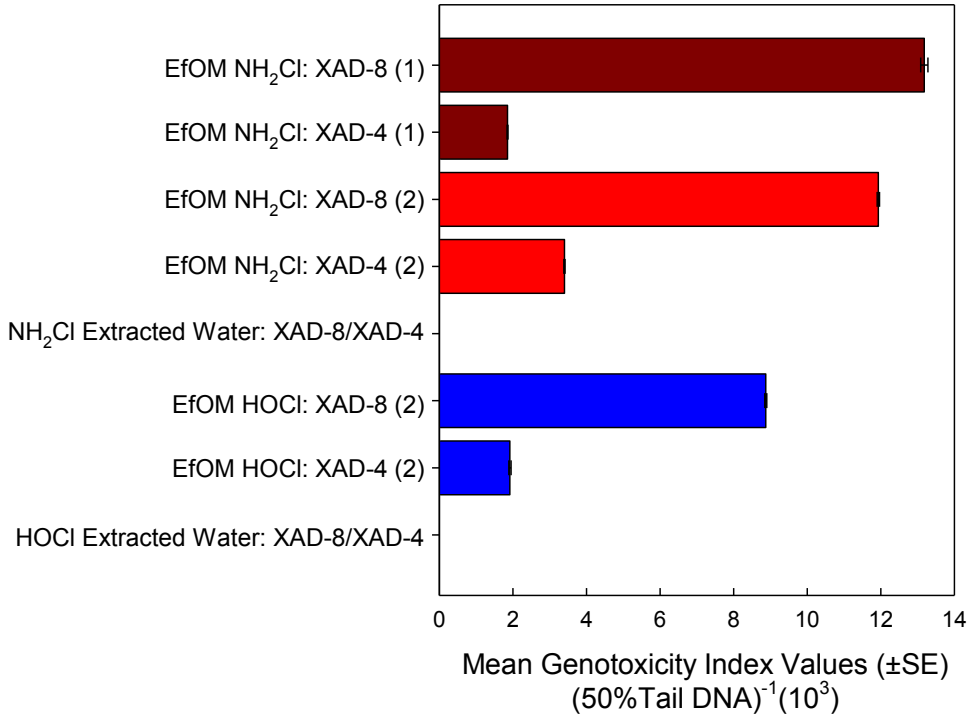

Figure 4.19. A comparison of the CHO cell genotoxicity index values for each group in experiment 1 and experiment 2.

4.6. REFERENCES

Bichsel Y, von Gunten U. 1999. Oxidation of iodide and hypoiodous acid in the disinfection of natural waters. Environmental Science & Technology 33(22):4040.

Box GEP, Hunter WG, Hunter JS. 1978. Statistics for Experimenters: An Introduction to Design, Data Analysis, and Model Building. New York, NY.: Wiley & Sons Inc.

Efron B. 1987. Better bootstrap confidence intervals. J Am Statis Assoc 82(397):171-185.

Food and Agriculture Organization of the United Nations. Health risks associated with wastewater use; http://www.fao.org/docrep/w5367e/w5367e04.htm - TopOfPage.

Krasner SW. 2009. The formation and control of emerging disinfection by-products of health concern. Philos Trans A Math Phys Eng Sci 367(1904):4077-4095.

Lovell DP, Omori T. 2008. Statistical issues in the use of the comet assay. Mutagenesis 23(3):171-182.

Phillips HJ. 1973. Dye exclusion tests for cell viability. In: Kruse PF, Patterson MJ, editors. Tissue Culture: Methods and Applications. New York: Academic Press. p 406.

Plewa MJ, Kargalioglu Y, Vankerk D, Minear RA, Wagner ED. 2002. Mammalian cell cytotoxicity and genotoxicity analysis of drinking water disinfection by-products. Environ Mol Mutagen 40(2):134-142.

Plewa MJ, Wagner ED. 2009. Mammalian Cell Cytotoxicity and Genotoxicity of Disinfection By-Products. Denver, CO: Water Research Foundation. 134 p.

Rundell MS, Wagner ED, Plewa MJ. 2003. The comet assay: genotoxic damage or nuclear fragmentation? Environ Mol Mutagen 42(2):61-67.

Singh K, Xie M. 2008. Bootstrap: A Statistical Method. Rutgers University. 14 p.

Tice RR, Agurell E, Anderson D, Burlinson B, Hartmann A, Kobayashi H, Miyamae Y, Rojas E, Ryu JC, Sasaki YF. 2000. Single cell gel/comet assay: guidelines for in vitro and in vivo genetic toxicology testing. Environ Mol Mutagen 35(3):206-221.

U. S. Environmental Protection Agency. 1999. Wastewater Technology Fact Sheet; Chlorine Disinfection. Report nr EPA 832-F-99-062.

Wagner ED, Plewa MJ. 2009. Microplate-based comet assay. In: Dhawan A, Anderson D, editors. The Comet Assay in Toxicology. London: Royal Society of Chemistry. p 79-97.

CHAPTER 5

TOXICITY OF PARTICLE ASSOCIATED POLYCYCLIC AROMATIC HYDROCARBONS IN URBAN LAKES

5.1. INTRODUCTION

Increased concentrations of particle associated contaminants (PACs) such as metals and highly stable organic compounds are often associated with urbanization (Lopes et al. 1999; Rice 1999). In New England, samples from sediment cores, streambed sediments, and suspended stream sediments showed higher concentrations of polycyclic aromatic hydrocarbons (PAHs), polychlorinated biphenyls (PCBs), DDT, and seven trace metals (Cd, Cr, Cu, Hg, Ni, Pb, Zn) than the reference concentrations, indicating a strong correlation with urbanization. The strongest relationships of PACs were observed to the percentage commercial, industrial and transportation land use. The urbanized watershed showed approximately 30 and 6 times higher concentrations of PAHs and metals than the reference concentrations, respectively (Chalmers et al. 2007). Atmospheric and fluvial pathways are the two main sources of PACs to aquatic system (Christensen and Xiaochun 1993). Atmospheric pathways for the Sources of PAHs and trace metals include waste incineration, fossil fuel combustion, and industrial emission from plating, smelting, and refining. The main sources of PACs with fluvial pathways to aquatic environment are, releases of contaminants to land surfaces by different means (such as pesticide use, disposal of wastes, and spills), erosion of historically contaminated soils, and wear of infrastructure (e.g. asphalt roads, driveways, parking-lot sealants, roofing materials, galvanized metals) (Chalmers et al. 2007).

In the US, there are different types of paved surfaces. However, most of the driveways and parking lots are either made of asphalt or concrete. In order to increase the longevity and improve appearance of these pavements, asphalt pavements, driveways, and parking lots are coated with a black, shiny material, known as “seal coat” (Dubey). In the US, the most common type of sealant is the coal tar; annually, 85 million gallons of coal tar-based sealcoat is used in the US (Scoggins et al. 2009). Particles abraded from these coal tar sealants on driveways, parking lots, and pavements flow into different water sources such as streams, and urban lakes via runoff and can be a primary source of different PACs (e.g. PAHs) in these water-bodies (Mahler et al. 2005; Yang et al. 2010).

PACs are highly stable; they are not only harmful to flora and fauna in the aquatic system but also harmful to humans. They are lipophilic in nature, bioaccumulative and toxic. Studies demonstrated that PACs were persistently found in nature even years after their use was diminished (Mahler and Van Metre 2003). Studies based on water quality surveys (Van Metre and Mahler 2005; Chalmers et al. 2007) showed that some of PACs (e.g. PAHs) concentration was correlated with urbanization. Since 1970's, metal, PCBs, and DDT concentrations decreased in water. However, total concentrations of PAHs have increased with increasing urbanization (Van Metre and Mahler 2005).

PAHs are organic compounds with two or more, single or fused benzene rings. They share a pair of carbon atoms between the rings in their molecules. PAHs containing less than four fused benzene rings have low molecular weight, easily soluble, biodegradable, and more volatile than those with four or more than four benzene rings. Compounds with four or less than four benzene rings are know as small PAHs and those with four or more benzene rings are know as large PAHs (Buha 2011; Mahler et al. 2012). The natural sources of PAHs are coal and petroleum products. They are produced due to the incomplete combustion of organic matter e.g. vehicle exhaust, cigarette smoke, residential wood burning, and wildfires. PAHs have many urban sources; sources of particle-associated PAHs in lake sediments are used motor oil, automobile exhaust, industrial emissions, tire particles, coal tar and asphalt based sealcoats on parking lots, abraded particles from driveway pavements, and municipal and industrial waste incineration (Hoffman et al. 1984; Mahler et al. 2005; Mahler et al. 2012).

PAHs are present in the environment as a mixture of different PAHs compounds. Out of all known PAH sources, coal tar has the highest concentration of PAHs (Mahler et al. 2012). Particles abraded from sealcoats, which enter streams and rivers are the major source of PAHs in urban lake sediments. Out of all different sealcoats, particles from coal tar sealcoats contribute the highest percentage (84%) of the total PAHs in urban lake sediments (Yang et al. 2010). Metre et al demonstrated through the contaminant mass-balance receptor modeling that coal tar was the main source of PAHs in 40 lakes located throughout the United States for the last 40 years (Van Metre and Mahler 2010). Due to the lipophilic nature of PAHs, they stay adsorbed on particle surfaces in water and can easily bioaccumulate in edible marine organisms. Background levels of PAHs in drinking water ranged from 4 to 24 ng per liter. The U.S. EPA selected 17

PAHs and profiled them in a single group based on their highest concentrations at national Priority List (NPL) sites, their level of harmful effects, exposure and the available information for these PAHs (Mumtaz and Julia 1995). Mahler et al demonstrated in a study that PAHs from coal tar and asphalt sealcoats are acutely toxic. In this study, *Ceriodaphnia dubia* and *Pimephales promelas* were exposed to undiluted runoff from unsealed asphalt pavement and ultraviolet radiation (UVR) that showed ≤10% mortality. However, when these test organisms were exposed to undiluted coal tar runoff after sealcoat applications, results showed 100% mortality (Mahler et al. 2015). PAHs were genotoxic and carcinogenic (Farmer 2003) and induced lung cancer in workers exposed to coal tar pitch volatiles measured as benzene-soluble matter (Armstrong 1994). Several fractions of creosote P1 were found as mutagenic in *Salmonella typhimurium* strain TA98. The mutagenicity of creosote fractions was due to the presence of 0.18 and 1.1% of benzo(α)pyrene and benz(α)anthracene, respectively (Bos et al. 1984).

The fate of PAHs from coal tar sealcoat in aquatic systems is not well understood. It is not clear if PAHs redistribute in water and lose their toxic potential or if they are lost to the water column with ageing. A mechanistic and quantitative approach is needed to understand the distribution of PAHs in water and the changes in the toxic potential of PAHs associated with its distribution in aquatic systems.

The objectives of this research were to evaluate the coal tar and soot associated PAHs for mutagenicity, and determine if they were direct-acting mutagens or promutagens. By using the *Salmonella typhimurium* his reversion assay for the mutagenicity evaluation we could determine if the agents induced base pair substitution mutations and/or frameshift mutations.

5.2. MATERIALS AND METHODS

PAHs Extraction and Characterization From Lake Sediments

The coal tar extracts (CTE) with PAHs were provided by Dr. Charles Werth laboratory in the Department of Civil and Environmental Engineering. For the PAH analysis, subsamples from the same depths selected for carbonaceous material (CM) characterization were directly subjected to PAH extraction by acetone and dichloromethane using accelerated solvent extraction (ASE, EPA method 3545). The extracts were cleaned with silica gel (EPA method

3630c), and 16 EPA priority PAHs were analyzed with GC/MS following EPA method 8270c. Quality assurance was provided by analyzing triplicate samples, blanks, and spiked reagent samples, and recovery of surrogate compounds was monitored. Mean and variance among triplicates were reported as described by Yang and his colleagues (Yang et al. 2010).

Chemicals and Reagents for Mutagenicity Test

Coal tar and soot extracts from lake sediments were provided by Dr. Charles Werth laboratory in Civil and Environmental Engineering Department. The coal tar and soot extracts were rotary evaporated. After rotary evaporation, coal tar and soot extract samples were solvent exchanged in 200 μL and 100 μL ethyl acetate, respectively and stored at at –22°C in sterile glass vials with Teflon seals. General laboratory chemicals and reagents were purchased from Sigma Chemical Co. (St. Louis, MO) or Fisher Scientific Co. (Fair Lawn, NJ). Aroclor 1254-induced rat hepatic S9 fraction was purchased from Molecular Toxicology, Inc. (Annapolis, MD).

Preparation of the Bacterial Suspensions

The experiments for this study involved two strains of *S. typhimurium* tester strains; TA98 (*hisD3052, rfa*$^{-}$; ΔuvrB-bio; pKM101, amp^{r}), TA100 (*hisG46*, rfa; ΔuvrB-bio; pKM101, amp^{r}). *S. typhimurium* strains TA98 and TA100 were originally obtained from Dr. B. N. Ames (Berkeley, CA), The bacterial strains were stored as frozen cultures in Luria-Bonner broth (LB) plus 10% DMSO at –80°C.

Plate Incorporation Assay With *S. typhimurium* Cells (TA100 and TA98)

S. typhimurium tester strain TA100 (*hisG46*, *rfa*$^{-}$; △uvrB-bio) + pKM10, amp^{r}) and TA98 (*hisD3052*, *rfa*$^{-}$; ΔuvrB-bio; pKM101, amp^{r}), with and without mammalian microsomal activation were used. Reverse mutation was measured at *hisG46* and *hisD3052* (Hartman et al. 1986). *S. typhimurium* strain TA100 was sensitive to PAHs (Kevekordes et al. 1998). TA100 and TA98 were stored in cryovials at −80°C as a frozen culture in Luria-Bonner (LB) plus 10% dimethylsulfoxide (DMSO). The TA98 and TA100 cells from their respective cryovials were used to construct master-plates; 100 μL cells from each cryovial were grown in 5 mL LB medium plus 10 μL ampicillin solution at 37°C while shaking and log-phase *S. typhimurium* TA100 or TA98 were used to construct master plates. The culture was streaked with a flame

sterilized platinum loop across the LB plate and incubated overnight at 37°C. The next day, master plate was stored at 4°C (Maron and Ames 1983). For the mutagenicity experiments, the single colony isolates of *S. typhimurium* TA100 and TA98 from there respective master plates were grown overnight in 50 mL LB medium 100 µL ampicillin stock solution at 37°C with shaking (200 rpm). The following day, the overnight cultures of TA100 or TA98 were utilized to check the coal-tar extract with PAHs induced mutagenicity using plate incorporation assay.

Most of the PAHs require metabolic activation to exhibit mutagenicity. Metabolic activation of PAHs is primarily dependent on cytochrome P-450 monooxygenase that converts PAHs into mutagens (Phillipson and Ioannides 1989). Oxidative transformation is an important route of metabolism of xenobiotics. The monooxygenase system is formed by the enzyme system of cytochrome P-450 and NADPH cytochrome P-450 reductase. The haemoprotein cytochrome P-450 functions as the terminal oxidase involved in the hydroxylation of xenobiotics such as PAHs.

S. typhimurium Plate Incorporation Mutagenicity Assay

For the plate incorporation assay, overlay tubes were prepared with 2 mL of his-bio supplemented top agar, 100 µL of overnight bacterial culture and ± 500 µL S9 mix. The S9 mix consisted of 0.2 M sodium phosphate, 0.5 M $MgCl_2$, 1.5 M KCl, 1 M glucose-6-phosphate, 0.5 M NADP and 40 µL/mL of Aroclor 1254-induced rat hepatic microsomal suspension. The required volume of the test agent was added to the overlay tube, mixed and the overlay tube was flamed sterilized and immediately poured onto a VB minimal plate. The VB plates were incubated at 37°C for 48-72 h. Histidine revertant colonies were counted by hand or with a New Brunswick Biotran III automatic colony counter. The data were saved in an Excel spreadsheet. The data were analyzed from the Excel spreadsheet using the statistical and graphical functions of SigmaPlot 12 (Systat Software, Inc., San Jose, CA). Photographs of specific plates (± 500 µL S9 mix) illustrating the induction of his revertants are presented in Figure 5.1-5.2.

To confirm the genotype of the TA100 and TA98 cells, 100 µL of the bacterial cell suspension was added to an LB plate, and spread with a flamed glass rod. Flamed tweezers were used to place a crystal violet disk onto the center of the plate, and the disk was tapped lightly in place. Due to the presence of the *rfa* mutation (Maron and Ames 1983), the large molecules of

crystal violet are able to enter and kill the TA100 and TA98 cells. This was indicated by a clear zone around the crystal violet disk (Figure 5.1 lower right hand plate). Similar experiments were repeated to study the mutagenicity induced by soot extracts in TA100 and TA98 strains.

5.3. RESULTS AND DISCUSSION

In the US, to increase the longevity and improve the appearance of the parking lots and, driveways; concrete or asphalt pavements are coated with a black material that is known as seal coat (Dubey). In the US, the most common type of seal coat is coal tar (Scoggins et al. 2009). The carbonaceous material based sealants (e.g. coal tar) have PAHs adsorbed in them. Usually, PAHs are present in the environment as a mixture. In the environment, PAHs have different sources but coal tar has the highest concentration of PAHs (Scoggins et al. 2009; Mahler et al. 2012). In urban lake sediments, particles abraded from coal tar sealcoats, which enter different water sources, are the main source of PAHs. These PAHs are highly toxic to biological systems and pose human health hazards.

To study the PAC based PAHs mutagenicity potential; we used the plate incorporation method with and without S9 microsomal activation system. The plate incorporation method was used with *S. typhimurium* TA100 and TA98 bacterial strains to screen for base pair substitution and frameshift mutations (Maron and Ames 1983).

The concentrations of PAHs were measured in different coal tar and soot extract samples using GCMS (Table 5.1-5.2) This study contained two samples for each extract i.e. coal tar extract sample 1(CTE-1), coal tar extract sample 2 (CTE-2) and soot extract 1 (SE-1) and soot extract 2 (SE-2). GCMS analysis of these samples demonstrated that CTE-2 and SE-1 had higher concentrations of PAHs as compared to CTE-1 and SE-1, respectively (Table 5.1-5.2). Out of EPA listed 16 priority PAHs (Campro Scientific), coal tar extracts had higher number of PAHs as compared to soot extracts.

The mutagenicity analysis demonstrated that coal tar and soot extracts were highly mutagenic and caused increased base pair substitution mutations by inducing higher frequencies of revertants in TA100 as compared to the induction of frameshift mutations in strainTA98. It was found that most of these the coal tar and soot samples were promutagens as the mutation frequencies were higher with S9 microsomal activation. Results demonstrated that SE-2 had a

highest mutagenic potency in TA100 and TA98 with S9 followed by SE-1. CTE-2 produced higher number of TA100 revertants as compared to CTE-1. However, CTE-2 had a lower mutagenic potency as compared to soot samples, despite the fact that CTE-2 had higher number of PAHs as compared to soot samples. Overall, all the soot and coal tar extracts induced base pair substitution mutations as compared to frameshift mutations (Table 5.3).

Results demonstrated that the average mutagenic potency of CTE-1 was 8 revertants/μg for the TA100 revertants with S9 microsomal activation system but without S9 microsomal activation system, the TA100 mutagenic potency rate was reduced to 1 revertant/μg. All the CTE-1 concentrations used in the experiment induced a significant response compared with their negative control after S9 microsomal activation system. CTE-1 without S9 microsomal activation system did not produce a significance difference as compared to the negative control. Due to the higher rate of random mutations, a large number of revertants were produced even in the plate with negative control. Therefore, data were corrected for the negative control (Figure 5.4.); the raw data are shown in Figure 5.3.

Results demonstrated that CTE-1 produced lower number of TA98 revertants as compared to the induction of TA100 revertants. The average mutagenic potency induced by CTE-1 in TA98 was 4 revertants/μg, with and without S9. Concentrations that induced a significance response was in the range of 20.5-205 μg/plate with S9 and 30.75-61.5 μg/plate without S9 (Table 5.3). In general, the difference between the number of TA98 revertants produced by CTE-1 with and without S9 was smaller than that of the TA100 with and without S9 (Figures 5.4-5.5, Table 5.3). CTE-2 had relatively higher concentrations of PAHs as compared to CTE-1 (Table 5.1). CTE-2 produced higher number of TA100 revertants with S9 with average mutagenic potency of 9 revertants/μg as compared to without S9 (3.7 revertants/μg) (Figure 5.6, Table 5.3). CTE-2 was a weaker frameshift mutagen (Figure 5.7). It only produced 3 revertants/μg in TA98 with S9 and 1 revertants/μg without S9. CTE-2 produced significantly higher number of TA100 revertants with S9 as compared to negative control with all the concentrations used in the experiment (10.4-166.4 μg/plate). However, only higher concentrations of CTE-2 produced significantly higher number of TA98 revertants with and without S9 (Table 5.3). This was corroborated by the previous studies where coal tar induced TA100 and TA98 revertants in the concentration range of 10-200 μg/plate and produced more

revertants with S9 activation as compared to without S9 activation system (Robinson et al. 1984; Cosmetic Ingredient Review Expert Panel 2008)

SE-1 induced a higher frequency of TA100 revertants with S9 with the average mutagenic potency rate of 10 revertants/μg then without S9 (6 revertants/μg). The significant concentration range was 11.5-103.5 μg/plate for the revertants produced with S9 and 103.5 μg/plate without S9 activation. SE-1 produced 9 TA98 revertants/μg with S9 and 5 revertants/μg without S9. Concentrations expressing significant mutagenic responses with S9 and without S9 were 11.5-103.5 μg/plate (Table 5.3). SE-1 produced higher number of TA98 and TA100 revertants with S9 as compared to without S9 (Figure 5.8-5.9). However, SE-2 had the higher PAHs concentrations as compared to SE-1 was highly mutagenic as compared to all other samples in the study. SE-2 produced the highest number of TA100 and TA98 revertants with S9 with the average mutagenic potency rate of 13 revertants/μg and 12 revertants/μg, respectively. All the concentrations (10.33-92.97 μg/plate) used for TA100 and TA98 mutagenicity experiment induced significantly higher numbers of revertants with S9. SE-2 had a relatively lower mutagenic potency rate for TA100 and TA98 without S9 and produced on 5 revertants/μg. Only higher concentrations showed a significant increase in the number of TA98 revertants (Table 5.3). Results demonstrated that SE-2 produced the highest number of TA100 and AT98 revertants with S9 as compared to without S9. However, the effect of S9 on TA98 revertants induced by SE-2 was not higher as much as it was on the TA100 revertants (Figure 5.10-5.11). (Godefroy et al. 2005)

The coal tar and soot extracts with higher concentrations of PAHs were compared for their mutagenic potency. Results demonstrated that out of the EPA listed 16 priority PAHs, SE-2 had relatively lower number of PAHs as compared to CTE-2, despite having lower number of PAHs, SE-2 showed a stronger mutagenic potency as compared to CTE-2. SE-2 produced higher number of TA100 and TA98 revertants with S9 as compared to CTE-2 (Figure 5.12-5.13).

5.4. CONCLUSIONS

These data demonstrated that coal tar particles adsorbed more PAHs as compared to soot. Soot extracts had lower number of PAHs. However, the mutagenic potency of soot extracts was greater than the coal tar extracts. Both kinds of PACs were promutagenic and required the S9

microsomal activation system. These PACs based PAHs induced more base pair substitution mutation as compared to frameshift mutations.

5.5. TABLES AND FIGURES

Table 5.1. Concentrations of PAHs extracted from two coal tar samples; sample 1 with 50 mg of coal tar and sample 2 with 60 mg of coal tar. Coal tar samples were extracted with 50:50 acetone: dichloromethane

	Concentration in extract (mg/L)	
Compound	Sample 1	Sample 2
Naphthalene	2.49	3.20
Acenaphthalene	0.09	0.09
Acenaphthylene	0.05	0.04
Fluorene	2.37	2.38
Phenanthrene	11.49	14.55
Anthracene	11.49	14.55
Fluoranthene	23.23	50.68
Pyrene	55.10	36.01
Chrysene	1.44	1.58
Benz[a]anthracene	8.94	12.41
Benzo[b]fluoranthene	3.94	4.93
Benzo[k]fluoranthene	1.66	1.82
Benz[a]pyrene	2.82	3.40
Indeno[123-cd]pyrene	2.60	0.16
Dibenz[ah]anthracene	0.14	0.24
Benzo[ghi]perylene	0.32	0.35

Table 5.2. PAHs extraction from SOOT samples, representing the mass and concentrations of PAHs in different soot samples extracts

	Mass PAH in 2 mL (μg)		Concentration of PAH (mg/L)	
	Sample 1	Sample 2	Sample 1	Sample 2
Naphthalene				
Acenaphthalene				
Acenaphthylene				
Fluorene				
Phenanthrene	0.584	0.612	0.292	0.306
Anthracene		0.130		0.065
Fluoranthene	0.869	0.854	0.434	0.427
Pyrene	1.379	1.366	0.690	0.683
Chrysene	0.233	0.232	0.116	0.116
Benz[a]anthracene	0.238	0.236	0.119	0.118
Benzo[b]fluoranthene	0.529	0.537	0.264	0.269
Benzo[k]fluoranthene		0.108		0.054
Benz[a]pyrene	0.711	0.738	0.355	0.369
Indeno[123-cd]pyrene	0.756	0.770	0.378	0.385
Dibenz[ah]anthracene				
Benzo[ghi]perylene	0.994	1.024	0.497	0.512
Total conc. (mg/L)			**3.146**	**3.303**

Table 5.3. Mutagenicity analysis of particle associated polyaromatic hydrocarbons using *S. typhimurium*

Carbonaceous material extract	Strain	S9	Treatment range (μg/plate)	Range with significant response	ANOVA test	Mutagenic potency (average revertants/μg)
CTE-1	TA100	+	10.25-61.5	10.25-61.5	F=6.113; P<0.001	8
	TA98	+	10.25-205	20.5-205	F=7.986; P<0.001	4
	TA100	−	10.25-61.5	Not significant	F=2.69;P=0.024	1
	TA98	−	10.25-205	30.75-61.5	F=3.376; P=0.011	4
CTE-2	TA100	+	10.4-166.4	10.4-166.4	F=7.96; P<0.001	9
	TA98	+	10.4-166.4	41.6-166.4	F=15.387;P<0.001	3
	TA100	−	10.4-166.4	166.4-104	F=8; P<0.001	3.7
	TA98	−	10.4-166.4	83.2-166.4	F=28.296;P<0.001	1
SE-1	TA100	+	11.5-103.5	11.5-103.5	F=253; P<0.001	10
	TA98	+	11.5-103.5	11.5-103.5	F=1079; P<0.001	9
	TA100	−	11.5-103.5	103.5	F=7.85; P=0.002	6
	TA98	−	11.5-103.5	11.5-103.5	F=485; P<0.001	5
SE-2	TA100	+	10.33-92.97	10.33-92.97	F=153; P<0.001	13
	TA98	+	10.33-92.97	10.33-92.97	F=293; P<0.001	12
	TA100	−	10.33-92.97	30.99-61.98	F=5.671; P=0.005	5
	TA98	−	10.33-92.97	10.33-92.97	F=445; P<0.001	5

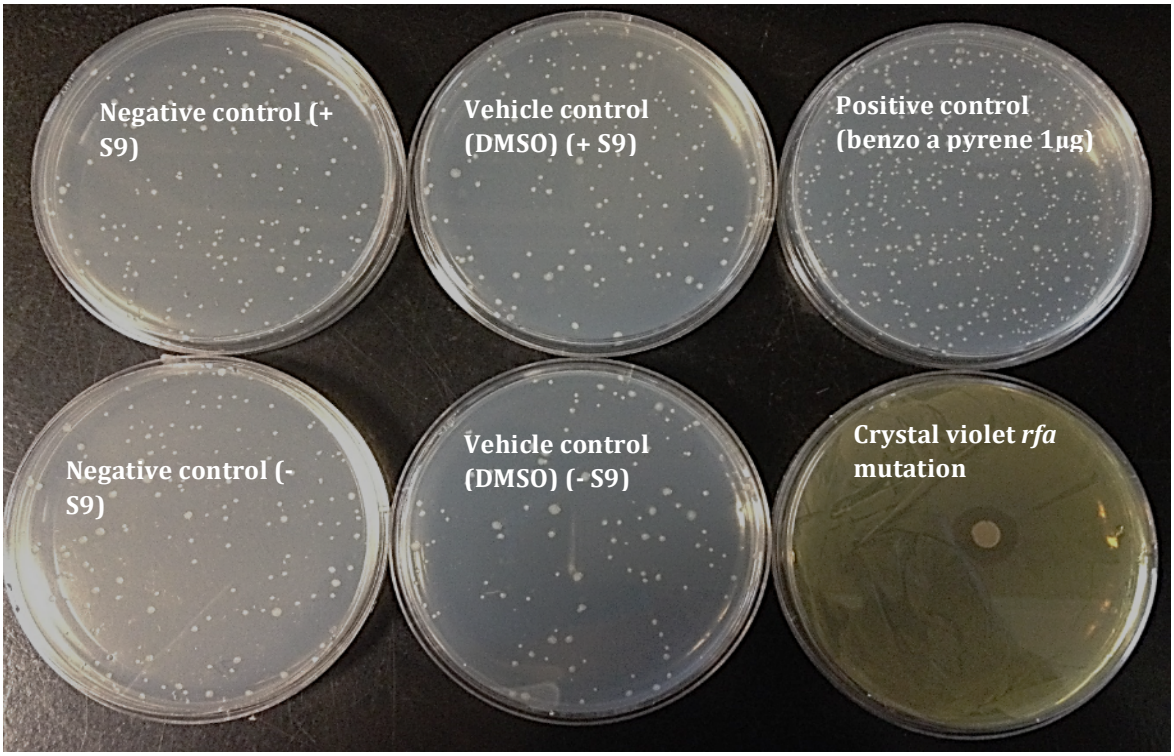

Figure 5.1. Diagnostic plates for the *S. typhimurium* plate incorporation mutagenicity assay. A negative control is illustrated by the left top and bottom plates with and without S9, the second top and bottom plates are showing vehicle control with and without S9, the top right plate is positive control (BaP) and the right bottom plate is the crystal violet *rfa*$^{-}$ plate showing a clear zone of inhibition.

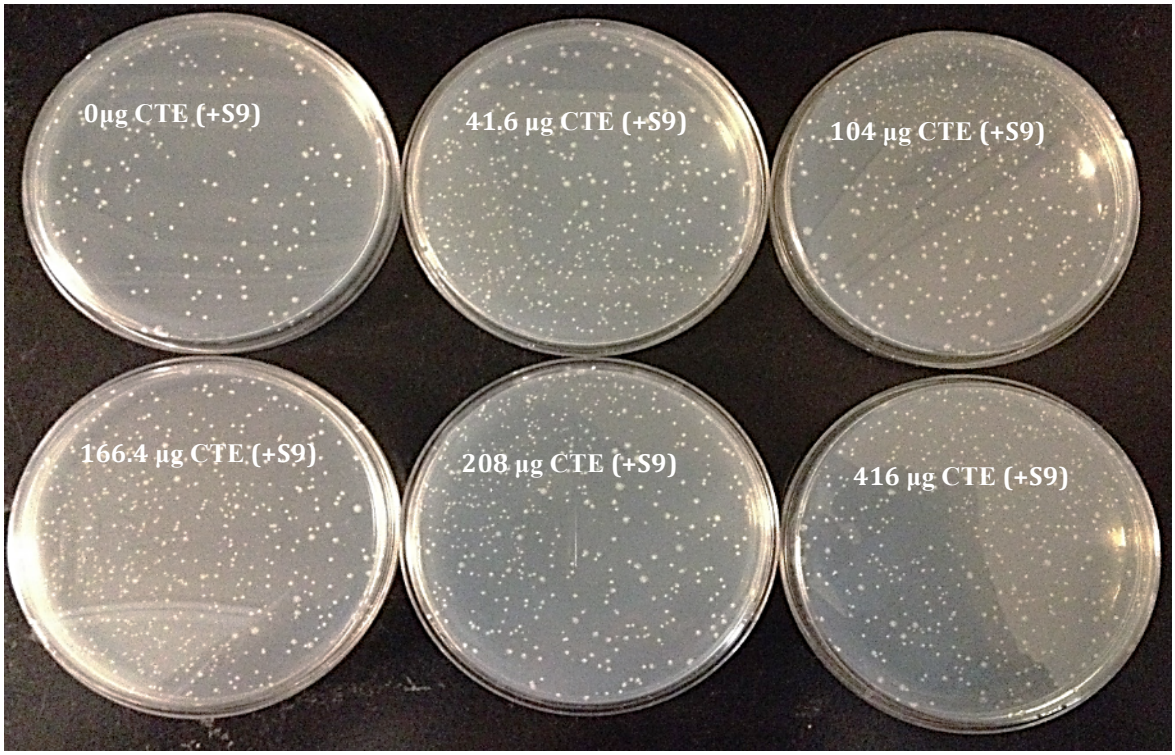

Figure 5.2. Mutagenicity of coal tar extract (CTE) from lake sediments with polyaromatic hydrocarbons in *S. typhimurium,* strain TA100, after mammalian hepatic microsomal activation showing increasing numbers of histidine revertants as a function of the concentration of the CTE.

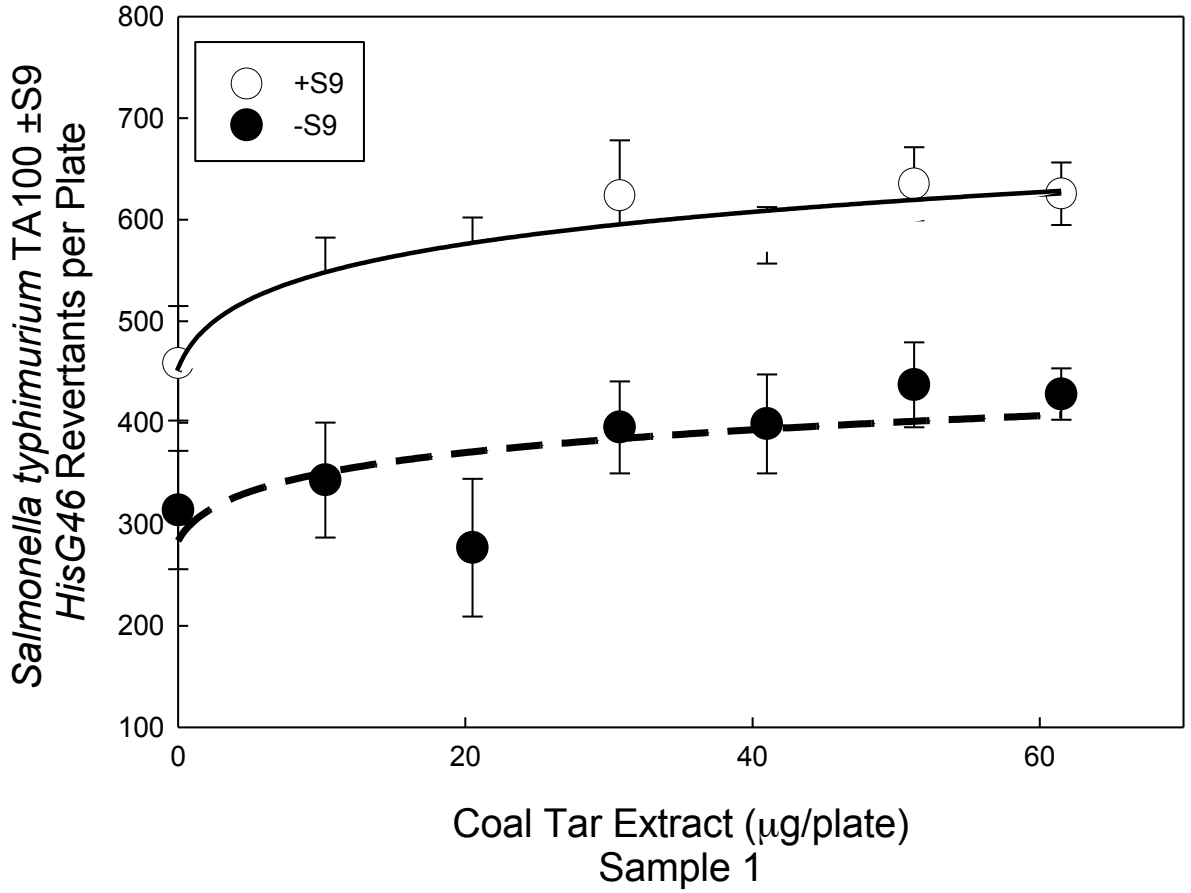

Figure 5.3. Mutagenicity of coal tar extract 1(CTE-1) from lake sediments with polyaromatic hydrocarbons (PAHs) in *S. typhimurium,* strain TA100 with and without microsomal activation. CTE-1 is showing increasing number of histidine revertants in the presence of S9 activation system as compared to without S9 activation system, as a function of the increasing CTE-1 concentration.

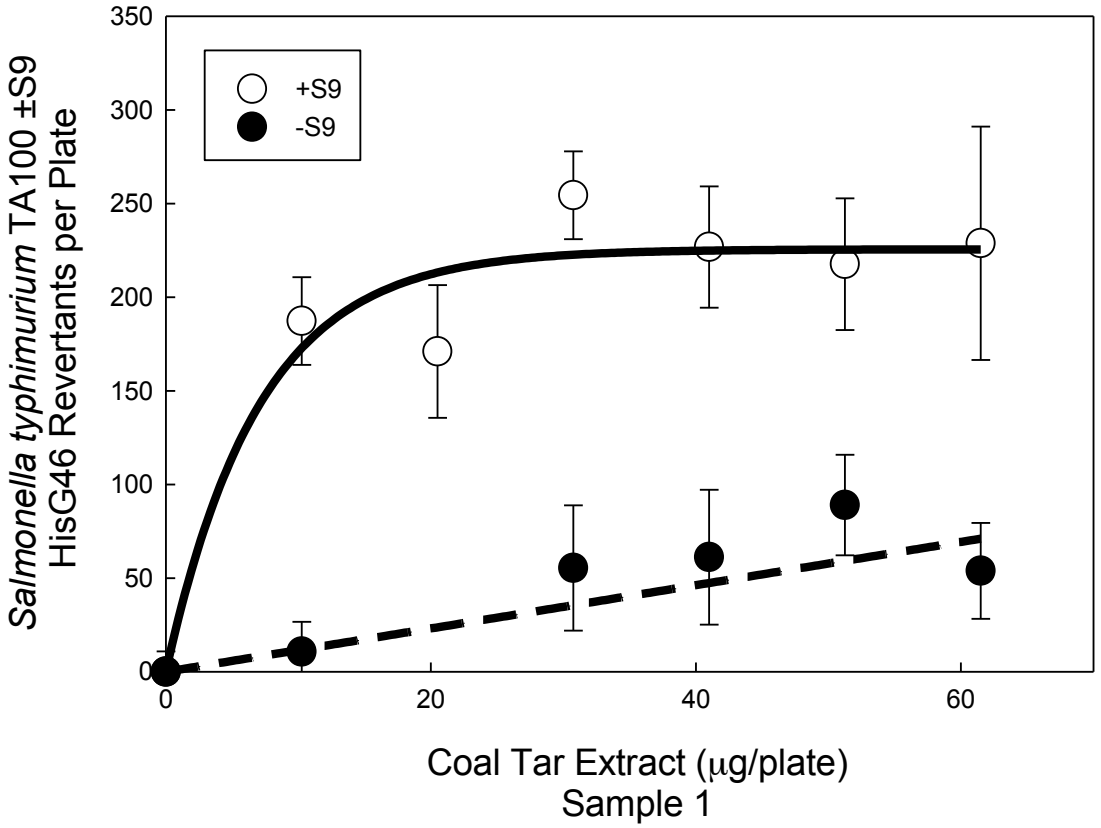

Figure 5.4. Mutagenicity of coal tar extract 1(CTE-1) from lake sediments with polyaromatic hydrocarbons (PAHs) in *S. typhimurium,* strain TA100 with and without microsomal activation, corrected for the negative control with higher rate random mutations induced revertants. CTE-1 is showing increasing number of histidine revertants in the presence of S9 activation system as compared to without S9 activation system, as a function of the increasing CTE-1 concentration.

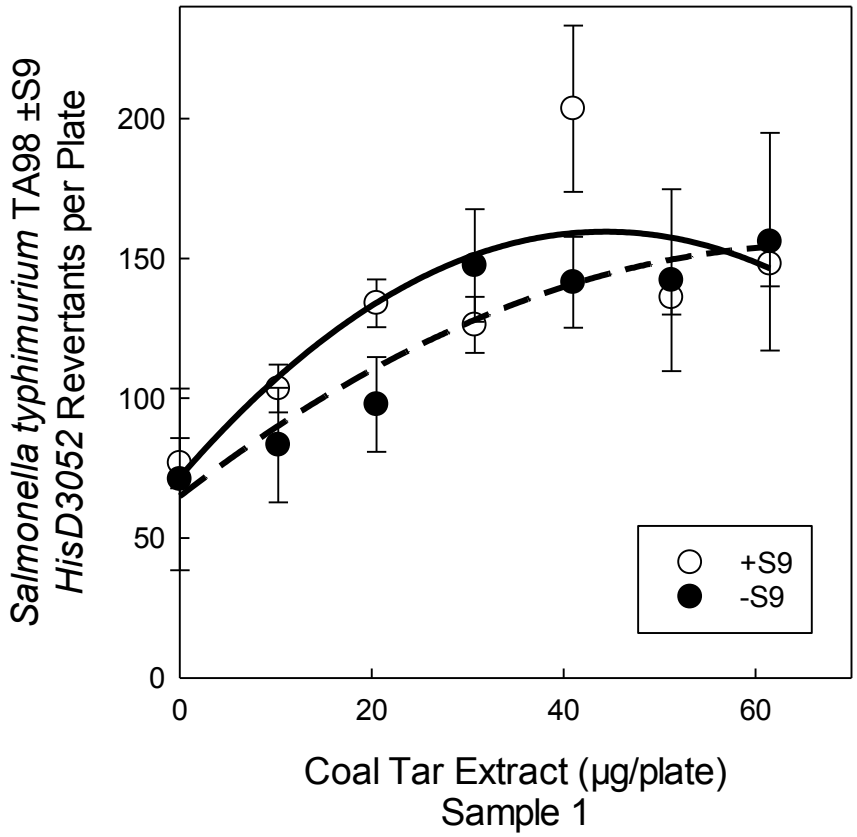

Figure 5.5. Mutagenicity of CTE-1 from lake sediments with PAHs in *S. typhimurium,* strain TA98 with and without microsomal activation. CTE-1 is showing increasing number of histidine revertants in the presence of S9 activation system as compared to without S9 activation system, as a function of the increasing CTE-1 concentration.

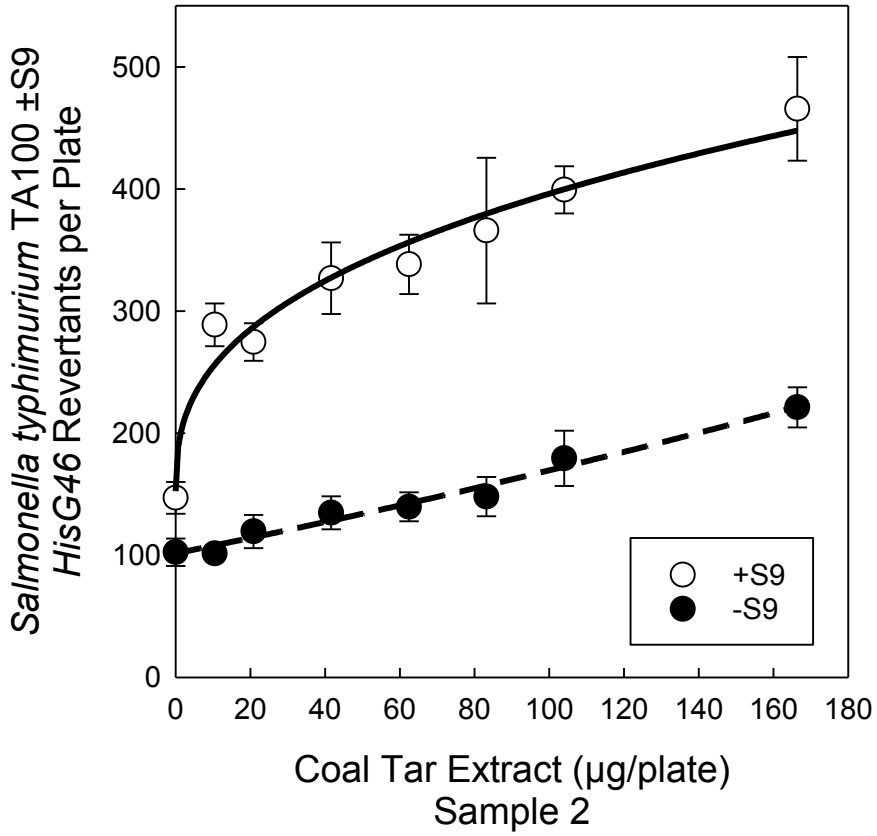

Figure 5.6. Mutagenicity of CTE-2 from lake sediments with PAHs in *S. typhimurium,* strain TA100 with and without microsomal activation. CTE-2 is showing increasing number of histidine revertants in the presence of S9 activation system as compared to without S9 activation system, as a function of the increasing CTE-2 concentrations.

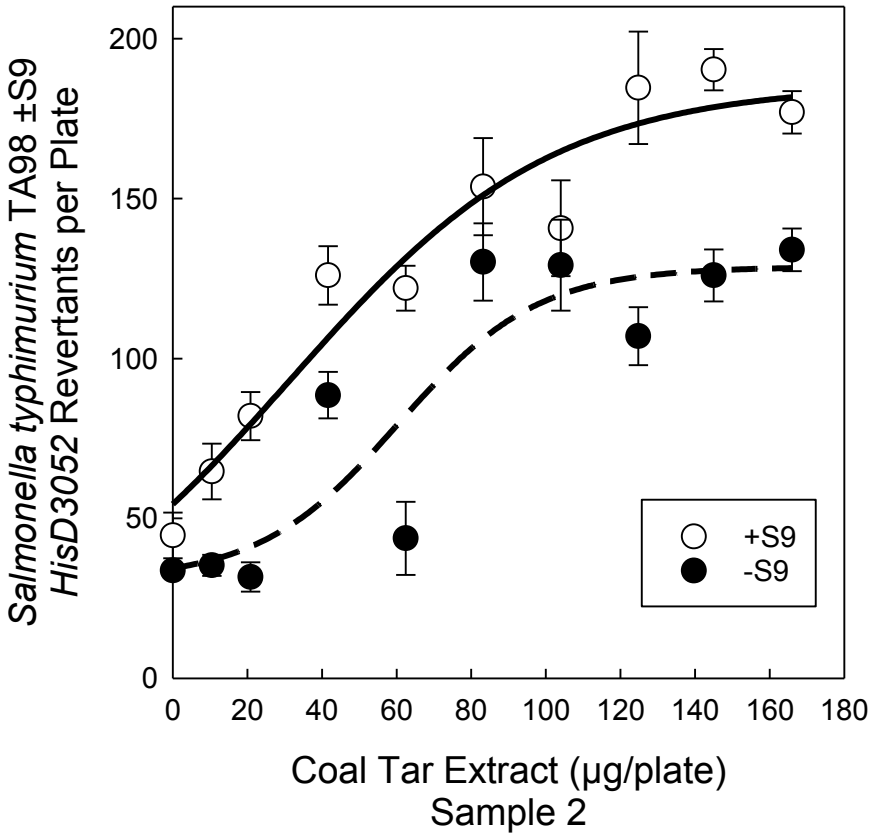

Figure 5.7. Mutagenicity of CTE-2 from lake sediments with PAHs in *S. typhimurium,* strain TA98 with and without microsomal activation. CTE-2 is showing increasing number of histidine revertants in the presence of S9 activation system as compared to without S9 activation system, as a function of the increasing CTE-2 concentrations.

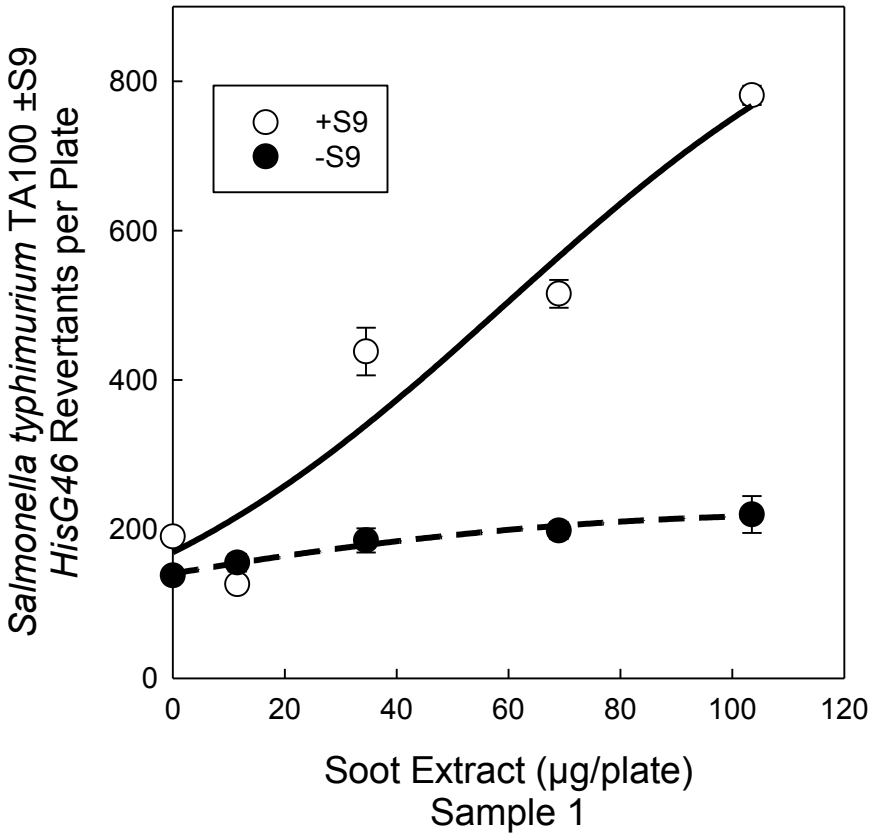

Figure 5.8. Mutagenicity of SE-1from lake sediments with PAHs in *S. typhimurium,* strain TA100 with and without microsomal activation. SE-1 is showing increasing number of histidine revertants in the presence of S9 activation system as compared to without S9 activation system, as a function of the increasing SE-1 concentrations.

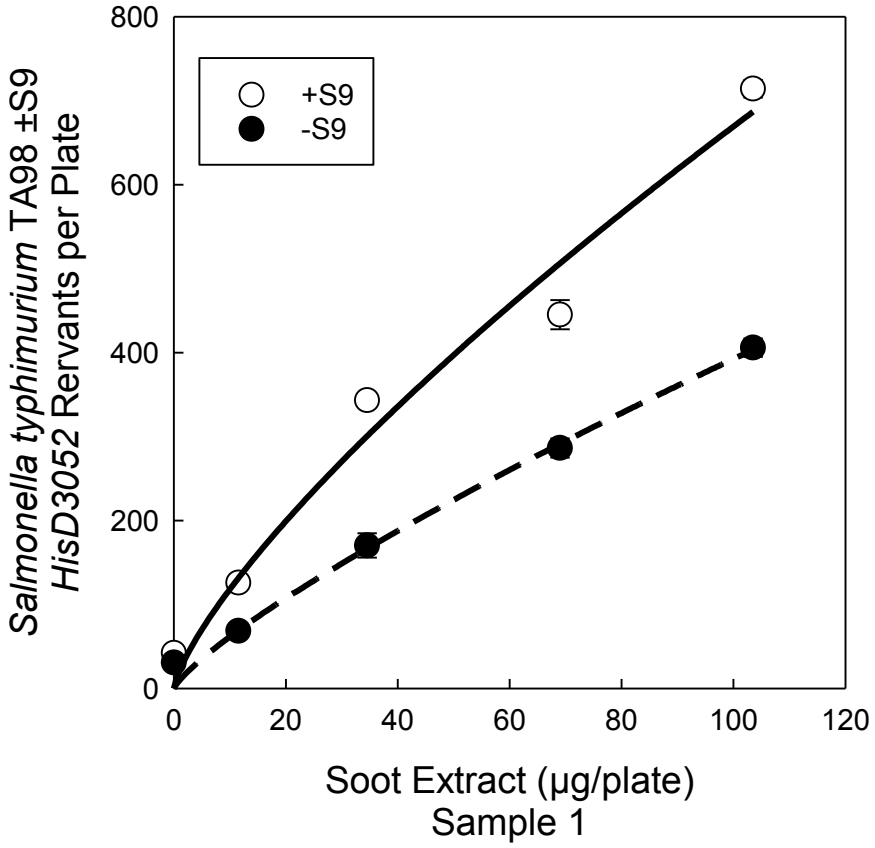

Figure 5.9. Mutagenicity of SE-1from lake sediments with PAHs in *S. typhimurium,* strain TA98 with and without microsomal activation. SE-1 is showing increasing number of histidine revertants in the presence of S9 activation system as compared to without S9 activation system, as a function of the increasing SE-1 concentrations.

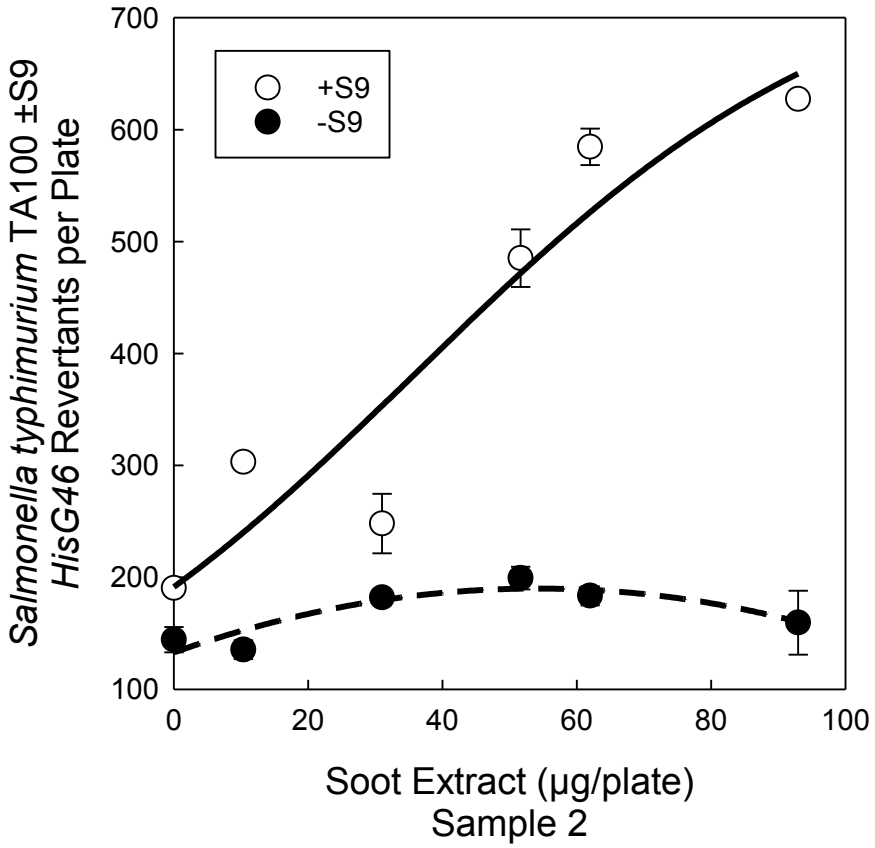

Figure 5.10. Mutagenicity of SE-2 from lake sediments with PAHs in *S. typhimurium,* strain TA100 with and without microsomal activation. SE-2 is showing increasing number of histidine revertants in the presence of S9 activation system as compared to without S9 activation system, as a function of the increasing SE-2 concentrations.

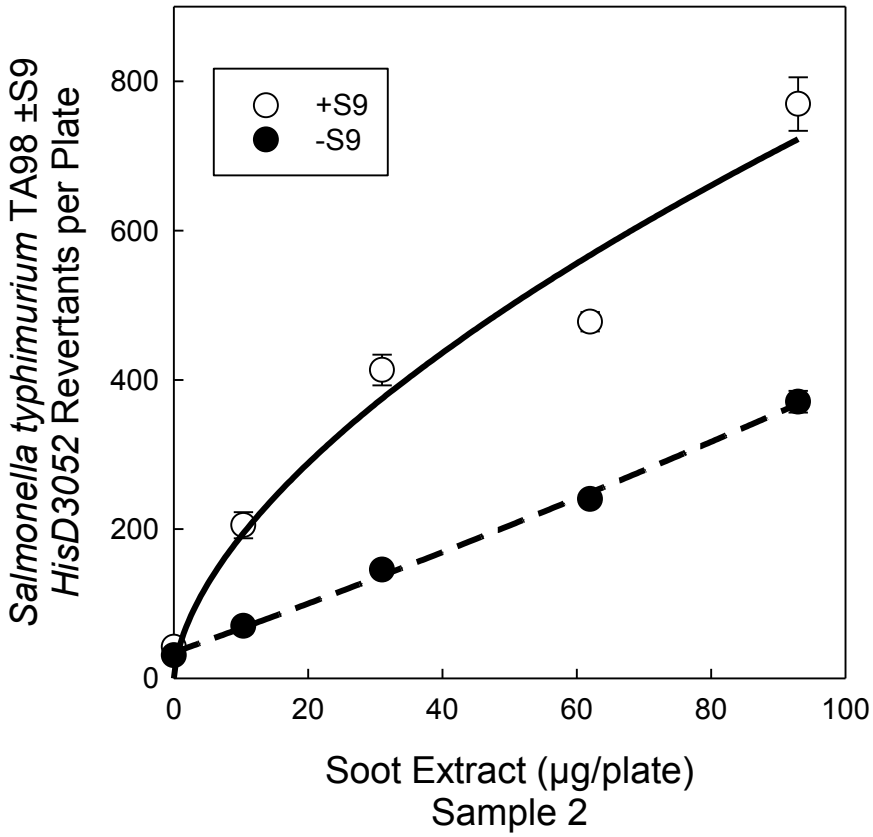

Figure 5.11. Mutagenicity of SE-2from lake sediments with PAHs in *S. typhimurium,* strain TA98 with and without microsomal activation. SE-2 is showing increasing number of histidine revertants in the presence of S9 activation system as compared to without S9 activation system, as a function of the increasing SE-2 concentrations.

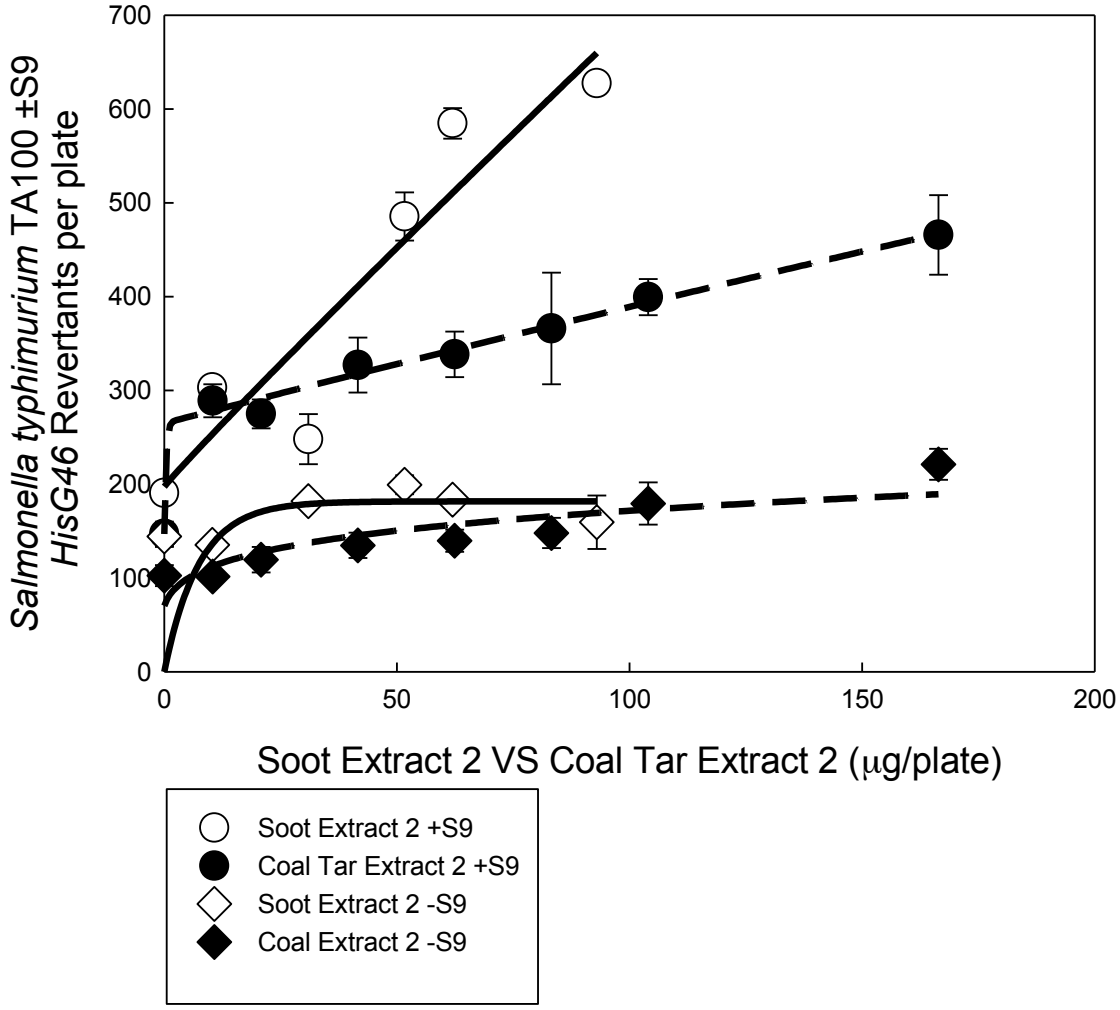

Figure 5.12. Mutagenicity of SE-2 VS CTE-2 from lake sediments with PAHs in *S. typhimurium,* strain TA100 with and without microsomal activation. SE-2 is showing relatively higher TA100 revertants as compared to CTE-2 with S9 activation system as a function of the increasing SE-2 concentrations.

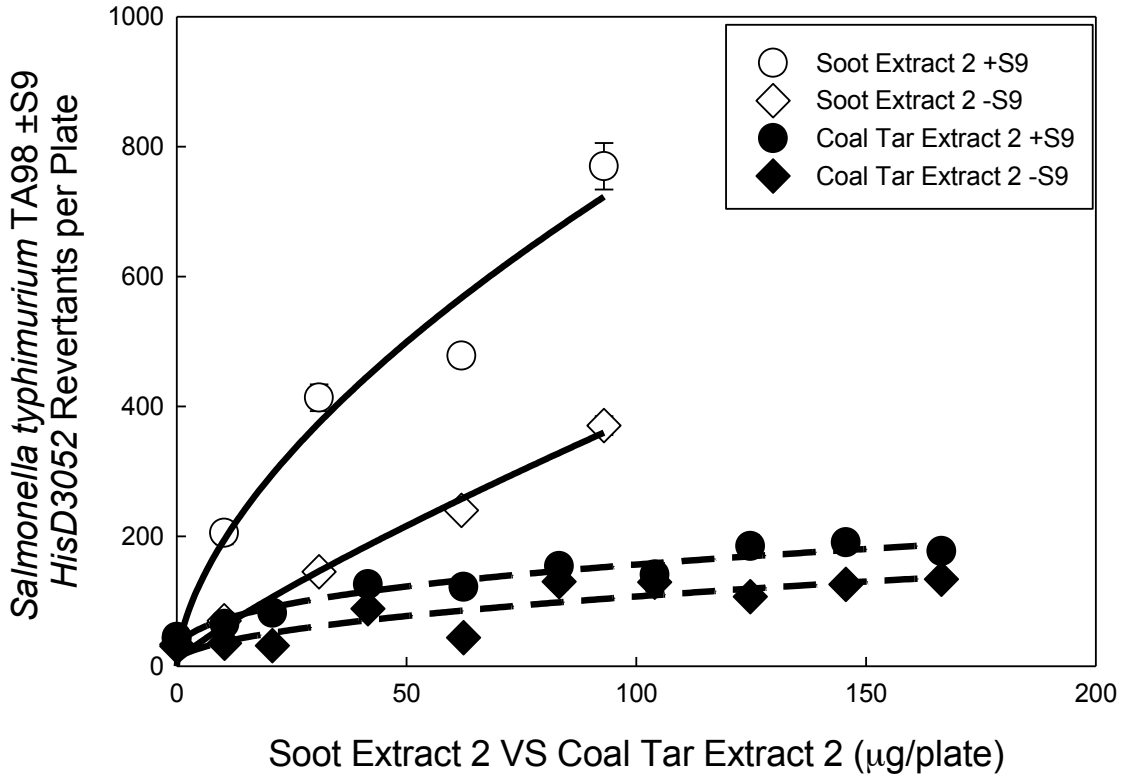

Figure 5.13. Mutagenicity of SE-2 VS CTE-2 from lake sediments with PAHs in *S. typhimurium,* strain TA98 with and without microsomal activation. SE-2 is showing relatively higher TA98 revertants as compared to CTE-2 with S9 activation system as a function of the increasing SE-2 concentrations.

5.6. REFERENCES

Armstrong B. 1994. Lung cancer mortality and polynuclear aromatic hydrocarbons: A case-cohort study of aluminum production workers in Arvida, Quebec, Canada. Am J Epidemiol 139(3):250-262.

Bos RP, Theuws JLG, Leijdekkers CM, Henderson PT. 1984. The presence of the mutagenic polycyclic aromatic hydrocarbons benzo(a)pyrene and benz(a)anthracine in creosote-P1 Mutat Res 130(3):153-158.

Buha A. 2011. Polycyclic Aromatic Hydrocarbons.

Campro Scientific. Priority PAHs. http://www.campro.eu/PDF/Brochures/Flyer-CHIRON/2009-09-BMF-40-PAHs.pdf.

Chalmers AT, Van Metre PC, Callender E. 2007. The chemical response of particle-associated contaminants in aquatic sediments to urbanization in New England, U.S.A. J Contam Hydrol 91(1-2):4-25.

Christensen ER, Xiaochun Z. 1993. Sources of polycyclic aromatic hydrocarbons to Lake Michigan determined from sedimentary records. Environmental Science & Technology 27(1):139-146.

Cosmetic Ingredient Review Expert Panel. 2008. Final Safety Assessment of Coal Tar as Used in Cosmetics. International Journal of Toxicology (Taylor & Francis) 27:1-24.

Dubey G. Understanding how sealcoating works ... and how it can save you money; http://pavementpro.org/understanding.htm.

Farmer PB. 2003. Molecular epidemiology studies of carcinogenic environmental pollutants - Effects of polycyclic aromatic hydrocarbons (PAHs) in environmental pollution on exogenous and oxidative DNA damage. Mutat Res 544(2-3):397-402.

Godefroy SJ, Martincigh BS, Salter LF. 2005. Measurements of polycyclic aromatic hydrocarbons and genotoxicity in soot deposited at a toll plaza near Durban, South Africa. South African Journal of Chemistry 58:61-66.

Hartman PE, Ames BN, Roth JR, Barnes WM, Levin DE. 1986. Target sequences for mutagenesis in Salmonella histidine-requiring mutants. Environ Mutagen 8(4):631-641.

Hoffman EJ, Mills GL, Latimer JS, Quinn JG. 1984. Urban runoff as a source of polycyclic aromatic-hydrocarbons to coastal waters Environ Sci Technol 18(8):580-587.

Kevekordes S, Porzig J, Gebel T, Dunkelberg H. 1998. [Mutagenicity of mixtures of halogenated aliphatic hydrocarbons and polycyclic aromatic hydrocarbons in the Ames test with TA98 and TA100]. Zentralbl Hyg Umweltmed 200(5-6):531-541.

Lopes TJ, Furlong ET, Pritt JW. 1999. Occurrence and distribution of semivolatile organic compounds in stream bed sediments, United States, 1992-95. ASTM Special Technical Publication(1333):105-119.

Mahler BJ, Ingersoll CG, Van Metre PC, Kunz JL, Little EE. 2015. Acute Toxicity of Runoff from Sealcoated Pavement to Ceriodaphnia dubia and Pimephales promelas. Environmental Science & Technology 49(8):5060-5069.

Mahler BJ, Van Metre PC. 2003. A simplified approach for monitoring hydrophobic organic contaminants associated with suspended sediment: Methodology and applications. Arch Environ Contam Toxicol 44(3):288-297.

Mahler BJ, van Metre PC, Bashara TJ, Wilson JT, Johns DA. 2005. Parking Lot Sealcoat: An Unrecognized Source of Urban Polycyclic Aromatic Hydrocarbons. Environ Sci Technol 39(15):5560-5566.

Mahler BJ, Van Metre PC, Crane JL, Watts AW, Scoggins M, Williams ES. 2012. Coal-Tar-Based Pavement Sealcoat and PAHs: Implications for the Environment, Human Health, and Stormwater Management. Environmental Science & Technology 46(6):3039-3045.

Maron DM, Ames BN. 1983. Revised methods for the Salmonella mutagenicity test. Mutat Res 113(3-4):173-215.

Mumtaz M, Julia G. 1995. Toxicologial profile for polycyclic aromatic hydrocarbons Toxic substances portal-polycyclic aromatic hydrocarbons (PAHs).

Phillipson CE, Ioannides C. 1989. Metabolic activation of polycyclic aromatic hydrocarbons to mutagens in the Ames test by various animal species including man. Mutat Res 211(1):147-151.

Rice KC. 1999. Trace-Element Concentrations in Streambed Sediment Across the Conterminous United States. Environmental Science & Technology 33(15):2499.

Robinson M, Bull RJ, Munch J, Meier J. 1984. Comparative carcinogenic and mutagenic activity of coal tar and petroleum asphalt paints used in potable water supply systems. J Appl Toxicol 4(1):49-56.

Scoggins M, Ennis TOM, Parker N, Herrington C. 2009. A Photographic Method for Estimating Wear of Coal Tar Sealcoat from Parking Lots. Environmental Science & Technology 43(13):4909-4914.

Van Metre PC, Mahler BJ. 2005. Trends in hydrophobic organic contaminants in urban and reference lake sediments across the United States, 1970-2001. Environ Sci Technol 39(15):5567-5574.

Van Metre PC, Mahler BJ. 2010. Contribution of PAHs from coal-tar pavement sealcoat and other sources to 40 U.S. lakes. Sci Total Environ 409(2):334-344.

Yang Y, Van Metre PC, Mahler BJ, Wilson JT, Ligouis B, Razzaque MD, Schaeffer DJ, Werth CJ. 2010. Influence of coal-tar sealcoat and other carbonaceous materials on polycyclic aromatic hydrocarbon loading in an urban watershed. Environ Sci Technol 44(4):1217-1223.

CHAPTER 6

CONCLUSIONS

The main focus of this dissertation was to study the toxicity mechanisms of anthropogenic water contaminants. The objectives were to i) analyze the toxicity mechanisms of haloacetic acids (HAAs) water disinfection by-products (DBPs) and to identify their molecular targets, ii) study the cytotoxicity and genotoxicity of chlorinated and chloraminated waste water effluents, iii) study the mutagenic effect of particle associated contaminants such as polycyclic aromatic hydrocarbons (PAHs) extracted from soot and coal tar particles in lake sediments. Following conclusions were derived from these studies.

It was concluded from the first study that HAAs were inducing their toxicity by affecting glycolytic and mitochondrial metabolism and by disrupting cellular energy homeostasis. However, there were differences among mono-, di-, and triHAAs toxicity mechanisms and their molecular targets. monoHAAs were the strongest inhibitors of gluceryldehyde-3-phosphate dehydrogenase (GAPDH) and greatly reduced the ATP contents of the cells. Di-, and triHAAs were weaker inhibitors of GAPDH and increased the ATP contents of the cells. HAAs not only affected the GAPDH kinetics but also affected the pyruvate dehydrogenase complex (PDC) activity. Most of the HAAs activated PDC. It was concluded that monoHAAs activated PDC because of the cellular metabolite ratios (ATP/ADP, NADH/NAD) which was a disruption induced by GAPDH inhibition. Reduction in cellular metabolites by the monoHAAs required cells to accelerate PDC activity based on the metabolite ratio-dependent pyruvate dehydrogenase (PDH) regulation. It was also concluded that the toxicity of monoHAAs was mainly due to the GAPDH inhibition as pyruvate supplementation rescued the cells against the monoHAAs induced genomic DNA damage and cellular ATP reductions. However, di- and triHAAs were the weaker inhibitors of GAPDH, increased celluar ATP levels, and increased the PDC activity. From this result I concluded that di-, and triHAAs induced increase in the PDC activity was due to the pyruvate dehydrogenase kinase (PDK) dependent regulation of PDH. Some di-, and triHAAs inhibited PDK, which blocked the PDK induced PDH inhibition and in turn increased the overall PDC activity.

From these results a global conclusion is that monoHAAs affect the mitochondrial metabolism by disturbing different metabolite ratios while di-, and triHAAs have a direct effect on mitochondrial metabolism by inhibiting PDK.

The second study involved a mammalian cell based cytotoxicity and genotoxicity analyses of concentrated organics of chlorinated and chloraminated wastewaters effluents. The wastewater XAD-8-isolated organic extracts were more cytotoxic and genotoxic than the XAD-4 extracts of the same wastewaters. It was concluded that halogenated hydrophobic acid fractions, aliphatic carboxylic acid fractions, and humic substances, which were eluted from XAD-8 were more cytotoxic and genotoxic than the organics eluted from XAD-4 resins. After passage over the XAD columns the remaining spent wastewater expressed very little residual toxicity indicating that XAD-8/XAD-4 extraction was highly efficient. The method of disinfection also affected the overall toxicity of the extracts. The organic extracts eluted from XAD-8 or XAD-4 for chlorinated water was more cytotoxic and genotoxic than that of the chloraminated wastewater extracts.

The final study involved the mutagenicity evaluation of PAHs extracted from different carbonaceous materials e.g. soot and coal tar from lake sediments. It was concluded from the data that coal tar and soot extracts were promutagens and required S9 microsomal activation to be converted into active mutagens. The coal tar and soot extracts induced more base pair substitution mutations as compared to frameshift mutations. Of the EPA listed 16 PAHs; soot samples had a lower number of PAHs as compared to coal tar extracts. However, soot extracts induced higher number of TA100 and TA98 revertants as compared to coal tar extracts.